

Sandia National Laboratories
Waste Isolation Pilot Plant

**Consumption of Carbon Dioxide by Precipitation of
Carbonate Minerals Resulting from Dissolution of
Sulfate Minerals in the Salado Formation
In Response to
Microbial Sulfate Reduction in the WIPP**

Laurence H. Brush,¹ Yongliang Xiong,¹ James W. Garner,²
Ahmed Ismail,² and Gregory T. Roselle¹

1. Repository Performance Dept. 6712
 2. Performance Assessment and Decision Analysis Dept. 6711
- Sandia National Laboratories
Carlsbad Programs Group
Carlsbad, NM 88220

APPROVAL PAGE

Author: _____
Laurence H. Brush, 6712 _____
Date

Author: _____
Yongliang Xiong, 6712 _____
Date

Author: _____
James W. Garner, 6711 _____
Date

Author: _____
Ahmed Ismail, 6711 _____
Date

Author: _____
Gregory T. Roselle, 6712 _____
Date

Technical Reviewer: _____
Haoran Deng, 6712 _____
Date

QA Reviewer: _____
Mario J. Chavez, 6710 _____
Date

Management Reviewer: _____
Mark Rigali, 6712 _____
Date

TABLE OF CONTENTS

TABLE OF CONTENTS.....	3
LIST OF TABLES.....	5
1 INTRODUCTION.....	8
2 BACKGROUND.....	9
3 CALCULATIONS.....	12
3.1 Reaction-Path Calculations.....	12
3.2 Compositions of Brines and Solids.....	14
3.2.1 Brines.....	14
3.2.2 MgO.....	14
3.2.3 Salado Minerals.....	15
3.3 Brine Volumes.....	16
3.3.1 Minimum Volume.....	16
3.3.2 Intermediate Volume.....	17
3.3.3 Maximum Volume.....	17
3.4 Quantities of Solids.....	17
3.4.1 CPR Materials.....	18
3.4.2 MgO.....	18
3.4.3 Salado Minerals.....	18
3.5 Scaling of Brine Volumes and Masses of Solids for EQ6 Input Files.....	19
3.6 Organic Ligands.....	20
3.6.1 Justification for Excluding Acetate and EDTA.....	20
3.6.2 Justification for Including Citrate and Oxalate.....	22
3.7 CaCO ₃ (am).....	23
4 SOFTWARE.....	24

TABLE OF CONTENTS (cont.)

5 RESULTS	26
5.1 Effects of Initial Brine Composition and Brine Volume	26
5.1.1 Effects on Brine Composition.....	26
5.1.2 Effects on Precipitation of Carbonate Minerals and Effective CO ₂ Yield.....	27
5.2 Effects of Hydromagnesite	28
5.2.1 Effects on Brine Composition.....	29
5.2.2 Effects on Precipitation of Carbonate Minerals and Effective CO ₂ Yield.....	29
5.3 Effects of Organic Ligands	29
5.3.1 Effects on Brine Composition.....	30
5.3.2 Effects on Precipitation of Carbonate Minerals and Effective CO ₂ Yield.....	30
5.4 Effects of CaCO ₃ (am).....	30
5.4.1 Effects on Brine Composition.....	31
5.4.2 Effects on Precipitation of Carbonate Minerals and Effective CO ₂ Yield.....	31
6 POSSIBLE ISSUES RELATED TO CALCITE PRECIPITATION.....	32
6.1 Possible Limitations on the Quantity of SO ₄ ²⁻ Available in the DRZ	32
6.2 Possible Kinetic Inhibition of Calcite Precipitation.....	34
6.2.1 Effects of Single Inhibitors	34
6.2.2 Effects of Multiple Inhibitors.....	37
7 CONCLUSIONS.....	38
8 REFERENCES	40
APPENDIX A. DOCUMENTATION OF EQ3/6 CALCULATIONS.....	97
APPENDIX B. LIST OF EQ6 INPUT FILES.....	98

LIST OF TABLES

Table 1.	Abbreviations, Acronyms, and Initialisms.....	49
Table 2.	Summary of Simulations Carried Out for This Analysis.....	52
Table 3.	Compositions of GWB and ERDA-6 Before and After Equilibration with MgO, Halite and Anhydrite.	53
Table 4.	Suffixes for EQ3/6 Files.	54
Table 5.	Input Parameters for the Simulation with 1,045 m ³ of GWB.....	55
Table 6.	Input Parameters for the Simulation with 1,045 m ³ of ERDA-6.....	56
Table 7.	Input Parameters for the Simulation with 7,763 m ³ of GWB.....	57
Table 8.	Input Parameters for the Simulation with 7,763 m ³ of ERDA-6.....	58
Table 9.	Input Parameters for the Simulation with 13,267 of m ³ ERDA-6.....	59
Table 10.	Input Parameters for the Simulation with 7,763 m ³ of GWB and Hydromagnesite.....	60
Table 11.	Input Parameters for the Simulation with 7,763 m ³ of ERDA-6 and Hydromagnesite.....	62
Table 12.	Input Parameters for the Simulations with 1,045 m ³ of GWB and Organic Ligands.....	64
Table 13.	Input Parameters for the Simulations with 1,045 m ³ of ERDA-6 and Organic Ligands.....	66
Table 14.	Input Parameters for the Simulations with 1,045 m ³ of GWB, Organic Ligands, and CaCO ₃ (am).....	68
Table 15.	Input Parameters for the Simulations with 1,045 m ³ of ERDA-6, Organic Ligands, and CaCO ₃ (am).....	70
Table 16.	Brine Compositions from the Simulation with 1,045 m ³ of GWB.....	72
Table 17.	Brine Compositions from the Simulation with 1,045 m ³ of ERDA-6.....	73

LIST OF TABLES (cont.)

Table 18.	Brine Compositions from the Simulation with 7,763 m ³ of GWB.....	74
Table 19.	Brine Compositions from the Simulation with 7,763 m ³ of ERDA-6.....	75
Table 20.	Brine Compositions from the Simulation with 13,267 m ³ of ERDA-6.....	76
Table 21.	Quantities of CO ₂ Consumed by Magnesite, Calcite, and Pirssonite; and Effective CO ₂ Yield in the Simulation with 1,045 m ³ of GWB..	77
Table 22.	Quantities of CO ₂ Consumed by Magnesite, Calcite, and Pirssonite; and Effective CO ₂ Yield in the Simulation with 1,045 m ³ of ERDA-6..	78
Table 23.	Quantities of CO ₂ Consumed by Magnesite, Calcite, and Pirssonite; and Effective CO ₂ Yield in the Simulation with 7,763 m ³ of GWB..	79
Table 24.	Quantities of CO ₂ Consumed by Magnesite, Calcite, and Pirssonite; and Effective CO ₂ Yield in the Simulation with 7,763 m ³ of ERDA-6 ..	80
Table 25.	Quantities of CO ₂ Consumed by Magnesite, Calcite, and Pirssonite; and Effective CO ₂ Yield in the Simulation with 13,267 m ³ of ERDA-6 ..	81
Table 26.	Brine Compositions from the Simulation with 7,763 m ³ of GWB and Hydromagnesite ..	82
Table 27.	Brine Compositions from the Simulation with 7,763 m ³ of ERDA-6 and Hydromagnesite ..	83
Table 28.	Quantities of CO ₂ Consumed by Hydromagnesite, Calcite, and Pirssonite; and Effective CO ₂ Yield in the Simulation with 7,763 m ³ of GWB.....	84
Table 29.	Quantities of CO ₂ Consumed by Hydromagnesite, Calcite, and Pirssonite; and Effective CO ₂ Yield in the Simulation with 7,763 m ³ of ERDA-6.....	85
Table 30.	Brine Compositions from the Simulation with 1,045 m ³ of GWB and Organic Ligands.....	86
Table 31.	Brine Compositions from the Simulation with 1,045 m ³ of ERDA and Organic Ligands.....	87
Table 32.	Quantities of CO ₂ Consumed by Magnesite, Calcite, and Pirssonite; and Effective CO ₂ Yield in the Simulation with 1,045 m ³ of GWB and Organic Ligands.....	89

LIST OF TABLES (cont.)

Table 33. Quantities of CO ₂ Consumed by Magnesite, Calcite, and Pirssonite; and Effective CO ₂ Yield in the Simulation with 1,045 m ³ of ERDA-6 and Organic Ligands.....	90
Table 34. Brine Compositions from the Simulation with 1,045 m ³ of GWB, Organic Ligands, and CaCO ₃ (am)	91
Table 35. Brine Compositions from the Simulation with 1,045 m ³ of ERDA-6, Organic Ligands, and CaCO ₃ (am)	92
Table 36. Quantities of CO ₂ Consumed by Magnesite, CaCO ₃ (am), and Pirssonite; and Effective CO ₂ Yield in the Simulation with 1,045 m ³ of GWB and Organic Ligands	94
Table 37. Quantities of CO ₂ Consumed by Magnesite, CaCO ₃ (am), and Pirssonite; and Effective CO ₂ Yield in the Simulation with 1,045 m ³ of ERDA-6 and Organic Ligands.....	95
Table 38. Logarithms of the Solubility Products for Minerals with the Composition CaCO ₃ or CaCO ₃ ·xH ₂ O.....	96

1 INTRODUCTION

This analysis report describes simulations of the effects of consumption of carbon dioxide (CO₂) by the precipitation of carbonate minerals on the excess factor for the magnesium oxide (MgO) being emplaced in the U.S. Department of Energy's (DOE's) Waste Isolation Pilot Plant (WIPP).

The MgO excess factor has been defined as the ratio of the total amount of MgO to be emplaced in the WIPP divided by the total amount required to consume all CO₂ that would be produced by microbial consumption of all cellulosic, plastic, and rubber (CPR) materials in the repository, calculated as specified by the U.S. Environmental Protection Agency (EPA) (Marcinowski, 2004).

This and other information needed to calculate the MgO effective excess factor were requested by the EPA as part of its review of a request by the DOE (Moody, 2006) to reduce the amount of excess MgO that it is required to emplace in the WIPP (Marcinowski, 2004). After the DOE submitted its request, the EPA asked that all uncertainties related to the MgO excess factor be described and that their effects be included to the extent possible. The MgO effective excess factor differs from the excess factor in that the former includes all uncertainties that can be quantified.

Precipitation of carbonates would result from the reaction of CO₂ with dissolved calcium (Ca²⁺) that would be released to WIPP brines by the dissolution of sulfate-bearing (SO₄²⁻-bearing) minerals in the Salado Formation surrounding the repository if microbial SO₄²⁻ reduction in the repository consumes all SO₄²⁻ available in the waste and continues by using SO₄²⁻ in brines and in minerals in the disturbed rock zone (DRZ). Carbonate precipitation could ameliorate the effects of SO₄²⁻ reduction that continues using naturally occurring SO₄²⁻.

This analysis report demonstrates that, to the extent that microbial SO₄²⁻ reduction delays or prevents methanogenesis, carbonate precipitation would compensate to a large extent for the effect on the MgO excess factor of additional SO₄²⁻ reduction using naturally occurring SO₄²⁻ in the DRZ. We thank Dr. Judith Wright of Carlsbad, NM, for her suggestion that consumption of CO₂ by carbonate minerals would affect the MgO excess factor in this manner.

A memorandum is being prepared to provide information on the following aspects of the geochemical behavior of MgO in the WIPP that could affect the excess factor: (1) the concentrations of the main reactive phase in MgO from two of the three vendors that have supplied this material to the DOE, (2) our expectation as to how much of this phase will actually react with CO₂, (3) the number of moles of CO₂ that will be consumed per mole of MgO emplaced in the repository, and (4) the likelihood of and extent to which CO₂ will be consumed by other materials.

2 BACKGROUND

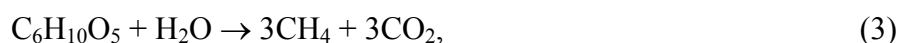
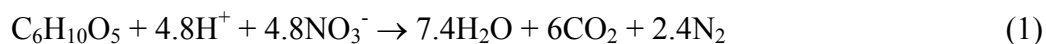
The DOE is emplacing MgO in the WIPP to serve as the engineered barrier by decreasing the solubilities of the actinide elements in transuranic (TRU) waste, such as uranium, thorium, neptunium, and plutonium. MgO will decrease actinide solubilities by consuming CO₂ that could be produced by microbial consumption of CPR materials in the TRU waste or waste containers in the repository and by controlling the pH of any brine present.

In this memorandum, “MgO” refers to the bulk, granular material being emplaced in the WIPP to serve as the engineered barrier. MgO comprises mostly periclase (pure, crystalline MgO – the main reactive constituent of the engineered barrier), which will consume CO₂ and water (H₂O) and form brucite (Mg(OH)₂) hydromagnesite (Mg₅(CO₃)₄(OH)₂·4H₂O), and – eventually - magnesite (MgCO₃). The terms “periclase,” “brucite,” “hydromagnesite,” and “magnesite” are mineral names and should, therefore, be restricted to naturally occurring forms of materials that meet all other requirements of the definition of a mineral (see, for example, Bates and Jackson 1984). However, mineral names are used herein for convenience.

MgO will decrease actinide solubilities by consuming essentially all carbon dioxide (CO₂) that would be produced by microbial consumption of all CPR materials in TRU waste or waste containers in the repository. Although MgO will consume nearly all CO₂, small quantities (relative to the quantity that would be produced by microbial consumption of all CPR materials) will persist in the aqueous and gaseous phases. The residual quantity will be so small relative to the initial quantity that the adverb “essentially” is omitted hereafter in this memorandum.

The excess factor is the ratio of the total amount of MgO to be emplaced in the WIPP divided by the total amount required to consume all CO₂ that would be produced by microbial consumption of all CPR materials in the repository, calculated as specified by the EPA (Marcinowski, 2004).

Hansen et al. (2004) and the U.S. DOE (2004, Appendix BARRIERS) concluded, based on the TRU waste inventory available at the time of the first WIPP Compliance Recertification Application (CRA-2004 PA) and results from the long-term laboratory study of microbial gas generation at Brookhaven National Laboratory, that microbial denitrification, SO₄²⁻ reduction, and fermentation and methanogenesis,



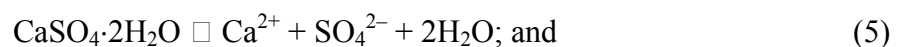
would consume 4.72, 0.82, and 94.46%, respectively, of the CPR materials in the repository in the event of microbial consumption of all CPR materials. Furthermore, the overall CO₂ yield would be 0.528 mol of CO₂ per mol of organic C consumed. This is because: (1) the CO₂ yields

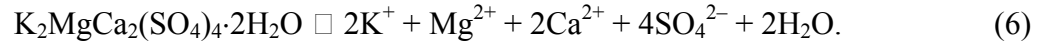
are 1 mol of CO₂ per mol of organic C consumed by denitrification (Reaction 1) and SO₄²⁻ reduction (Reaction 2), and 0.5 mol of CO₂ per mol of C from methanogenesis (Reaction 3); and (2) the total quantity of CPR materials in the repository greatly exceeds the quantities of NO₃⁻ and SO₄²⁻ in the waste. This was also the case at the time of the WIPP Compliance Certification Application (CCA) (U.S. DOE, 1996) and the 1997 Performance Assessment Verification Test (PAVT), and is still the case with the inventory used for the Performance Assessment Baseline Calculations (PABC). Based on the PABC inventory (Crawford, 2005a; 2005b), denitrification, SO₄²⁻ reduction, and methanogenesis would consume 4.89, 0.84, and 94.27%, respectively, of the CPR materials in the repository in the event of consumption of all CPR materials; and the overall CO₂ yield would be 0.529 mol of CO₂ per mol of organic C.

However, the EPA questioned whether “sulfate available in the anhydrite (CaSO₄) marker beds and repository fluids ... would or would not be expected to confound this methanogenesis” (Marcinowski, 2003, Enclosure 1, Issue 7). This issue is central to the MgO excess factor, because: (1) the CO₂ yield from methanogenesis (0.5 mol of CO₂ per mol of organic C) is half that from denitrification and SO₄²⁻ reduction (1 mol of CO₂ per mol of C); (2) the amount of MgO required to consume the CO₂ that would be produced from microbial consumption of all CPR materials via denitrification (4.89%), SO₄²⁻ reduction (0.84%), and methanogenesis (94.27%) is 52.9% of the amount required to consume the CO₂ that would be produced from denitrification (4.89%) and SO₄²⁻ reduction (95.11%) without methanogenesis; and (3) the MgO safety factor calculated including methanogenesis is almost twice that calculated without methanogenesis.

Kanney et al. (2004) analyzed of the effects of naturally occurring SO₄²⁻ on the MgO excess factor. They concluded, based on conservative assumptions, that advective transport of SO₄²⁻ from the underlying Castile Fm. in the event of human intrusion, and diffusive transport of SO₄²⁻ from the surrounding Salado would not preclude methanogenesis. However, the EPA required that the DOE “maintain the current 1.67 MgO safety factor ... calculated assuming all [C] could be converted to [CO₂],” because “DOE’s analysis may be correct ... [but] more [SO₄²⁻] may be present in the waste or the waste area environment than currently estimated” (Marcinowski, 2004, p. 3 and Enclosure).

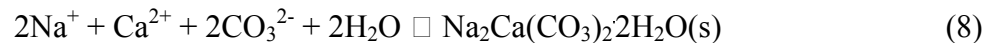
Diffusive transport of SO₄²⁻ from the Salado to the disposal rooms – if it occurs to a significant extent – would occur because microbial SO₄²⁻ reduction would consume the SO₄²⁻ in the waste and in brines in contact with the waste via Reaction 2 (see above), thereby creating a concentration gradient from the DRZ to the waste. If SO₄²⁻ diffuses from the DRZ through saturated voids to the waste, the dissolved SO₄²⁻ concentrations in the DRZ would decrease. However, this decrease would result in dissolution of SO₄²⁻-bearing minerals such as anhydrite, gypsum (CaSO₄·2H₂O), and polyhalite (K₂MgCa₂(SO₄)₄·2H₂O), present in both the marker beds and the nearly pure halite (NaCl) in the Salado, via the reactions:





Clearly, dissolution of anhydrite and other SO_4^{2-} -bearing minerals would yield abundant Ca^{2+} if microbes use naturally occurring SO_4^{2-} to a significant extent after consuming all SO_4^{2-} in the waste.

The Ca^{2+} released by Reactions 4, 5, and 6 would consume CO_2 by precipitating calcite (CaCO_3), metastable polymorphs of calcite, hydrated CaCO_3 , or minerals such as pirssonite ($\text{Na}_2\text{Ca}(\text{CO}_3)_2 \cdot 2\text{H}_2\text{O}$):



Reaction 7 could produce calcite because it is the stable Ca^{2+} -bearing phase in systems containing CO_2 at ambient temperatures (Butler, 1982; Stumm and Morgan, 1996). Furthermore, calcite is known to precipitate rapidly at low temperatures in many natural environments, which accounts for the fact that it is the solubility-controlling phase for Ca^{2+} in natural waters containing CO_2 (see, for example; Stumm and Morgan, 1996).

However, inorganic elements and compounds, and organic ligands known to inhibit or suspected of inhibiting the precipitation of calcite by decreasing the rate at which it nucleates and grows will be present in WIPP brines. Therefore, Reaction 7 will could also produce metastable polymorphs of calcite such as aragonite and vaterite, amorphous CaCO_3 ($\text{CaCO}_3(\text{am})$), and hydrated phases such as monohydrocalcite ($\text{CaCO}_3 \cdot \text{H}_2\text{O}$) and ikaite ($\text{CaCO}_3 \cdot 6\text{H}_2\text{O}$).

Our simulations also predicted that Reaction 8 would also produce pirssonite in most cases, although it did not consume as much CO_2 as Reaction 7.

Consumption of CO_2 by precipitation of carbonates would in turn reduce the quantity of MgO required to consume all CO_2 produced by complete microbial consumption of CPR materials. Carbonate precipitation would in turn increase the MgO excess factor to values close to those calculated previously based on the prediction that methanogenesis would be the dominant microbial reaction in the WIPP.

3 CALCULATIONS

We used the reaction-path code EQ6 (Wolery and Daveler, 1992) to simulate the precipitation of carbonate minerals caused by reaction of microbial CO_2 with Ca^{2+} from the dissolution of anhydrite, gypsum, and polyhalite resulting from the drawdown of SO_4^{2-} in the DRZ by microbial SO_4^{2-} reduction in WIPP disposal rooms. EQ6 is part of the EQ3/6 geochemical software package (Daveler and Wolery, 1992; Wolery, 1992a; 1992b; Wolery and Daveler, 1992).

We then used the results of the EQ6 reaction-path simulations to calculate: (1) the quantity of magnesite (or hydromagnesite) produced during each phase of the microbial consumption of CPR materials, and the total quantity of magnesite (or hydromagnesite) formed after consumption of all CPR materials; (2) the quantities of carbonate minerals produced during each phase of microbial activity, and the total quantity formed; and (3) the effective yields of CO_2 per mole of organic C in CPR materials consumed during each phase of microbial activity, and the overall effective yields.

We determined the effects of the following factors on brine composition, the quantities of carbonate minerals produced, and the effective yield of CO_2 per mole of organic C: (1) the initial brine composition and the brine volume, (2) whether carbonation of brucite produces magnesite or hydromagnesite, (3) the effects of organic ligands, and (4) the effects of precipitation of $\text{CaCO}_3(\text{am})$ instead of calcite. Table 2 provides a description of the simulations that we carried out to quantify the effects of these factors.

3.1 Reaction-Path Calculations

We simulated the precipitation of carbonate minerals by carrying out the following sequential reaction-path calculations with EQ6: (1) reaction of WIPP brines with brucite and the minerals in the DRZ surrounding the repository (referred to herein as “Step 1”); and (2) consumption of CPR materials by microbial SO_4^{2-} reduction (see Reaction 2 above); dissolution of anhydrite, gypsum, and polyhalite (Reactions 4, 5, and 6 above); and consumption of CO_2 by calcite or $\text{CaCO}_3(\text{am})$ (Reaction 7) and (in most cases) pirssonite (Reaction 8) (referred to as “Step 2”).

We used sequential EQ6 calculations (Steps 1 and 2 above) to be consistent with the conceptual models for WIPP near-field chemistry and their implementation in WIPP PA (U.S. DOE, 1996, Chapter 6 and Appendices BARRIERS, MASS, and SOTERM; U.S. EPA, 1997; 1998a). According to the conceptual model for chemical conditions in the repository, it is assumed that many reactions will reach equilibrium instantaneously and reversibly throughout a domain in which all components are well mixed and homogeneously distributed. In particular, it has been assumed for the CCA, PAVT, CRA-2004 PA, and PABC that (most) reactions among Salado and Castile brines, the MgO engineered barrier, and major Salado minerals are fast relative to the 10,000-year regulatory period, thereby allowing the use of

thermodynamic models implemented in codes such as EQ3/6 and Fracture-Matrix Transport (FMT) (Babb and Novak, 1997 and addenda; Wang, 1998) to predict equilibrium conditions in the repository. Of course, there are some exceptions to the assumption of instantaneous equilibrium in modeling these reactions. For example, the EPA has specified since 1997 that we use the brucite-hydromagnesite carbonation reaction to buffer the fugacity of CO_2 (f_{CO_2}) for the actinide-solubility calculations for WIPP PA instead of using the brucite-magnesite reaction. The EPA has specified this exception because of concern that metastable hydromagnesite might not dehydrate to form stable magnesite to a significant extent during the 10,000-year regulatory period (Trovato, 1997; U.S. EPA, 1998b).

On the other hand, the conceptual model for gas generation also acknowledges that some reactions will proceed at experimentally measured rates that are much slower than those assumed to occur instantaneously. These include anoxic corrosion of steels and other iron-base (Fe-base) alloys, which will produce hydrogen (H_2); and microbial consumption of CPR materials, which will produce mainly CO_2 and methane (CH_4) with lesser amounts of nitrogen (N_2) and hydrogen sulfide (H_2S) (see Reactions 1-3 above). Abstracted versions of anoxic corrosion of Fe-base metals and microbial consumption of CPR materials are incorporated in BRAGFLO using ranges of rates based on WIPP-relevant experimental studies (Nemer and Stein, 2005). The effective rates of these gas-generation reactions in BRAGLO are typically even slower than the experimentally measured rates because they cannot occur unless water is present in brine or, in the case of microbial activity, in the gaseous phase. Anoxic corrosion and microbial activity have not been included explicitly in geochemical modeling with EQ3/6 or FMT to date because of code limitations. However, the effects of microbial activity have been included to some extent by incorporation of thermodynamic data for the $\text{MgO-CaO-H}_2\text{O-CO}_2$ system in these models.

Sequential execution of Steps 1 and 2 above recognized the differences in the rates of these reactions and was consistent with their implementation in PA (i.e., BRAGFLO). However, after brine reached equilibrium with brucite and the DRZ minerals in Step 1, we constrained it to remain in equilibrium with these minerals throughout Step 2.

We ran Step 1 by titrating brucite, halite, anhydrite, gypsum, polyhalite, and magnesite (or hydromagnesite) into brine until the system reached equilibrium. Brucite simulated the engineered barrier; halite, anhydrite, gypsum, polyhalite, and magnesite (or hydromagnesite) represented the DRZ minerals.

We then ran Step 2 by titrating -2H^+ , $-\text{SO}_4^{2-}$, and $+2\text{CO}_2$ into brine to simulate SO_4^{2-} reduction (Reaction 2). Titration of -2H^+ and $-\text{SO}_4^{2-}$ into the brine simulated the use of these components by the community of microorganisms responsible for SO_4^{2-} reduction; titration of CO_2 into the system simulated the production of this gas by these microbes. We had to simulate SO_4^{2-} reduction indirectly by titrating in -2H^+ , $-\text{SO}_4^{2-}$, and $+2\text{CO}_2$ because this and other microbial reactions are not included in EQ3/6 yet. We did not titrate $\text{C}_6\text{H}_{10}\text{O}_5$ out of the system or include it in the solid phase assemblage. We did not titrate H_2O into the system because we do not think that SO_4^{2-} reduction actually produces H_2O ; instead, consumption of H_2O by hydrolysis of the cellulose molecules in the waste prior to the onset of Reactions 1 and 2 probably consumes as much H_2O as Reactions 1 and 2 produce. Furthermore, we did not titrate

H₂S into the system because there are no Pitzer ion-interaction parameters for dissolved H₂S species, and because corrosion of steels and other Fe-base alloys will probably consume H₂S as fast as it is produced.

We did not force EQ6 to dissolve anhydrite, gypsum, and polyhalite in response to the drawdown of SO₄²⁻ by Reaction 2. Instead, the code predicted that these minerals would dissolve. Furthermore, we did not force calcite precipitation; the code predicted that this would occur in response to the build-up of Ca²⁺ and CO₂.

3.2 Compositions of Brines and Solids

For this analysis, we used: (1) two brines to determine the sensitivity of our results to the composition of the aqueous phase; (2) one solid phase to represent uncarbonated MgO, and two solids for its carbonation product; and (3) a mineralogical composition typical of the Salado at or near the stratigraphic horizon of the repository, along with other possible compositions to determine whether enough SO₄²⁻-bearing minerals would be available in the DRZ for significant calcite precipitation.

3.2.1 Brines

Generic Weep Brine (GWB) and Energy Research and Development Administration (WIPP Well) 6 (ERDA-6) were used to simulate WIPP brines in this analysis. Snider (2003) established GWB as a standard Salado brine based on the average composition of intergranular fluids collected from the stratigraphic horizon of the repository by Krumhansl et al, (1991). ERDA-6, the average composition of samples collected from that well by Popielak et al. (1983), is typical of fluids from brine reservoirs in the Castile Fm. Both of these brines have been used extensively for laboratory and modeling studies of WIPP chemistry.

Table 3 provides the initial compositions of GWB and ERDA-6 and their predicted compositions after reaction with brucite, hydromagnesite, halite, and anhydrite (Brush, 2005). These calculations were carried out for the CRA-2004 PABC.

Section 5 describes the compositions of these brines after reaction with brucite, halite, anhydrite, gypsum, polyhalite, and magnesite (or hydromagnesite) (Step 1 in Subsection 3.1 above); and after SO₄²⁻ reduction, dissolution of anhydrite, gypsum, and polyhalite, and precipitation of calcite and magnesite (or hydromagnesite) (Step 2 in Subsection 3.1).

3.2.2 MgO

We used brucite to simulate uncarbonated MgO in this analysis. We did not use periclase because the hydration of this phase to form brucite could have consumed all H₂O and terminated our simulations prior to microbial consumption of all CPR materials. The use of brucite as a reactant instead of periclase is consistent with previous geochemical modeling.

We used both magnesite and hydromagnesite to simulate carbonated MgO. A separate analysis report that is being prepared will demonstrate that it is likely that essentially all thermodynamically metastable hydromagnesite will convert to stable magnesite during the 10,000-year regulatory period, because the rate of conversion of hydromagnesite to magnesite is rapid relative to the microbial CO₂ production rate (Vugrin et al., 2006, Subsection 7.1). However, we carried out one simulation in which we assumed that hydromagnesite will persist indefinitely instead of dehydrating to form magnesite. This run was necessary to determine the sensitivity of our results to which Mg carbonate formed by carbonation of brucite (hydromagnesite or magnesite), and to perform a simulation consistent with the EPA specification that we assume that hydromagnesite will persist indefinitely instead of forming magnesite for predictions of the conditions used to calculate actinide solubilities (Trovato, 1997; U.S. EPA, 1998b). For this run, constraints imposed by EQ6 necessitated substitution of hydromagnesite for magnesite in our Salado mineral assemblage (see Subsection 3.1.3 below).

Xiong (2004) incorporated two similar forms of hydromagnesite ($\text{Mg}_4(\text{CO}_3)_3(\text{OH})_2 \cdot 3\text{H}_2\text{O}$ and $\text{Mg}_5(\text{CO}_3)_4(\text{OH})_2 \cdot 4\text{H}_2\text{O}$), and four other solid phases (CaO, MgCl₂, MgO and MgSO₄), into the EQ3/6 database (see Section 4 below). In many of our analysis plans, analysis reports, presentations, and publications, we have referred to hydromagnesite ($\text{Mg}_4(\text{CO}_3)_3(\text{OH})_2 \cdot 3\text{H}_2\text{O}$) and hydromagnesite ($\text{Mg}_5(\text{CO}_3)_4(\text{OH})_2 \cdot 4\text{H}_2\text{O}$) as “hydromagnesite (4323)” and “hydromagnesite (5424),” respectively. Although both of these forms of hydromagnesite are now in the EQ3/6 and FMT databases, these codes have always predicted that hydromagnesite (5424) will form under expected WIPP conditions instead of hydromagnesite (4323) if we suppress magnesite (i.e., prevent the more stable magnesite from forming at the expense of hydromagnesite (5424) by switching off magnesite in the input file). This is because hydromagnesite (5424) has a lower free energy of formation and hence a lower solubility product than hydromagnesite (4323). Furthermore, we have consistently observed hydromagnesite (5424) in laboratory studies of the carbonation of MgO under expected WIPP conditions, but we have never observed hydromagnesite (4323). Therefore, we will use “hydromagnesite” to refer to “hydromagnesite (5424)” throughout the remainder of this analysis report.

3.2.3 Salado Minerals

We used a Salado mineralogical composition of 93.2 wt % halite and 1.7 wt % each anhydrite, gypsum, magnesite, and polyhalite for these simulations. Brush (1990, pp. 80-81) used the results of Stein (1985) to establish this mineralogical composition for the Salado at or near the stratigraphic horizon of the repository for use in geochemical modeling studies. Stein (1985) studied the mineralogy of two 50-ft, vertical cores drilled through the back and floor of Test Room 4. She sampled each core at intervals of “approximately every other foot along the length of the cores.” From the results in Stein (1985, Table 1) it is clear that these samples included both the nearly pure halites and the marker beds. However, it is not clear whether Stein (1985) sampled the cores randomly. Stein (1985) determined the concentrations of halite, quartz (SiO₂), and clay minerals gravimetrically (i.e., by weighing the water-insoluble and ethylenediaminetetraacetic acid-insoluble (EDTA-insoluble) residues, respectively). Therefore, the uncertainties in the concentrations of halite (93.2 wt %) and of quartz and clays (0.64 wt %) are probably smaller than those associated with anhydrite, gypsum, magnesite, and polyhalite,

which Stein (1985) identified by routine X-ray diffraction (XRD) analysis. However, it should be noted that Brush (1990, p. 80) calculated a mean of 93.23 wt % for halite from Stein (1985, Table 1), not the value of 94.44 wt % reported by Stein (1985, p. 16). Brush (1990, p. 81) then neglected the quartz and clays in the rock because geochemical models did not (and, in the case of EQ3/6 and FMT, still do not) include Pitzer parameters for Al and Si. He thus assumed that anhydrite, gypsum, magnesite, and polyhalite constitute the entire water-insoluble residue of 6.8 wt %. Furthermore, he assumed the concentrations of these four minerals are equal (1.7 wt % each), because Stein (1985) did not use a quantitative XRD technique in her study. Brush (1990, p. 81) reported that the Salado comprises 93.2 wt % halite and 1.7 wt % each anhydrite, gypsum, magnesite, and polyhalite; and stated that “this estimate [of 1.7 wt % each] is probably not accurate to more than one significant figure.” Given the uncertainties inherent in sampling and routine XRD analysis, it would probably be reasonable to estimate that, for this analysis, the Salado consists of about 90-95 wt % halite and about 1-3 wt % each of anhydrite, gypsum, magnesite, and polyhalite.

We considered the effects of varying the proportions of these minerals to determine the sensitivity of our results to the mineralogical composition of the Salado. For this test, we used compositions of 88 wt % halite and 3 wt % each of anhydrite, gypsum, magnesite, and polyhalite; and 96 wt % halite and 1 wt % each of anhydrite, gypsum, magnesite, and polyhalite.

In one set of EQ6 runs, it was necessary to use an alternative Salado mineralogical composition of 93.2 wt % halite and 1.7 wt % each anhydrite, gypsum, hydromagnesite, and polyhalite. Substitution of hydromagnesite for magnesite in Step 1 of the sequential EQ6 calculations was necessary to specify that carbonation of brucite in Step 2 produce hydromagnesite (see Subsection 3.1.2 above).

3.3 Brine Volumes

We used a wide range of brine volumes for this analysis to determine the sensitivity of our results to this parameter and to simulate the large differences in the volumes of Salado and Castile brines that could be present in the WIPP.

To select these volumes, we considered the quantities of brines that could be present in a seven-room WIPP panel. This is consistent with PA (i.e., BRAGFLO), which uses a panel as the basis for its calculations (Nemer and Stein, 2005). In the case of the minimum brine volume (see Subsection 3.1.2.1 below), we multiplied a volume established for the repository by 0.1044 to scale it down to a seven-room panel. We multiplied this volume by 0.1044 instead of 0.1 because the volume of the eight seven-room panels is slightly larger than the two equivalent panels in the access drifts (Lappin et al, 1989).

3.3.1 Minimum Volume

We selected Stein’s (2005) volume of 10,011 m³ for the minimum brine volume. This value, “a reasonable minimum volume of brine in the repository required for a brine release” Stein (2005), was used to calculate the concentrations of acetate, citrate, EDTA, and

oxalate for the PABC actinide-solubility calculations (Brush and Xiong, 2005a; 2005b; Brush 2005). We multiplied $10,011 \text{ m}^3$ by 0.1044 (see Subsection 3.1 above) and obtained a minimum volume of $1,045 \text{ m}^3$ of brine in one seven-room panel. We used this volume for both GWB and ERDA-6 because it is possible that this volume of ERDA-6 could also be present in a panel.

Stein (2005) used BRAGFLO results from the CRA-2004 PA to obtain a minimum brine volume of $10,011 \text{ m}^3$ for the PABC. This was because the actinide solubility calculations had to be completed by the time the BRAGFLO calculations were completed to expedite the execution of a complete WIPP PA. This value is now out of date because Nemer and Stein (2005) reran BRAGFLO for the PABC. Therefore, Clayton (2006) updated Stein's (2005) analysis by repeating it using the BRAGFLO results from the PABC. Clayton (2006) obtained a revised minimum brine volume of $13,746 \text{ m}^3$ for the repository; multiplication of $13,746 \text{ m}^3$ yielded a minimum brine volume of $1,435 \text{ m}^3$ for a seven-room panel. However, we did not use this revised volume because it is only about 37.3 % greater than the minimum volume of $1,045 \text{ m}^3$ and would not have introduced a wide enough range of volumes. However, Clayton's (2006) revised minimum brine volume of $13,746 \text{ m}^3$ could be used to recalculate the concentrations of organic ligands for future actinide-solubility calculations.

3.3.2 Intermediate Volume

For the intermediate brine volume, we selected the maximum volume of GWB that was present in a seven-room panel at one time according to the BRAGFLO results obtained for the PABC (Clayton, 2006). This volume, $7,763 \text{ m}^3$, was present in the panel at 10,000 years, and was obtained from Scenario 5 (an E2 intrusion at 1,000 years), Replicate 2, Vector 53 (see Clayton, 2006, Table 3). Again, we used this volume for both GWB and ERDA-6 because it is possible that this volume of ERDA-6 could also be present in a panel.

3.3.3 Maximum Volume

We used a volume of $13,267 \text{ m}^3$ of brine for a panel for the maximum brine volume. This was the largest volume of ERDA-6 that was present at one time in a seven-room panel. It occurred at 354 years in Scenario 2, Replicate 1, Vector 93 (Clayton, 2006, Table 3). It was used only for ERDA-6 because it greatly exceeded the largest volume of GWB that was present at one time ($7,763 \text{ m}^3$).

3.4 Quantities of Solids

We used spreadsheet calculations to determine: (1) the quantity of organic C remaining in CPR materials after microbial denitrification and SO_4^{2-} reduction using SO_4^{2-} in the waste; (2) the quantity of brucite remaining at that time; (3) the quantities of halite, anhydrite, gypsum, polyhalite, and magnesite present in the DRZ; and (4) the quantities of these minerals that would be required to provide enough naturally occurring SO_4^{2-} for microbes to consume all CPR materials remaining after denitrification and SO_4^{2-} reduction using SO_4^{2-} in the waste. These spreadsheets are contained in the file entitled "Calcite.xls," which is included in

the records package for this analysis and which can be obtained from the SNL/WIPP Records Center.

3.4.1 CPR Materials

We used the quantities of CPR materials to be emplaced in the WIPP and the quantities of NO_3^- and SO_4^{2-} in the waste provided by Crawford (2005a, 2005b) for the CRA-2004 PABC to calculate that: (1) the total quantity of organic C in the CPR materials to be emplaced in the WIPP will be about 1.10×10^9 mol; (2) microbial denitrification and SO_4^{2-} reduction using SO_4^{2-} in the waste would consume about 4.89 and 0.84%, respectively, of the CPR materials in the repository (see Section 2 above); and (3) these processes would decrease the quantity of organic C remaining in CPR materials from its initial value 1.10×10^9 mol to 1.03697×10^9 mol, or about 1.04×10^9 mol. These results are consistent with the CRA-2004 PABC.

3.4.2 MgO

To calculate the quantity of brucite (hydrated periclase) initially present in the WIPP, we assumed that a total of 1.2 mol brucite/mol organic C will be emplaced in the repository and multiplied 1.2 mol MgO/mol organic C $\times 1.10 \times 10^9$ mol organic C to obtain 1.32×10^9 mol of brucite. We used brucite instead of periclase to simulate uncarbonated MgO because the hydration of periclase to form brucite could have consumed all water and terminated our runs prior to microbial consumption of all CPR materials. We used an MgO excess factor of 1.2 instead of 1.67 to be consistent with other analyses supporting the DOE response to the EPA request that all uncertainties related to the MgO excess factor be described and that their effects be included to the extent possible.

We then decreased the initial quantity of brucite by subtracting the quantity that would be converted to magnesite by CO_2 from microbial denitrification and SO_4^{2-} reduction using SO_4^{2-} in the waste, which would consume 4.89 and 0.84%, respectively, of the CPR materials in the repository (see Section 2). We thus subtracted $(0.0489 + 0.0084) \times 1.10 \times 10^9$ mol organic C $\times 1$ mol CO_2 /mol organic C $\times 1$ mol brucite/mol $\text{CO}_2 = 0.06303$ mol $\times 10^9$ mol brucite from 1.32×10^9 mol of brucite to obtain about 1.25697×10^9 mol brucite, or about 1.26×10^9 mol, present at the start of SO_4^{2-} reduction using naturally occurring SO_4^{2-} .

3.4.3 Salado Minerals

We assumed that the DRZ comprises all rock in the four BRAGFLO computational grid cells above the disposal rooms and the three cells below the rooms. This is identical to the DRZ used for the CRA-2004 PABC (Nemer and Stein, 2005). The thickness of the upper DRZ is about 11.9 m; the thickness of the lower DRZ is 2.23 m. The waste area of the repository (the total surface area of the rooms and access drifts in which waste will be emplaced) is about 1.12×10^5 m² (Lappin et al, 1989). We multiplied the total thickness of the upper and lower DRZ by the waste area and obtained a total volume of about 1.58×10^6 m³ for the DRZ above and below the waste area.

We used the Salado mineralogical composition of 93.2 wt % halite and 1.7 wt % each anhydrite, gypsum, magnesite, and polyhalite (Subsection 3.1.3); the molecular weights of these minerals, and a density of $2,180 \text{ kg/m}^3$ for the Salado from the PA parameter database (Hansen et al., 2003) to calculate that the DRZ contains about $3.48 \times 10^4 \text{ mol/m}^3$ halite, $2.72 \times 10^2 \text{ mol/m}^3$ anhydrite, $2.15 \times 10^2 \text{ mol/m}^3$ gypsum, $6.15 \times 10^1 \text{ mol/m}^3$ polyhalite, and $4.39 \times 10^2 \text{ mol/m}^3$ magnesite. Therefore, the total (solid-phase) SO_4^{2-} content of the DRZ is $7.33 \times 10^2 \text{ mol/m}^3$, and the total quantity of SO_4^{2-} in the DRZ is $1.58 \times 10^6 \text{ m}^3 \times 7.33 \times 10^2 \text{ mol/m}^3 = 1.16 \times 10^9 \text{ mol}$.

The quantity of naturally occurring SO_4^{2-} required for microbial consumption of the CPR materials remaining after denitrification and SO_4^{2-} reduction using SO_4^{2-} in the waste is $5.18485 \times 10^8 \text{ mol}$, or about $5.18 \times 10^8 \text{ mol}$. We obtained this result by halving $1.03697 \times 10^9 \text{ mol}$ organic C, the quantity of organic C remaining after denitrification and SO_4^{2-} reduction using SO_4^{2-} in the waste. Multiplication of this quantity of organic C by 0.5 is consistent with the overall reaction for SO_4^{2-} reduction (Reaction 2), during which microbes consume 0.5 mol SO_4^{2-} /mol organic C.

Finally, the quantity of naturally occurring SO_4^{2-} required for microbial consumption of the CPR materials remaining after denitrification and SO_4^{2-} reduction using SO_4 in the waste ($5.18 \times 10^8 \text{ mol}$) is about 44.7% of the solid-phase SO_4 in the DRZ used for the CRA-2004 PABC.

3.5 Scaling of Brine Volumes and Masses of Solids for EQ6 Input Files

EQ6 allows the user to specify the composition of the aqueous phase present at the start of a simulation. However, the code calculates the initial volume of this fluid by assuming that exactly 1 kg of H_2O is present and using the specific gravity specified by the user. Therefore, we scaled down the volumes of brine described in Subsection 3.1.2 by scaling down the masses of H_2O in these brines to 1 kg of H_2O for our EQ6 input files. We then used the same scaling factor to reduce the masses of solids (see Calcite.xls).

The following example illustrates our approach. We used the chemical composition of GWB before reaction with brucite, hydromagnesite, halite, and anhydrite (see Table 3) and a specific gravity of 1.2321 kg/L of GWB to calculate that there are 0.3617108 kg solids/L GWB and, by subtraction of 0.3617108 kg solids/L GWB from 1.2321 kg solids and H_2O /L GWB, 0.8703892 kg H_2O /L GWB. We used a specific gravity of 1.2321 kg/L for GWB instead of 1.2 kg/L (the value in Table 3) because we concluded that the former value, from the output file from FMT Run 7 for the CRA-2004 PABC, is a better estimate than the latter value, which was measured for Brine A and assigned to GWB by analogy because both Brine A and GWB are Salado brines. The volume of GWB that contains 1 kg H_2O is then $1 \text{ kg } \text{H}_2\text{O} \div 0.8703892 \text{ kg } \text{H}_2\text{O}/\text{L GWB} = 1.148911 \text{ L}$, or about 1.15 L. The minimum volume of GWB that we used, $1.0011 \times 10^4 \text{ m}^3$ (Subsection 3.1.2.1), contains $1.0011 \times 10^7 \text{ L GWB}$. The scaling factor is then $1.045 \times 10^6 \div 0.1044 \text{ L of GWB/repository} \div 1.148911 \text{ L GWB/EQ6} = 8.7122 \times 10^6$, or about 8.17×10^6 .

Tables 5-15 provide various EQ6 input parameters scaled to the repository, a seven-room panel, and the EQ6 input files. These include: (1) the volumes of brine and the masses of the solutes and solvent in these brines; (2) the masses and volumes of rock in the DRZ, the moles of SO_4^{2-} in the DRZ, and the moles of anhydrite, gypsum, magnesite, and polyhalite in DRZ minerals required to simulate SO_4^{2-} reduction using SO_4^{2-} in the DRZ; and (3) the moles of organic C in CPR materials, brucite in the MgO engineered barrier, and CO_2 produced by microbial SO_4^{2-} reduction using SO_4^{2-} in the DRZ.

3.6 Organic Ligands

Organic ligands in the TRU waste being emplaced in the WIPP could affect equilibria among brines and carbonate minerals. After considering the potential effects of acetate, citrate, EDTA, and oxalate on carbonate equilibria (e.g., precipitation of calcite, amorphous CaCO_3 , or pirssonite), we concluded that acetate and EDTA would not have a significant effect, but that citrate and oxalate might. Because we concluded that citrate and oxalate might affect carbonate equilibria, we included them in some of our simulations. The justification for excluding acetate and EDTA from and including citrate and oxalate in our EQ6 simulations is described below (see Subsections 3.5.1 and 3.5.2, respectively).

3.6.1 Justification for Excluding Acetate and EDTA

Apelblat and Manzurola (1999) measured the solubility of the solid Ca acetate, $(\text{Ca}(\text{CH}_3\text{CO}_2)_2)$ via the reaction:



In this equation, CH_3CO_2^- is acetate, the deprotonated form of acetic acid ($\text{CH}_3\text{CO}_2\text{H}$). They determined an equilibrium concentration (solubility) of 2.1738 m. The ionic strength of the resulting solution was 6.5214 m. Loos et al. (2004) also studied the solubility of $\text{Ca}(\text{CH}_3\text{CO}_2)_2$ in water; they determined an equilibrium concentration of 2.166 m, with an ionic strength of 6.498 m. Assuming stoichiometric dissolution of $\text{Ca}(\text{CH}_3\text{CO}_2)_2$ and that the concentrations of Ca^{2+} and acetate are equal to their activities (i.e. unit activity coefficients), then the concentration of Ca^{2+} and CH_3CO_2^- in solution should be at least 2.166 m and 4.332 m, respectively, for $\text{Ca}(\text{CH}_3\text{CO}_2)_2$ to precipitate. However, Brush and Xiong (2005b) estimated a total dissolved acetate concentration of 1.06×10^{-2} M for WIPP brines, and the FMT calculations for the PABC predicted CH_3CO_2^- concentrations of 6.54×10^{-3} m in GWB and 7.92×10^{-3} m in ERDA-6 (Brush, 2005, Runs 7 and 11, respectively). Because these estimated and predicted CH_3CO_2^- concentrations are orders of magnitude lower than that required for precipitation of $\text{Ca}(\text{CH}_3\text{CO}_2)_2$, we screened out the possibility of precipitation of $\text{Ca}(\text{CH}_3\text{CO}_2)_2$ and concluded that precipitation of this solid would not affect carbonate equilibria (e.g., precipitation of calcite or other carbonates). Therefore, we did not include solid or dissolved acetate species in our EQ6 calculations.

It is important to note that the assumption of unit activity coefficients is conservative because the predicted activity coefficients from the EQ6 calculations are less than unity.

For example, in PABC Run 7 the activity coefficient for Ca^{2+} is 0.9135 and that of CH_3CO_2^- is 0.5575 (Brush, 2005). Since the activity coefficients are less than 1.0, the activities of the ions would be less than their concentrations. Therefore, the required equilibrium concentrations would need to be even larger for precipitation of $\text{Ca}(\text{CH}_3\text{CO}_2)_2$.

Fiorucci et al. (2002) measured a value of 7.027×10^{-3} M for the solubility of CaH_2EDTA via the reaction:



In this equation, $\text{H}_2\text{EDTA}^{2-}$ is one of the deprotonated forms of EDTA. The solubility product constant for this phase at infinite dilution can be estimated using the activity coefficients determined with the Davies equation (Davies, 1962):

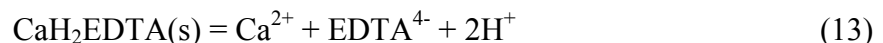
$$\log \gamma_i = -A_\gamma z_i^2 \left(\frac{\sqrt{I_m}}{1 + \sqrt{I_m}} + 0.3I_m \right) \quad (11)$$

in which A_γ has a value of 0.5102 and the ionic strength of the solution is equal to 0.0281 M. Assuming the stoichiometric dissolution of CaH_2EDTA and logarithmic (\log) γ values of -0.310, as calculated with Equation 11, the $\log K_{\text{sp}}$ of reaction 10 at infinite dilution is -4.926.

The ionic complex, $\text{H}_2\text{EDTA}^{2-}$, will further dissociate in solution via the reaction:



The dissociation constant of Reaction 12 is calculated to be -17.4498 according to the dimensionless standard chemical potentials from FMT_050405.CHEMDAT (Xiong, 2005) for the species shown in Reaction 12. The combination of Reactions 10 and 12 gives the following total dissolution reaction:



The equilibrium constant for Reaction 13 is obtained by adding the $\log K_{\text{sp}}$ for Reactions 10 and 12, which yields -22.376 in logarithmic units. The $\log K_{\text{sp}}$ for Reaction 13 is described with the following equation:

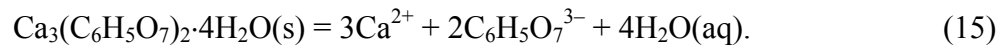
$$\log K_{\text{sp, CaH}_2\text{EDTA}} = -22.376 = \log ([\text{Ca}^{2+}][\text{EDTA}^{4-}][\text{H}^+]^2) \quad (14)$$

in which the brackets ($[\]$) signify the activities of the enclosed species. Assuming the stoichiometric dissolution of CaH_2EDTA and unit activity coefficients, Equation 14 can be solved for a fixed $[\text{H}^+]$ concentration (pH) to determine the equilibrium concentration of free EDTA (EDTA^{4-}) required for precipitation of CaH_2EDTA . Solving Equation 14 at an assumed pH of 9.0, the equilibrium concentration of EDTA^{4-} should be at least 6.49×10^{-3} M in order for CaH_2EDTA precipitation. This concentration is about three orders of magnitude higher than the total EDTA concentration of 8.14×10^{-6} M estimated by Brush and Xiong (2005b, Table 4)

for WIPP brines, and is at least six orders of magnitude higher than EDTA⁴⁻ concentration of 8.37×10^{-11} M predicted for GWB by the FMT calculations for the PABC, or the EDTA⁴⁻ concentration of 1.74×10^{-11} M predicted for ERDA-6 by FMT (Brush, 2005, Runs 7 and 11). Therefore, we screened out the possibility of precipitation of CaH₂EDTA and concluded that precipitation of this solid would not affect the carbonate equilibria in our simulations.

3.6.2 Justification for Including Citrate and Oxalate

We included citrate (C₆H₅O₇³⁻) and oxalate (C₂O₄²⁻) in our EQ6 calculations because their concentrations in the WIPP brines are close to or higher than those required for saturation of the solubility-controlling solid phases. In the case of citrate, the solubility controlling solid is earlandite (Ca₃(C₆H₅O₇)₂·4H₂O). The dissolution reaction of earlandite is:



The log K_{sp} for Reaction 15 is -17.81 (Xiong, 2006a). The solubility of earlandite at infinite dilution can be determined from the log K_{sp} via the relation:

$$K_{\text{sp, earlandite}} = [\text{Ca}^{2+}]^3 [\text{C}_6\text{H}_5\text{O}_7^{3-}]^2 \quad (16)$$

in which [Ca²⁺] and [C₆H₅O₇³⁻] are the activities of Ca²⁺ and free citrate, respectively. If we assume unit activity coefficients and stoichiometric dissolution, then every mole of earlandite that dissolves produces 3 moles of calcium ion and 2 moles of citrate ion. This relation can be expressed as:

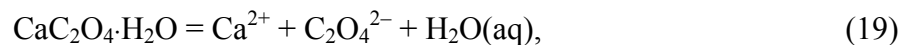
$$[\text{Ca}^{2+}] = 3x \text{ and } [\text{C}_6\text{H}_5\text{O}_7^{3-}] = 2x, \quad (17)$$

in which x is the solubility of earlandite. Substitution of Equation 17 into Equation 16 yields:

$$\log K_{\text{sp, earlandite}} = \log([3x]^3 [2x]^2) = -17.81. \quad (18)$$

Solving Equation 18 for x yields a value of 1.07×10^{-4} m. Substitution of this value in Equation 17 implies that a citrate concentration of 2.14×10^{-4} m is required for the precipitation of earlandite, which is close to the total dissolved citrate concentration of 8.06×10^{-4} M estimated for the PABC (Brush and Xiong, 2005b, Table 4). Therefore, we screened in the possibility of precipitation of earlandite, concluded that precipitation of this solid could affect the precipitation of calcite and other carbonates, transferred the thermodynamic data for citrate (the solubility product for earlandite, stability constants for dissolved Ca²⁺-citrate and Mg²⁺-citrate complexes, and Pitzer parameters for dissolved citrate species) from the FMT database to the EQ3/6 database, and included it in our EQ6 calculations.

The solubility of oxalate is controlled by the mineral whewellite (CaC₂O₄·H₂O). For the dissolution reaction of whewellite,



$\log K_{sp}$ is -8.75 (Xiong, 2004). Using the same approach discussed for earlandite, the K_{sp} can be used to determine the solubility of whewellite by assuming equimolar amounts of the dissolution products, Ca^{2+} and $\text{C}_2\text{O}_4^{2-}$. The calculated solubility of whewellite at infinite dilution is 4.22×10^{-5} m. Assuming stoichiometric dissolution of whewellite, the oxalate concentration required for its precipitation is 4.22×10^{-5} m, lower than the oxalate concentration of 4.55×10^{-2} M in the PABC (Brush and Xiong, 2005). Therefore, we included oxalate in our simulations.

Xiong (2006a) converted the standard chemical potentials for earlandite, whewellite, and the dissolved Ca^{2+} -citrate, Mg^{2+} -citrate, Ca^{2+} -oxalate, and Mg^{2+} -oxalate complexes in the FMT thermodynamic database to the logs of the solubility products and stability constants used in the EQ3/6 databases, and added them to the HMP database. He also transferred the Pitzer parameters for all available dissolved citrate and oxalate species from the FMT database to the HMP database. He did not transfer the comparable data for actinide-bearing solids and complexes to HMP because we did not include actinide elements in any of our simulations. The version of HMP that includes citrate and oxalate is designated “HMY.”

3.7 $\text{CaCO}_3(\text{am})$

Several inorganic elements or compounds and organic compounds are known to inhibit calcite precipitation and are expected to be present in WIPP brines (see Subsection 6.2 below). Results from the literature reviewed in Subsection 6.2 imply that these inhibitors result in precipitation of metastable CaCO_3 -bearing solids such as aragonite, vaterite, ikaite, monohydrocalcite, and $\text{CaCO}_3(\text{am})$. Therefore, we carried out a few simulations in which we substituted $\text{CaCO}_3(\text{am})$ for calcite in the EQ3/6 database. This resulted in a conservative test of the effects of the precipitation of these metastable phases because $\text{CaCO}_3(\text{am})$ is more soluble than aragonite, vaterite, or ikaite. (We could not find a solubility product for monohydrocalcite, so we do not know if $\text{CaCO}_3(\text{am})$ is more soluble than monohydrocalcite.)

Xiong (2006b) added the logarithm of the solubility product of $\text{CaCO}_3(\text{am})$ to the HMY version of the EQ3/6 database. The version of the EQ3/6 database that includes $\text{CaCO}_3(\text{am})$ is Version HML.

4 SOFTWARE

We used EQ6 (Wolery and Daveler, 1992) for our reaction-path calculations. EQ6 is part of the EQ3/6 geochemical software package (Daveler and Wolery, 1992; Wolery, 1992a; 1992b; and Wolery and Daveler, 1992). We used Version 7.2c, which was qualified according to the SNL/WIPP software quality-assurance (QA) requirements by Emily R. Giambalvo in 2001 (see SNL/WIPP Records Package entitled “EQ3/6, Version 7.2c,” ERMS 519559).

To carry out EQ6 reaction-path calculations, the user first sets up an EQ3NR input file to run EQ3NR and generate a pickup file (Wolery, 1992b; Wolery and Daveler, 1992). The pickup file generated by EQ3NR is then used to run EQ6. The suffixes for these and other EQ3/6 input and output files are listed in Table 3, and their meanings are described in Wolery (1992b) and Wolery and Daveler (1992). The QA requirements per Appendix B of NP 9-1 concerning calculations performed for this analysis report are included in Appendix A of this analysis report.

The user specifies the concentrations of elements and species included in a given database for the solution of interest in the EQ3NR input file (Wolery, 1992b). For example, the HMP database includes the following elements and species: H^+ , Na, Mg, K, Ca, Mg, HCO_3^- , OH^- , SO_4^{2-} , and Cl^- . EQ3NR then predicts the speciation of each element among the various uncomplexed and complexed species of each element. For example, the code predicts how much inorganic C is present as dissolved CO_2 , HCO_3^- , and CO_3^{2-} . Note that EQ3NR (and EQ6) lump dissolved, unhydrated CO_2 and hydrated carbonic acid (H_2CO_3) together as CO_2 .

The user can specify one of three types of reaction-path calculations in the EQ6 input file (Wolery and Daveler, 1992). In closed-system mode, the code titrates various quantities of solid, aqueous, and/or gaseous phases specified in the EQ6 input file into the solution defined in the EQ3NR pickup file at rates selected by the user. The code can also titrate negative quantities of aqueous species into the solution to simulate removal of these species (e.g., titration of $-2H^+$, $-SO_4^{2-}$, and CO_2 into GWB or ERDA-6 to simulate the effects of microbial SO_4^{2-} reduction according to Reaction 2 above). As the titration proceeds, the solution remains in contact with the reaction product(s) and continues to react with them if necessary to maintain equilibrium. Use of this option requires experimentally measured or estimated kinetic data, which are unavailable for many geochemical reactions. The titration mode is similar to the closed-system mode, except that the code does not require kinetic data. In the open-system mode, which does not require rate data, the solution reacts with solid, aqueous, and/or gaseous phases; but the reaction products are removed from the system after they form. Thus, the open-system mode can be used to simulate a slug of groundwater flowing through an aquifer. For this analysis, we used the titration mode, because: (1) the conceptual model for WIPP near-field chemistry assumes that the contents of a panel (brine, waste, waste containers, MgO, and DRZ minerals) constitute a homogeneous system (batch reactor); and (2) there are insufficient kinetic data to use the closed-system option.

There are nine databases associated with EQ3/6: ALT, CMP, HML, HMP, HMW, HMY, NEA, PIT, and SUP. ALT, CMP, NEA, and SUP use either the Davies or the B-Dot equation to calculate activity coefficients of aqueous species. HML, HMP, HMW, HMY, and PIT all support the Pitzer activity-coefficient option, which uses the Pitzer equations to calculate activity coefficients of aqueous species. HMW uses the Pitzer ion-interaction parameters developed by Harvie et al. (1984); PIT uses the Pitzer parameters developed by K. S. Pitzer and his students.

Previously, Xiong (2004) modified HMW and designated the revised database “HMP.” He established HMP by incorporating the necessary parameters (the common logarithms of the solubility products for solid phases, the logs of the stability constants for aqueous complexes, and the various Pitzer parameters) for hydromagnesite (5424), hydromagnesite (4323), CaO, MgCl₂, MgO and MgSO₄ into HMW. As noted above in Subsection 3.1.1.2, EQ3/6 (and FMT) have always predicted that hydromagnesite (5424) will form instead of hydromagnesite (4323) if magnesite is suppressed, even though both phases are in the database(s). This is because hydromagnesite (5424) has a lower free energy of formation and a lower solubility product than hydromagnesite (4323). Furthermore, hydromagnesite (5424) has been observed frequently in laboratory studies of the carbonation of MgO, but hydromagnesite (4323) has never been observed. Therefore, we use “hydromagnesite” to refer to “hydromagnesite (5424)” in this analysis report.

For this analysis, Xiong (2006a) modified HMP and established HMY by adding the necessary thermodynamic data and Pitzer parameters for dissolved citrate and oxalate species and citrate- and oxalate-bearing solids to HMP. Xiong (2006b) then added the log of the solubility product of CaCO₃(am) to HMY to establish HML.

5 RESULTS

This section describes the effects of the following factors on brine composition, the quantities of carbonate minerals produced, and the effective yield of CO₂ per mole of organic C: (1) the initial brine composition and the brine volume, (2) whether carbonation of brucite produces magnesite or hydromagnesite, (3) the effects of organic ligands, and (4) the effects of precipitation of CaCO₃(am) instead of calcite.

5.1 Effects of Initial Brine Composition and Brine Volume

This subsection describes the results of the simulations carried out with 1,045 and 7,763 m³ of GWB in a seven-room panel, and with 1,045, 7,763, and 13,267 m³ of ERDA-6 in a panel to determine the effects of initial brine composition and brine volume on brine composition, the quantities of carbonate minerals produced, and the effective yields of CO₂ per mole of organic C.

5.1.1 Effects on Brine Composition

Tables 16-20 show the effects of the initial brine composition and brine volume on brine chemistry. Each of these tables provides the composition of GWB or ERDA-6 before Step 1, after Step 1, and after Step 2. As explained in Subsection 3.1 (see above), Step 1 consisted of reaction of GWB or ERDA-6 with brucite and the minerals in the DRZ surrounding the repository. Step 2 involved consumption of CPR materials by microbial SO₄²⁻ reduction (Reaction 2 above); dissolution of anhydrite, gypsum, and polyhalite (Reactions 4, 5, and 6); and consumption of CO₂ by calcite (Reaction 7) and (in most cases) pirssonite (Reaction 8). Therefore, the compositions of these brines after Step 1 reflect equilibration of the brines with brucite, halite, anhydrite, gypsum, magnesite, and polyhalite; the compositions after Step 2 result from microbial consumption of 94.27% of the CPR materials initially present in the repository via SO₄²⁻ reduction, and concomitant dissolution of anhydrite, gypsum, and polyhalite and fixation of CO₂ by calcite and pirssonite.

The compositions of GWB and ERDA-6 after Step 1 are similar, but not identical to, the compositions of these brines calculated by FMT for the PABC (compare the results from Tables 16-20 with those from Table 3, columns labeled “GWB [or ERDA-6] after Reaction with MgO, Halite, and Anhydrite”). The differences result mainly from: (1) equilibration of GWB or ERDA-6 with the four most important Salado minerals (halite, anhydrite, gypsum, polyhalite; and magnesite) in the runs that produced the results in Tables 16-20, but with just two of them in the FMT runs for the PABC (halite and anhydrite, but note that the hydromagnesite used to represent carbonated MgO in these runs can be viewed as a “stand-in” for the magnesite in the Salado); (2) equilibration of the brines with brucite and magnesite in Tables 16-20, but with brucite and hydromagnesite in Table 3.

The most important parameters predicted by geochemical modeling from the standpoint of WIPP PA are the f_{CO_2} and the pH. This is because they affect actinide speciation and solubilities more than the concentrations of any other major or minor element in these brines. EQ6 calculated a value of -6.92 for $\log f_{\text{CO}_2}$ after Step 1 (see Tables 16-20). This is lower than the value of -5.50 predicted by FMT for PABC Runs 7 and 11 (Brush, 2005, Table 5). This is because the brucite-magnesite carbonation reaction buffered f_{CO_2} in the runs that produced the results in Tables 16-20, but the brucite-hydromagnesite carbonation reaction buffered f_{CO_2} in PABC Runs 7 and 11. It is worth noting that when FMT used the brucite-magnesite reaction, it predicted a value -6.92 for $\log f_{\text{CO}_2}$ for GWB (Brush, 2005, Table 5, Run 5) and a value of -6.91 for ERDA-6 (Brush, 2005, Table 5, Run 9).

EQ6 calculated a range of values of 8.27 to 8.45 for the pH after Step 1 (Tables 16-20). These are similar to the values of 8.69 and 8.94 calculated by FMT for the PABC (Table 3).

On the other hand, the compositions of GWB and ERDA-6 after Step 2 are quite different from anything reported previously for WIPP disposal rooms. These differences probably reflect the dissolution of significant quantities of the SO_4^{2-} minerals in the DRZ (anhydrite, gypsum, and especially polyhalite), which resulted from the drawdown of dissolved SO_4^{2-} by microbial SO_4^{2-} reduction (simulated by titration of $-\text{SO}_4^{2-}$ during Step 2).

The most significant difference from the standpoint of PA is the pH predicted by EQ6 after Step 2: Four of these five simulations predicted a final pH of 11.3 (Tables 16, 17, 19, and 20); one predicted a value of 8.53 (Table 18). This high pH resulted from including polyhalite among the minerals that dissolved in response to microbial SO_4^{2-} reduction. However, the precise mechanism that increased the pH above the values of 8.69 and 8.94 predicted by FMT for the PABC (Brush, 2005, Table 5, Runs 7 and 11) is still unclear.

The values of $\log f_{\text{CO}_2}$ calculated by EQ6 after Step 2 are -6.93 or -6.92, essentially identical to those calculated after Step 1.

5.1.2 Effects on Precipitation of Carbonate Minerals and Effective CO_2 Yield

Tables 21-25 show the effects of the initial brine composition and brine volume on the quantities of carbonate minerals precipitated, and the effective yields of CO_2 per mole of organic C calculated by these simulations. Each of these tables shows these results: (1) at the beginning of microbial activity (before any CPR materials were consumed); (2) for microbial denitrification, which will consume 4.89% of the CPR materials initially present in the WIPP; (3) for microbial SO_4^{2-} reduction using SO_4^{2-} in the waste, which will consume 0.84% of the CPR materials; (4) for SO_4^{2-} reduction using SO_4^{2-} in the DRZ minerals anhydrite, gypsum, and polyhalite, which will consume 94.27% of the CPR materials; and (5) at the end of microbial activity (after consumption of all CPR materials, or the cumulative effects of all microbial activity).

EQ6 calculated that precipitation of calcite or (in most cases) calcite and pirssonite consumed 40-46% of the CO_2 from microbial SO_4^{2-} reduction using SO_4^{2-} in DRZ minerals, and

38-43% of the CO₂ from all microbial activity. The ranges of effective CO₂ yields were 0.54-0.60 mol CO₂/mol organic C for SO₄²⁻ reduction, and 0.57-0.62 mol CO₂/mol organic C for all microbial activity.

Calcite consumed significantly more CO₂ than pirssonite. The range of CO₂ precipitated by calcite was 38-42% of the CO₂ from SO₄²⁻ reduction using SO₄²⁻ in DRZ minerals, and 36-40% of the CO₂ from all microbial activity. The comparable ranges for pirssonite were 0-8% and 0-7%, respectively.

In the simulations with 1,045 and 7,763 m³ of GWB and ERDA-6, carbonates consumed somewhat more CO₂ in ERDA-6 than in GWB. For ERDA-6, a mean of 45.5% of the CO₂ from SO₄²⁻ reduction using SO₄²⁻ in DRZ minerals was precipitated by carbonates, and a mean of 42.5% of the CO₂ from all microbial activity was fixed by carbonates. The comparable values for GWB were 42.5 and 40%.

The effective CO₂ yield was somewhat lower with ERDA-6 than with GWB in the simulations with 1,045 and 7,763 m³ of brine. For ERDA-6, a mean of 0.545 mol CO₂/mol organic C was obtained for SO₄²⁻ reduction using SO₄²⁻ in DRZ minerals, and a mean of 0.575 mol CO₂/mol organic C was obtained for all microbial activity. The comparable values for GWB were 0.575 and 0.60 mol CO₂/mol organic C.

Increasing the brine volume decreased the quantity of CO₂ consumed by carbonates slightly in both brines. Carbonate precipitation from GWB fixed 45 and 40% of the CO₂ from SO₄²⁻ reduction using SO₄²⁻ in DRZ minerals, and 42 and 38% the CO₂ from all microbial activity with brine volumes of 1,045 and 7,763 m³, respectively. Carbonate precipitation from ERDA-6 fixed 46, 45 and 44% of the CO₂ from SO₄²⁻ reduction, and 43, 42 and 41% for all microbial activity with volumes of 1,045, 7,763, and 13,267 m³, respectively.

Increasing the brine volume increased the effective CO₂ yield slightly. The yields for GWB were 0.55 and 0.60 mol CO₂/mol organic C for SO₄²⁻ reduction using SO₄²⁻ from DRZ minerals, and 0.58 and 0.62 mol CO₂/mol organic C for all microbial activity with brine volumes of 1,045 and 7,763 m³, respectively. The yields for ERDA-6 were 0.54, 0.55 and 0.56 for SO₄²⁻ reduction, and 0.57, 0.58 and 0.59 mol CO₂/mol organic C for all microbial activity with volumes of 1,045, 7,763, and 13,267 m³, respectively.

5.2 Effects of Hydromagnesite

This subsection describes the results of the simulations carried out with 7,763 m³ of GWB and ERDA-6 to determine the effects of hydromagnesite on brine composition, the quantities of carbonate minerals produced, and the effective yields of CO₂.

5.2.1 Effects on Brine Composition

Tables 26 and 27 show the effects of hydromagnesite on brine chemistry. The compositions of GWB and ERDA-6 after Steps 1 and 2 were similar to those described above (see Tables 18 and 19). EQ6 calculated a value of -5.48 for $\log f_{\text{CO}_2}$ for both GWB and ERDA-6 after Steps 1 and 2. In these simulations, the brucite-hydromagnesite carbonation reaction buffered f_{CO_2} . This value is essentially identical to that of -5.50 calculated by FMT for PABC Runs 7 and 11, in which the brucite-hydromagnesite reaction also buffered f_{CO_2} (Brush, 2005, Table 3).

However, the pH values predicted after Step 2 were slightly lower with hydromagnesite (8.32 in GWB and 10.6 in ERDA-6) than with magnesite and a brine volume of 7,763 m³ (8.53 in GWB and 10.6 in ERDA-6).

5.2.2 Effects on Precipitation of Carbonate Minerals and Effective CO₂ Yield

Tables 28 and 29 show the effects of hydromagnesite on the production of carbonates and the effective CO₂ yield.

Comparison of Tables 28 and 23 shows that whether hydromagnesite or magnesite formed had little effect on carbonate production and the effective CO₂ yield in the case of GWB. Calcite consumed 41% of the CO₂ from microbial SO₄²⁻ reduction using SO₄²⁻ in DRZ minerals and 38% of the CO₂ from all microbial activity when hydromagnesite formed, and 40% of the CO₂ from SO₄²⁻ reduction and 38% of the CO₂ from all microbial activity when magnesite formed. The effective CO₂ yields were 0.59 mol CO₂/mol organic C for SO₄²⁻ reduction and 0.62 mol CO₂/mol organic C for all microbial activity with hydromagnesite, and 0.60 mol CO₂/mol organic C for SO₄²⁻ reduction and 0.62 mol CO₂/mol organic C for all CPR materials with magnesite.

Comparison of Tables 29 and 24 shows similar results for ERDA-6. Calcite and pirssonite consumed 45% of the CO₂ from SO₄²⁻ reduction using SO₄²⁻ from DRZ minerals and 43% of the CO₂ from all microbial activity when hydromagnesite formed, and 45% of the CO₂ from SO₄²⁻ reduction and 42% of the CO₂ from all microbial activity when magnesite formed. The effective CO₂ yields were 0.55 mol CO₂/mol organic C for SO₄²⁻ reduction and 0.58 mol CO₂/mol organic C for all microbial activity with hydromagnesite; the comparable values for magnesite are identical.

5.3 Effects of Organic Ligands

This subsection discusses the results of the simulations carried out with 1,045 m³ of GWB and ERDA-6 to determine the effects of citrate and oxalate on brine composition, the quantities of carbonate minerals produced, and the effective CO₂ yields.

5.3.1 Effects on Brine Composition

Tables 30 and 31 show that the simulations with citrate and oxalate resulted in brine compositions essentially identical to those obtained with 1,045 m³ of GWB and ERDA-6, but without these organic ligands (compare Tables 30 and 16, and Tables 31 and 17). For both of these brines, all values of log f_{CO_2} and pH, and the concentrations of major and minor elements are nearly identical after both Steps 1 and 2 in these simulations. In particular, the values of log f_{CO_2} , -6.93 and -6.92, reflect the fact that f_{CO_2} was buffered by the brucite-magnesite carbonation reaction in these runs. The pH increased to a value of 11.3 in both brines after Step 2.

Note that the concentrations of citrate and oxalate fluctuated during these simulations. We are examining the EQ6 output files to determine whether precipitation and dissolution of citrate- and oxalate-bearing solids occurred during these runs, or changes in the brine volumes were responsible.

5.3.2 Effects on Precipitation of Carbonate Minerals and Effective CO₂ Yield

Tables 32 and 33 show the effects of citrate and oxalate on the production of carbonates and the effective CO₂ yields.

Comparison of Tables 32 and 21 shows that citrate and oxalate had no effect on carbonate production and the effective CO₂ yield in the case of GWB. Calcite and pirssonite consumed 45% of the CO₂ from microbial SO₄²⁻ reduction using SO₄²⁻ in DRZ minerals and 42% of the CO₂ from all microbial activity with or without citrate and oxalate. The effective CO₂ yields were 0.55 mol CO₂/mol organic C for SO₄²⁻ reduction and 0.58 mol CO₂/mol organic C for all microbial activity with or without these organic ligands.

Comparison of Tables 33 and 22 shows citrate and oxalate also had no effect with ERDA-6. Calcite and pirssonite consumed 46% of the CO₂ from SO₄²⁻ reduction using SO₄²⁻ from DRZ minerals and 43% of the CO₂ from all microbial activity with or without citrate and oxalate. The effective CO₂ yields with and without these organic ligands were 0.54 mol CO₂/mol organic C for SO₄²⁻ reduction and 0.57 mol CO₂/mol organic C for all microbial activity.

5.4 Effects of CaCO₃(am)

This subsection discusses the results of the simulations carried out with 1,045 m³ of GWB and ERDA-6 to determine the effects of CaCO₃(am) on brine composition, the quantities of carbonate minerals produced, and the effective CO₂ yields.

5.4.1 Effects on Brine Composition

Tables 34 and 35 show the effects of $\text{CaCO}_3(\text{am})$ on brine chemistry. The compositions of GWB and ERDA-6 after Steps 1 and 2 were similar to those with organic ligands and calcite (see Tables 30 and 31). The values of $\log f_{\text{CO}_2}$ were identical after Step 1 (-6.92) and Step 2 (-6.93) with $\text{CaCO}_3(\text{am})$ and calcite in both GWB and ERDA-6 (compare Tables 34 and 30). This is because f_{CO_2} was buffered by the brucite-hydromagnesite carbonation reaction.

However, the pH value predicted after Step 2 was slightly lower with $\text{CaCO}_3(\text{am})$ (10.3 in both GWB and ERDA-6) than with calcite (11.3 in both brines).

5.4.2 Effects on Precipitation of Carbonate Minerals and Effective CO_2 Yield

Tables 36 and 37 show the effects of $\text{CaCO}_3(\text{am})$ on the production of carbonates and the effective CO_2 yields.

Comparison of Tables 36 and 32 shows that $\text{CaCO}_3(\text{am})$ had little effect on carbonate production and the effective CO_2 yield in the case of GWB. Calcite and pirssonite consumed 45% of the CO_2 from microbial SO_4^{2-} reduction using SO_4^{2-} in DRZ minerals and 42% of the CO_2 from all microbial activity with both $\text{CaCO}_3(\text{am})$ and calcite. However, $\text{CaCO}_3(\text{am})$ did affect the relative contributions from calcite and pirssonite slightly. The effective CO_2 yields were 0.55 mol CO_2 /mol organic C for SO_4^{2-} reduction and 0.58 mol CO_2 /mol organic C for all microbial activity with both $\text{CaCO}_3(\text{am})$ and calcite.

Tables 37 and 33 show that $\text{CaCO}_3(\text{am})$ also had no effect with ERDA-6. Calcite and pirssonite consumed 46% of the CO_2 from SO_4^{2-} reduction using SO_4^{2-} from DRZ minerals and 43% of the CO_2 from all microbial activity with both $\text{CaCO}_3(\text{am})$ and calcite, but $\text{CaCO}_3(\text{am})$ affected the relative contributions from calcite and pirssonite slightly. The effective CO_2 yields with both $\text{CaCO}_3(\text{am})$ and calcite were 0.54 mol CO_2 /mol organic C for SO_4^{2-} reduction and 0.57 mol CO_2 /mol organic C for all microbial activity.

6 POSSIBLE ISSUES RELATED TO CALCITE PRECIPITATION

This section addresses two more potential issues related to calcite, $\text{CaCO}_3(\text{am})$, and pirssonite precipitation from the reaction of CO_2 with dissolved Ca^{2+} released to WIPP brines by the dissolution of anhydrite, gypsum, and polyhalite in the DRZ if microbial SO_4^{2-} reduction in the repository consumes all SO_4^{2-} in the waste. These issues are: (1) possible limitations on the availability of SO_4^{2-} in the DRZ; (2) possible kinetic inhibition of calcite precipitation by Mg, phosphate (PO_4), Fe, and organic ligands.

6.1 Effects of Limited Availability of SO_4^{2-} in the DRZ

We have assumed so far that the SO_4^{2-} in anhydrite, gypsum, and polyhalite in the DRZ will be available to SO_4^{2-} -reducing microbes for consumption of the CPR materials remaining in the repository after microbial denitrification and SO_4^{2-} reduction using SO_4^{2-} in the waste (94.27% of the CPR materials initially emplaced in the WIPP). We showed that the amount of SO_4^{2-} required, 5.18×10^8 mol, is about 44.7% of the quantity contained in these minerals in the DRZ used for the CRA-2004 PABC, 1.16×10^9 mol (Subsection 3.3.3). However, it is by no means clear that advective transport of SO_4^{2-} from the underlying Castile Fm. in the event of human intrusion, and diffusive transport of SO_4^{2-} from the surrounding Salado Fm. would be sufficient to prevent methanogenesis (Kanney et al, 2004). Therefore, it is reasonable to consider the consequences of limitations on the availability of SO_4^{2-} (i.e., whether there are possible scenarios in which more CO_2 could be generated if methanogenesis occurs than if SO_4^{2-} reduction using SO_4^{2-} in the DRZ consumes 94.27% of the CPR materials.)

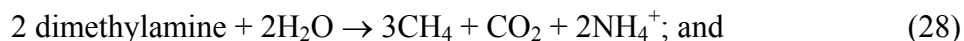
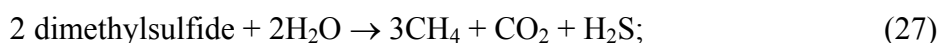
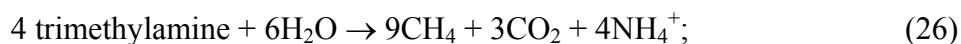
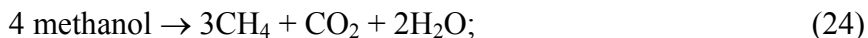
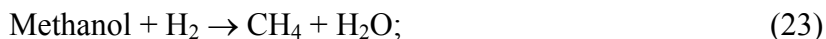
Garcia et al. (2000) reviewed the taxonomic, phylogenetic, and ecological diversity of methanogenic *Archaea*. In particular, they included 11 methanogenic reactions and compared the changes in free energies for these reactions (Garcia et al, 2000, Table 1). The methanogenic reaction in their Table 1 that is most similar to the reaction for fermentation and methanogenesis implemented in BRAGFLO is:



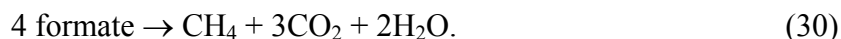
Note that Reaction 20 is not identical to the reaction for fermentation and methanogenesis in BRAGFLO (see Reaction 3 in Section 2 above) because Reaction 3 includes both fermentation (which produces short-chain organic acids such as acetic and formic acid, and alcohols such as ethanol and methanol) and methanogenesis (which consumes these organic acids and alcohols), but Reaction 20 includes only methanogenesis. (It is technically correct to refer to Reaction 3 in Section 2 as “fermentation and methanogenesis;” however, we typically omit “fermentation” for brevity.)

Inspection of Table 1 in Garcia et al. (2000) reveals that: (1) 9 of the 11 reactions that Garcia et al, (2002) considered representative of those carried out by methanogenic *Archaea* produce more CH_4 than CO_2 (Reactions 21 through 29 below); (2) 4 of the 11 reactions produce

no CO₂ at all (Reactions 21, 22, 23); and (3) 3 of the 11 reactions actually consume CO₂ (Reactions 21, 22, and 29). These reactions are:



On the other hand, only 1 of the 11 typical methanogenic reactions compiled by Garcia et al, (2002, Table 1) produces more CO₂ than CH₄:



Therefore, Reaction 20 would produce somewhat more CO₂, and Reaction 30 would produce significantly more CO₂, if methanogenesis occurs than if SO₄²⁻ reduction using SO₄²⁻ in the DRZ consumes 94.27% of the CPR materials initially emplaced in the repository. However, Reactions 21 through 29 would produce significantly less CO₂ if methanogenesis occurs than if SO₄²⁻ reduction using SO₄²⁻ in the DRZ consumes 94.27% of the CPR materials. This is because the implementation of fermentation and methanogenesis in BRAGFLO (see Reaction 3 above) is very conservative. Garcia et al. (2000, Table 1) showed that Reaction 21 is the most energetically favored of all methanogenic reactions. The value of ΔG^o for Reaction 21 calculated by Garcia et al. (2000, Table 1) is -135.6 kJ/mol CH₄, which is more negative than the values for the other 10 reactions. Thus, according to the conceptual model for WIPP near-field chemistry, Reaction 21 should occur preferentially to all other methanogenic reactions if both H₂ and CO₂ are present in the repository, a condition that would be quite common because anoxic corrosion of steels and other Fe-base metals will produce significant quantities of H₂ if brine is present. Clearly methanogenesis via Reaction 21 will consume significant quantities of CO₂ until all H₂ is consumed, at which time methanogenesis via Reaction 20 (or fermentation and methanogenesis via Reaction 3) would replace methanogenesis by Reaction 21.

6.2 Possible Kinetic Inhibition of Calcite Precipitation

The previous discussion in this report has assumed for the most part that calcite will precipitate rapidly after reaching saturation in WIPP brines. However, a number of inorganic elements and compounds, and organic ligands expected to be present in the WIPP are known to inhibit calcite precipitation. These include Mg, PO₄, SO₄, and Fe; and citrate, EDTA, oxalate, and humic acid. Therefore, it is necessary to consider whether these elements and compounds could prevent calcite precipitation in the WIPP.

It is also important to note that a number of other CaCO₃-bearing minerals can still precipitate if the formation of calcite is inhibited. These minerals, which are metastable with respect to calcite, include aragonite (CaCO₃), vaterite (CaCO₃), monohydrocalcite (CaCO₃·H₂O), ikaite (CaCO₃·6H₂O), and CaCO₃(am) (Brooks et al., 1950; Gal et al., 1996). Table 37 provides the logs of the solubility products for these phases at 301 K (28 °C), the in-situ temperature of the WIPP at the repository horizon (Munson et al., 1987). These phases are known to precipitate in order of increasing solubility product (i.e., in order of increasing free energy of formation). Thus, if the precipitation of calcite is inhibited, the next phase to form will be aragonite, which has the next lowest solubility product (and free energy of formation); this process continues in this manner until CaCO₃(am) forms.

In addition, the precipitation of a number of other CaCO₃-bearing minerals is possible. These include gaylussite (Na₂Ca(CO₃)₂·5H₂O), pirssonite (Na₂Ca(CO₃)₂·2H₂O), and dolomite (CaMg(CO₃)₂). The formation of these other CaCO₃-bearing phases could be significant because most of the minerals containing more than one cation will precipitate multiple carbonate ions, thereby increasing the quantity of CO₂ consumed per mole of Ca. The formation of Mg-bearing carbonates (e.g., dolomite) might seem disadvantageous because it effectively removes MgO from the system. However, in these minerals one mole of CO₂ is removed from the system for every mole of MgO that is sequestered by a carbonate phase. Thus, incorporation of Mg into these minerals still consumes 1 mole CO₂ per mole of MgO.

The potential for each of these species (see above) to inhibit calcite precipitation is discussed in the next section.

6.2.1 Effects of Single Inhibitors

The presence of Mg²⁺ has been shown to have a significant impact on the kinetics and thermodynamics of CaCO₃ precipitation. Fernández-Díaz et al. (1996) reported that Mg²⁺ inhibits calcite growth by increasing the supersaturation threshold required to initiate precipitation, but appears to have no effect on the kinetics of aragonite precipitation. In addition, Mg may coprecipitate in the reaction, leading to formation of as much as 20% MgCO₃ in addition to CaCO₃ (Morse, 1983). Finally, for values of [Mg²⁺]/[Ca²⁺] greater than approximately 2, experiments indicate that calcite may not precipitate at all; instead, CaCO₃ precipitates as aragonite (Katz, 1973). In GWB, the concentration ratio of Mg to Ca will be roughly 68:1 after this brine reacts with the MgO engineered barrier, halite, and anhydrite; the activity ratio will be nearly 130:1 (Brush, 2005, Run 7). In ERDA-6, the concentration ratio will be 15:1 after reaction and the activity ratio will be 27:1. Consequently, we conclude that

aragonite could be a significant component of the CaCO_3 precipitated in the WIPP. In addition, Mg may also enhance the conversion of metastable vaterite to calcite (Chen et al, 2006).

On the other hand, Xiong and Lord (2006) observed calcite precipitation in their experiments to define the reaction path(s) during hydration and carbonation of Premier MgO under simulated WIPP conditions. XRD analysis, used to characterize the solids formed during these experiments, demonstrated that calcite was present among the solids sampled after 381 hours in ERDA-6 and after 3025 hours (and perhaps as early as 1197 hours) in GWB (see their Figures 3 and 4, respectively). The fact that calcite appeared earlier in ERDA-6 than it did in GWB is not surprising in view of the fact the initial Mg concentrations of these brines were 19 mM and 1.00 M, respectively. However, precipitation of calcite instead of aragonite from GWB is surprising in view of the results reviewed above.

PO_4 can reduce the rate of precipitation of both calcite and aragonite, but does not affect the kinetics of vaterite formation (van Langerak et al., 1999). However, since vaterite precipitation is somewhat slower than that of calcite and aragonite, the observed precipitation of CaCO_3 is reduced, primarily through formation of calcium orthophosphate ($\text{Ca}_3(\text{PO}_4)_2$) (Lin and Singer, 2006). The minimum concentration of PO_4 observed to inhibit precipitation is approximately 1.6×10^{-5} M. We used the method of Brush and Xiong (2005b) to estimate the PO_4 concentration in the WIPP. Crawford (2005, Table 10) established a total mass of 85.1 kg of PO_4 in the TRU waste to be emplaced in the WIPP. We then used a brine volume of $10,011 \text{ m}^3$ (the minimum volume that results in a release from the repository) from Stein (2005), to calculate a dissolved PO_4 concentration of 9.0×10^{-5} M. However, even at this concentration, the observed reduction of precipitation was only about 15% of the total volume of CaCO_3 that would form in 8 days if no inhibitors were present (van Langerak et al., 1999, Figure 1). Thus, we conclude that PO_4 inhibition of CaCO_3 precipitation will not be significant during the 10,000-year WIPP regulatory period.

SO_4^{2-} may also inhibit calcite precipitation (Paquette et al., 1996), largely by increasing the solubility of CaCO_3 . However, neither Akin and Lagerwerff (1965) nor Zuddas and Mucci (1994) discussed the formation of metastable CaCO_3 or $\text{CaCO}_3 \cdot x\text{H}_2\text{O}$ minerals. However, Xiong and Lord (2006, Figures 3 and 4) observed calcite formation from GWB and ERDA-6, which had initial SO_4^{2-} concentrations of 175 and 170 mM, respectively.

The effects of a number of other metals, including Fe(II), Mg(II), Ni(II), Co(II), Zn, Cd, and Cu(II), were also examined (Wada et al., 1995). Except for Cd, which had no discernible effect, all these cations led to increased aragonite formation. By contrast, it has been shown that Pb(II) can be incorporated in the crystal structure of CaCO_3 , thereby reducing the amount of Ca^{2+} required to react with CO_3^{2-} (Godelitsas, 2003). Similar results have been observed through simulation for Sr^{2+} (De Leeuw et al., 2002).

Citrate could have a measurable impact on calcite precipitation. A 20% reduction in the precipitation rate of calcite was observed at a citrate concentration of 4×10^{-5} M, while a 30-fold reduction was observed for aragonite at the same citrate concentration (Westin and Rasmuson, 2005). The citrate concentration estimated for the PABC was 8.06×10^{-4} M (Brush and Xiong, 2005b). Thus, since the high Mg/Ca ratio in the WIPP brine favors the formation of

aragonite instead of calcite, one might conclude that there would be a substantial reduction in the precipitation of CaCO_3 at this citrate concentration. Under the conditions present in the WIPP, however, we do not expect the formation of either calcite or aragonite to be completely inhibited (Meldrum and Hyde, 2001); we will discuss this in greater detail in Section 6.2.2.

EDTA can slow the precipitation of aragonite; Fredd and Fogler (1998) observed that CaCO_3 dissolution increases by a factor of three for high concentrations of EDTA (0.01-0.1 M). However, the EDTA concentration in the WIPP brine, 8.14×10^{-6} M (Brush and Xiong, 2005b), is several orders of magnitude lower than these experimental conditions. Therefore, we conclude that EDTA will not have a significant effect on CaCO_3 formation in the repository.

Oxalate can have a slight inhibitory effect on CaCO_3 precipitation through the formation of calcium oxalate. However, the rate of Ca oxalate aggregation is an order of magnitude smaller than calcite precipitation; therefore, even under conditions in which Ca oxalate should precipitate, we expect that it will not have a major impact on the calcite precipitation rate (Collier and Hounslow, 1999). In addition, the Ca^{2+} concentration is approximately 30 times that of the total oxalate concentration. Therefore, even complete precipitation of oxalate as calcium oxalate would still leave sufficient Ca^{2+} for complete reaction with the CO_3^{2-} present in the brine.

Finally, humic acid has been shown to have an inhibitory effect on calcite precipitation, decreasing the rate by an order of magnitude at a concentration of 1 g humic acid per 1 kg solution. In the WIPP, the concentration of humic acid was estimated to be in the range of 1.5-2.0 mg/L (U.S. DOE, 1996, Appendix SOTERM). Therefore, the rate of inhibition should be substantially less than one order of magnitude. In addition, it has not been shown that humic acid blocks the formation of any of the other forms of CaCO_3 (Zuddas et al, 2003).

To summarize, our review of the effects of individual inhibitors of CaCO_3 precipitation implies that, while many elements and compounds that will be present in the WIPP have been shown to inhibit the precipitation of calcite and other forms of CaCO_3 , none of them have been shown to completely inhibit the precipitation of all forms of CaCO_3 . For example, if the high Mg/Ca ratios in WIPP brines inhibit calcite precipitation, the predominant form of CaCO_3 could be aragonite. Furthermore, the presence of other elements and compounds in the repository will reduce the rate of, but not entirely prevent, aragonite precipitation. Furthermore, nearly complete inhibition of all six of the CaCO_3 or $\text{CaCO}_3 \cdot \text{H}_2\text{O}$ minerals listed in Table 37 — as well as Na-Ca carbonates such as gaylussite and pirssonite — would be required to prevent sequestration of significant amounts of CO_2 in CaCO_3 -bearing minerals in the repository.

Additionally, due to the high ionic strength of WIPP brines, any increase in the concentration of inhibitory ions would also lead to an increase in the activity coefficients γ_i (Pitzer, 1991). This would in turn lead to a reduction in the concentration of CO_3^{2-} required for precipitation, thereby partially offsetting any reduction in reaction rates caused by the inhibitors. In fact, a number of studies, including those of Zuddas and Mucci (1998) and Zhang and Dawe (1998) suggest that the rate of CaCO_3 precipitation increases with increasing ionic strength. Tomson (1983) proposes that the minimum concentration of anions needed to have a possible inhibitory effect on calcite formation is equal to the concentration of CO_3^{2-} for divalent ions, and double the concentration of CO_3^{2-} for monovalent ions. Several other factors can also increase

the precipitation rate of calcite. For instance, increasing the P_{CO_2} can lead to increased precipitation rates through increased charge concentration on the calcite surface and the increased activity of CaHCO_3^+ (Lebron and Suarez, 1998). In addition, the presence of bacteria has been shown to inhibit calcite dissolution (Lüttge and Conrad, 2004). The presence of citrate, EDTA, and oxalate enhance the dissolution of dolomite in alkaline solutions, and cause a small increase in the dissolution rate (Pokrovsky and Schott (2001).

6.2.2 Effects of Multiple Inhibitors

Although the literature demonstrates that many of the species expected in WIPP brines may inhibit precipitation of CaCO_3 when considered individually, very few papers have analyzed the effects of multiple inhibitors acting simultaneously on the same solution. Thus, predicting the cumulative effect of the many inhibitors that can be found in WIPP brines is a challenging task. The existence of numerous species in WIPP brines creates numerous other solubility criteria that must be satisfied, as well as many other kinetic pathways that could prevent those species from participating in the inhibition of CaCO_3 precipitation.

For instance, while studies have shown that Mg^{2+} inhibits calcite formation (Katz, 1973) and citrate inhibits aragonite formation (Westin and Rasmuson, 2005), the simultaneous presence of Mg^{2+} and citrate can lead to the formation of so-called “magnesian calcites,” $\text{Mg}_x\text{Ca}_{1-x}\text{CO}_3$, where the magnesium content $x < 0.5$; at high Mg^{2+} concentrations, aragonite precipitation is also observed (Meldrum and Hyde, 2001). The concentration of MgCO_3 in magnesian calcite depends upon the source of the calcite. Naturally occurring magnesian calcites from inorganic sources typically have very low MgCO_3 concentrations; typically $x < 0.05$. Organisms that produce CaCO_3 yield magnesian calcite with greater magnesium content ($x < 0.20$). Synthetically produced magnesian calcite can yield higher magnesium levels ($x > 0.40$), but only in the absence of SO_4^{2-} . In the presence of SO_4^{2-} , the MgCO_3 content is typically the same as organically produced magnesian calcite (Busenberg and Plummer, 1989).

Meldrum and Hyde’s experiments (2001) demonstrated that the percentage of MgCO_3 incorporated into the calcite depended on the ratios of both Mg^{2+} and citrate to Ca^{2+} . However, for a given citrate concentration, the amount of MgCO_3 incorporated does not show a clear trend. According to Brush and Xiong (2005b), the ratio of Ca^{2+} to citrate is approximately 10.4:1 for GWB and 13.7:1 for ERDA-6; these values correspond closely to the “C2” class of experiments performed by Meldrum and Hyde (2001, Tables 1 and 3). For these experiments, the MgCO_3 concentration in the magnesian calcite varied between 5.5 and 14.2 percent, with anywhere from 0 to 50 percent of the total CaCO_3 precipitation occurring as aragonite. Unlike calcite, aragonite tends not to incorporate Mg in more than trace amounts (Deer, Howie, and Zussman, 1992). Because aragonite formation increases with increasing Mg^{2+} concentration, it is possible that, under the conditions present in WIPP brines (Mg/Ca ratios of anywhere between 15:1 and 130:1), aragonite could be the dominant CaCO_3 phase, with magnesian calcite containing up to 22% MgCO_3 as the secondary form of precipitated CaCO_3 .

7 CONCLUSIONS

We used the reaction-path code EQ6 (Wolery and Daveler, 1992) to simulate the precipitation of calcite (or $\text{CaCO}_3(\text{am})$), and pirssonite caused by reaction of microbial CO_2 with Ca^{2+} from the dissolution of anhydrite, gypsum, and polyhalite resulting from the drawdown of SO_4^{2-} in the DRZ by microbial SO_4^{2-} reduction in WIPP disposal rooms.

We then used the results of the EQ6 reaction-path simulations to calculate: (1) the quantity of magnesite (or hydromagnesite) produced during each phase of the microbial consumption of CPR materials, and the total quantity of magnesite (or hydromagnesite) formed after consumption of all CPR materials; (2) the quantities of calcite (or $\text{CaCO}_3(\text{am})$) and pirssonite produced during each phase of microbial activity, and the total quantities formed; and (3) the effective CO_2 yields for each phase of microbial activity, and the overall effective yield.

We determined the effects of the following factors on brine composition, the quantities of carbonate minerals produced, and the effective CO_2 yields: (1) the initial brine composition and the brine volume, (2) whether carbonation of brucite produces magnesite or hydromagnesite, (3) the effects of citrate and oxalate, and (4) the effects of precipitation of $\text{CaCO}_3(\text{am})$ instead of calcite.

We simulated the precipitation of carbonate minerals by carrying out the following sequential reaction-path calculations with EQ6: (1) reaction of WIPP brines with brucite and the minerals in the DRZ surrounding the repository (Step 1); and (2) consumption of CPR materials by microbial SO_4^{2-} reduction (see Reaction 2 above); dissolution of anhydrite, gypsum, and polyhalite (Reactions 4, 5, and 6 above); and consumption of CO_2 by calcite (Reaction 7) and (in most cases) pirssonite (Reaction 8) (Step 2).

The compositions of GWB and ERDA-6 predicted by EQ6 after Step 1 are similar, but not identical to, the compositions of these brines calculated by FMT for the PABC (Brush, 2005). On the other hand, the compositions of GWB and ERDA-6 after Step 2 are quite different from anything reported previously for WIPP disposal rooms. These differences probably reflect the dissolution of significant quantities of the SO_4^{2-} minerals in the DRZ (anhydrite, gypsum, and especially polyhalite), which resulted from the drawdown of dissolved SO_4^{2-} by microbial SO_4^{2-} reduction. The most significant difference is the pH predicted by EQ6 after Step 2: Most of the simulations predicted final pH values of 10.4-11.3, significantly higher than the values of ~ 9 predicted for the PABC.

Precipitation of calcite (or $\text{CaCO}_3(\text{am})$) and pirssonite from GWB and ERDA-6 consumed 40-46% of the CO_2 from microbial SO_4^{2-} reduction using SO_4^{2-} in DRZ minerals, and 38-43% of the CO_2 from all microbial activity. Calcite (or $\text{CaCO}_3(\text{am})$) consumed significantly more CO_2 than pirssonite. The range of CO_2 precipitated by calcite (or $\text{CaCO}_3(\text{am})$) was 38-42% of the CO_2 from SO_4^{2-} reduction using SO_4^{2-} in DRZ minerals, and 36-40% of the CO_2 from all microbial activity. The comparable ranges for pirssonite were 0-8% and 0-7%, respectively.

Carbonate minerals consumed somewhat more CO₂ in ERDA-6 than in GWB. For 1,045 and 7,763 m³ ERDA-6, a mean of 45.5% of the CO₂ from SO₄²⁻ reduction using SO₄²⁻ in DRZ minerals was precipitated by carbonates, and a mean of 42.5% of the CO₂ from all microbial activity was fixed by carbonates. The comparable values for GWB were 42.5 and 40%.

Increasing the brine volume decreased the quantity of CO₂ consumed by carbonate minerals slightly in both brines. Carbonate precipitation from GWB fixed 45 and 40% of the CO₂ from SO₄²⁻ reduction using SO₄²⁻ in DRZ minerals, and 42 and 38% the CO₂ from all microbial activity with brine volumes of 1,045 and 7,763 m³, respectively. Carbonate precipitation from ERDA-6 fixed 46, 45 and 44% of the CO₂ from SO₄²⁻ reduction, and 43, 42 and 41% the CO₂ from all microbial activity with volumes of 1,045, 7,763, and 13,267 m³, respectively.

The ranges of effective CO₂ yields for both brines were 0.54-0.60 for SO₄²⁻ reduction using SO₄²⁻ in DRZ minerals, and 0.57-0.62% for all microbial activity.

The effective CO₂ yields were somewhat lower with ERDA-6 than with GWB in the simulations with 1,045 and 7,763 m³ of brine. For ERDA-6, a mean of 0.545 was obtained for SO₄²⁻ reduction using SO₄²⁻ in DRZ minerals, and a mean of 0.575 was obtained for all microbial activity. The comparable values for GWB were 0.575 and 0.60.

Increasing the brine volume also increased the effective CO₂ yield slightly. The yields for GWB were 0.55 and 0.60 for SO₄²⁻ reduction using SO₄²⁻ from DRZ minerals, and 0.58 and 0.62 for all microbial activity with brine volumes of 1,045 and 7,763 m³, respectively. The yields for ERDA-6 were 0.54, 0.55 and 0.56 for SO₄²⁻ reduction, and 0.57, 0.58 and 0.59 for all microbial activity with volumes of 1,045, 7,763, and 13,267 m³, respectively.

Based on studies of the effects of single inhibitors, a number of inorganic elements and compounds, and organic ligands expected to be present in WIPP brines are known to decrease the rate of calcite precipitation. These include Mg, PO₄, SO₄, and Fe; and citrate, EDTA, oxalate, and humic acid. However, a number of other metastable, CaCO₃-bearing minerals can still precipitate if calcite precipitation is inhibited. These minerals, which include aragonite, vaterite, monohydrocalcite, ikaite, and CaCO₃(am), precipitate in order of increasing metastability (i.e., in order of increasing solubility product or free energy of formation). Although these species have been shown to inhibit the precipitation of calcite and other forms of CaCO₃, none of them have been shown to completely inhibit the precipitation of all forms of CaCO₃.

There have been few studies of the effects of multiple inhibitors acting simultaneously. However, results are available that imply that the simultaneous presence of Mg²⁺ and citrate can lead to the formation of magnesian calcites and, at high Mg²⁺ concentrations, aragonite precipitation. Based on a study of the effects of the Mg²⁺/citrate and Ca²⁺/citrate ratios on the MgCO₃ content of magnesian calcite, and the expected Mg²⁺/Ca²⁺ ratios in WIPP brines, we conclude that aragonite could be the dominant CaCO₃ phase precipitated in the repository, along with magnesian calcite containing up to 22% MgCO₃.

8 REFERENCES

- Akin, G.W., and J.V. Lagerwerff. 1965. "Calcium Carbonate Equilibria in Solutions Open to the Air. II. Enhanced Solubility of CaCO_3 in the Presence of Mg^{2+} and SO_4^{2-} ," *Geochimica et Cosmochimica Acta*. Vol. 29, no. 4, 353-360.
- Anadón, P., L. Roswell, and M.R. Talbot. 1992. "Carbonate Replacement of Lacustrine Gypsum Deposits in Two Neogene Continental Basins, Eastern Spain," *Sedimentary Geology*. Vol. 78, 201–216.
- Apelblat, A, and E. Manzurola. 1999. "Solubilities of Magnesium, Calcium, Barium, Cobalt, Nickel, Copper, and Zinc Acetates in Water from $T = (278.15 \text{ to } 348.15) \text{ K}$," *Journal of Chemical Thermodynamics*. Vol. 31, no. 10, 1347-1357.
- Babb, S.C., and C.F. Novak. 1997 and addenda. "User's Manual for FMT Version 2.3: A Computer Code Employing the Pitzer Activity Coefficient Formalism for Calculating Thermodynamic Equilibrium in Geochemical Systems to High Electrolyte Concentrations." Albuquerque, NM: Sandia National Laboratories. ERMS 243037.
- Bates, R.L., and J.A. Jackson, Eds. 1984. *Dictionary of Geological Terms*, Third Edition. New York, NY: Anchor Books (Doubleday).
- Brečević, L., A.E. Nielsen. 1989. "Solubility of Amorphous Calcium Carbonate," *Journal of Crystal Growth*. Vol. 98, 504-510.
- Brooks, R., L.M. Clark, and E.F. Thurston. 1950. "Calcium Carbonate and its Hydrates." *Philosophical Transactions of the Royal Society of London, Series A*. Vol. 243, 145-168.
- Brush, L.H. 1990. *Test Plan for Laboratory and Modeling Studies of Repository and Radionuclide Chemistry for the Waste Isolation Pilot Plant*. SAND90-0266. Albuquerque, NM: Sandia National Laboratories.
- Brush, L.H. 2005. "Results of Calculations of Actinide Solubilities for the WIPP Performance Assessment Baseline Calculations." Analysis report, May 18, 2005. Carlsbad, NM: Sandia National Laboratories. ERMS 539800.
- Brush, L.H., and Y. Xiong. 2003a. "Calculation of Actinide Solubilities for the WIPP Compliance Recertification Application, Analysis Plan AP-098, Rev. 1." April 14, 2003. Carlsbad, NM: Sandia National Laboratories. ERMS 527714.
- Brush, L.H., and Y. Xiong. 2003b. "Calculation of Actinide Solubilities for the WIPP Compliance Recertification Application." Analysis report, May 8, 2003. Carlsbad, NM: Sandia National Laboratories. ERMS 529131.

- Brush, L.H., and Y.-L. Xiong, 2005a. "Calculation of Actinide Solubilities for the WIPP Performance-Assessment Baseline Calculations, Analysis Plan AP-120, Rev. 0. April 4, 2005. Carlsbad, NM: Sandia National Laboratories. ERMS 539255.
- Brush, L.H., and Y.-L. Xiong. 2005b. "Calculation of Organic-Ligand Concentrations for the WIPP Performance-Assessment Baseline Calculations." Analysis report, May 4, 2005. Carlsbad, NM: Sandia National Laboratories. ERMS 539635.
- Busenberg, E., and L.N. Plummer. 1989. "Thermodynamics of Magnesian Calcite Solid Solutions at 25 Degrees C and 1 Atm Total Pressure," *Geochimica et Cosmochimica Acta*. Vol. 53, 1189-1208.
- Butler, J.N. 1982. *CO₂-Equilibria and Their Applications*. Chelsea, MI: Lewis Publishing Co.
- Chen, T., A. Neville, and M.D. Yuan. 2006. "Influence of Mg²⁺ on CaCO₃ Formation – Bulk Precipitation and Surface Deposition," *Chemical Engineering Science*. Vol. 61, no. 16, 5318-5327
- Clarkson, J.R., T.J. Price, and C.J. Adams. 1992. "Role of Metastable Phases in the Spontaneous Precipitation of Calcium Carbonate," *Journal of the Chemical Society, Faraday Transactions*. Vol. 88, no. 2, 243-249.
- Clayton, D. 2006. "Update of the Minimum Brine Volume for a Direct Brine Release and New Maximum Castile and Salado Brine Volumes in a Waste Panel." Memorandum to L.H. Brush, October 11, 2006. Carlsbad, NM: Sandia National Laboratories. ERMS 544453.
- Collier, A.P., and M.J. Hounslow. 1999. "Growth and Aggregation Rates for Calcite and Calcium Oxalate Monohydrate," *American Institute of Chemical Engineering Journal*. Vol. 45, no. 11, 2298-2305.
- Crawford, B.A. 2005a. "Determination of Waste Stream Oxyanions using TWBID Revision 2.1, Version 3.13, Data Version 4.15." Analysis report, February 24, 2005. Carlsbad, NM: Los Alamos National Laboratory. ERMS 538811.
- Crawford, B.A. 2005b. "Waste Material Densities in TRU Waste Streams from TWBID Revision 2.1, Version 3.13, Data Version D.4.15." Analysis report, April 13, 2005. Carlsbad, NM: Los Alamos National Laboratory. ERMS 539323.
- Daveler, S.A., and T.J. Wolery. 1992. *EQPT, A Data File Preprocessor for the EQ3/6 Software Package: User's Guide and Related Documentation (Version 7.0)*. UCRL-MA-110662 PT II. Livermore, CA: Lawrence Livermore National Laboratory.
- Davies, C.W. 1962. *Ion Association*. Washington, DC: Butterworths.

- Deer, W.A., R.A. Howie, and J. Zussman. 1992. *An Introduction to the Rock-Forming Minerals*. New York, NY: Longman Scientific and Technical.
- Fernández-Diáz, L., A. Putnis, M. Prieto, and C.V. Putnis. 1996. "The Role of Magnesium in the Crystallization of Calcite and Aragonite in a Porous Medium," *Journal of Sedimentary Research*. Vol. 66, no. 3, 482-491.
- Fiorucci, A.R., L.R. de Paula, E.A. Neves, and E.T.G. Cavalheiro. 2002. "Solubility of Alkali and Alkali Earth Salts of Dihydrogen Ethylenediaminetetraacetate in Aqueous Solutions," *Journal of Chemical and Engineering Data*. Vol. 47, 1510-1513.
- Fredd, C.N., and H.S. Fogler. 1998. "The Influence of Chelating Agents on the Kinetics of Calcite Dissolution," *Journal of Colloid and Interface Science*. Vol. 204, no. 1, 187-197.
- Gal, J. Y., J. C. Bollinger, H. Tolosa, and N. Gache. 1996. "Calcium Carbonate Solubility: A Reappraisal of Scale Formation and Inhibition," *Talanta*. Vol. 43, no. 9, 1497-1509.
- Garcia, J.-L., B.K.C. Patel, and B. Ollivier. 2000. "Taxonomic, Phylogenetic, and Ecological Diversity of Methanogenic *Archaea*," *Anaerobe*. Vol. 6, 205-226.
- Godelitsas, A., J.M. Astilleros, K. Hallam, S. Harissopoulos, and A. Putnis. 2003. "Interaction of Calcium Carbonates with Lead in Aqueous Solutions," *Environmental Science and Technology*. Vol. 37, 3351-3360.
- Hansen, C.W., L.H. Brush, M.B. Gross, F.D. Hansen, B.-Y. Park, J.S. Stein, and T.W. Thompson. 2004. "Effects of Supercompacted Waste and Heterogeneous Waste Emplacement on Repository Performance, Rev. 2." Analysis report, January 19, 2004. Sandia National Laboratories. ERMS 533551.
- Hansen, F.D., D.L. Lord, and T.W. Pfiefler. "Parameter Justification Report for DRSPALL, Rev. 0." Analysis report, August 11, 2003. Carlsbad, NM: Sandia National Laboratories. ERMS 531057.
- Kanney, J.F., A.C. Snider, T.W. Thompson, and L.H. Brush. 2004. "Effect of Naturally Occurring Sulfate on the MgO Safety Factor in the Presence of Supercompacted Waste and Heterogeneous Waste Emplacement." Analysis report, March 5, 2004. Carlsbad, NM: Sandia National laboratories. ERMS 534150.
- Kanney, J.F., and W. Zelinski. 2004. "Ratio of Brine Volume to Rock Volume in the DRZ Adjacent to the Repository." Memorandum to Y.-L. Xiong, September 9, 2004. Carlsbad, NM: Sandia National Laboratories. ERMS 536665.
- Katz, A. 1973. "The Interaction of Magnesium with Calcite during Crystal Growth at 25–90 °C and One Atmosphere," *Geochimica et Cosmochimica Acta*. Vol. 37, no. 6, 1563-1578.

- Kazmierczak, T.F., M.B. Tomson, and G.H. Nancollas. 1982. "Crystal Growth of Calcium Carbonate: A Controlled-Composition Kinetic Study," *Journal of Physical Chemistry*. Vol. 86, 103-107.
- van Langerak, E.P.A., M.M.H. Beekmans, J.J. Beun, H.V.M. Hamelers, and G. Lettinga. 1999. "Influence of Phosphate and Iron on the Extent of Calcium Carbonate Precipitation during Anaerobic Digestion," *Journal of Chemical Technology and Biotechnology*. Vol. 74, no. 11, 1030-1036.
- Lappin, A.R., R.L. Hunter, D.R. Garber, and P.B. Davies, Eds. 1989. *Systems Analysis, Long-Term Radionuclide Transport, and Dose Assessments, Waste Isolation Pilot Plant (WIPP), Southeastern New Mexico; March 1989*. SAND89-0462. Albuquerque, NM: Sandia National Laboratories.
- Larson, K.W. 1996. "Brine-Waste Contact Volumes for Scoping Analysis of Organic Ligand Concentration." Memorandum to R.V. Bynum, March 13, 1996. Albuquerque, NM: Sandia National Laboratories. ERMS 236044.
- Lebron, I., and D.L. Suarez. 1998. "Kinetics and Mechanisms of Precipitation of Calcite as Affected by P_{CO_2} and Organic Ligands at 25 Degrees C," *Geochimica et Cosmochimica Acta*. Vol. 62, no. 3, 405-416.
- de Leeuw, N.H., J.H. Harding, and S.C. Parker. 2002. "Molecular Dynamics Simulations of the Incorporation of Mg^{2+} , Cd^{2+} and Sr^{2+} at Calcite Growth Steps: Introduction of a $SrCO_3$ Potential Model," *Molecular Simulation*. Vol. 28, 573-589.
- Lin, Y.P., and P. C. Singer. 2006. "Inhibition of Calcite Precipitation by Orthophosphate: Speciation and Thermodynamic Considerations," *Geochimica et Cosmochimica Acta*. Vol. 70, 2530-2539.
- Lüttge, A., and P.G. Conrad. 2004. "Direct Observation of Microbial Inhibition of Calcite Dissolution," *Applied and Environmental Microbiology*. Vol. 70, no. 3, 1627-1632.
- Loos, D, C. Pasel, M. Luckas, K.G. Schmidt, and J.D. Herbell. 2004. "Experimental Investigation and Modelling of the Solubility of Calcite and Gypsum in Aqueous Systems at Higher Ionic Strength," *Fluid Phase Equilibria*. Vol. 219, no. 2, 219-229.
- Marcinowski, F. 2003. Untitled letter from F. Marcinowski to I.R. Triay with additional issues from the EPA's review of DOE's request to dispose of supercompacted waste from the Advanced Mixed Waste Treatment Program in the WIPP, December 9, 2003. Washington, DC: U.S. Environmental Protection Agency Office of Air and Radiation. ERMS 533464.

- Marcinowski, F. 2004. Untitled letter with attachment from F. Marcinowski to R.P. Detwiler approving the DOE's request to dispose of compressed (supercompacted) waste from the Advanced Mixed Waste Treatment Program in the WIPP, March 26, 2004. Washington, DC: U.S. Environmental Protection Agency Office of Air and Radiation. ERMS 534327.
- Matty, J.M., and M.B. Tomson. 1988. "Effect of Multiple Precipitation Inhibitors on Calcium Carbonate Nucleation," *Applied Geochemistry*. Vol. 3, 549-556.
- Meldrum, F.C., and S.T. Hyde. 2001. "Morphological Influence of Magnesium and Organic Additives on the Precipitation of Calcite," *Journal of Crystal Growth*. Vol. 231, no. 4, 544-558.
- Moody, D.C. 2006. Untitled letter from D.C. Moody to E.A. Cotsworth requesting EPA approval of the DOE's request reduce the amount of excess MgO currently being emplaced in the WIPP, April 10, 2006. Carlsbad, NM: U.S. Department of Energy Carlsbad Field Office. ERMS 543262.
- Morse, J.W. 1983. "The Kinetics of Calcium Carbonate Dissolution and Precipitation," *Carbonates: Mineralogy and Chemistry*. Ed. R.J. Reeder. Blacksburg, VA: Mineralogical Society of America. Reviews in Mineralogy, Vol. 11, 227-264.
- Nemer, M.B. and J.S. Stein. 2005. "Analysis Package for BRAGFLO: 2004 Compliance Recertification Application Performance Assessment Baseline Calculation." Analysis Report, June 28, 2005. Carlsbad, NM: Sandia National Laboratories. ERMS 540527.
- Paquette, J., H. Vali, and A. Mucci. 1996. "TEM Study of Pt-C Replicas of Calcite Overgrowths Precipitated from Electrolyte Solutions," *Geochimica et Cosmochimica Acta*. Vol. 60, no. 23, 4689-4699.
- Peckmann, J., J. Paul, and V. Thiel. 1999. "Bacterially Mediated Formation of Diagenetic Aragonite and Native Sulfur in Zechstein Carbonates (Upper Permian), Central Germany)," *Sedimentary Geology*. Vol. 126, 205-222.
- Phillips, B.L., Y.J. Lee, and R.J. Reeder. 2005. "Organic Coprecipitates with Calcite: NMR Spectroscopic Evidence," *Environmental Science and Technology*. Vol. 39 no. 12, 4533-4539.
- Pitzer, K.S. 1991. *Activity Coefficients in Electrolyte Solutions*. Boca Raton, FL: CRC Press.
- Plummer, L.N., and E. Busenberg. 1982. "The Solubilities of Calcite, Aragonite and Vaterite in CO₂-H₂O Solutions between 0 and 90 °C, and an Evaluation of the Aqueous Model for the System CaCO₃-CO₂-H₂O," *Geochimica et Cosmochimica Acta*. Vol. 46, 1011-1040.

- Pokrovsky, O.S., and J. Schott. 2001. "Kinetics and Mechanism of Dolomite Dissolution in Neutral to Alkaline Solutions Revisited," *American Journal of Science*. Vol. 301, no. 7, 597-628.
- Popielak, R.S., R.L. Beauheim, S.R. Black, W.E. Coons, C.T. Ellingson and R.L. Olsen. 1983. *Brine Reservoirs in the Castile Formation, Waste Isolation Pilot Plant Project, Southeastern New Mexico*. TME 3153. Carlsbad, NM: U.S. Department of Energy WIPP Project Office.
- Sabbides, T.G., and P.G. Koutsoukos. 1993. "The Crystallization of Calcium-Carbonate in Artificial Seawater - Role of the Substrate," *Journal of Crystal Growth*. Vol. 133, no. 1-2, 13-22.
- Snider, A.C. 2003. "Verification of the Definition of Generic Weep Brine and the Development of a Recipe for This Brine." Analysis report, April 8, 2003. Carlsbad, NM: Sandia National Laboratories. ERMS 527505.
- Stein, C.L. 1985. *Mineralogy in the Waste Isolation Pilot Plant (WIPP) Facility Stratigraphic Horizon*. SAND85-0321. Albuquerque, NM: Sandia National Laboratories.
- Stein, J.S. 2005. "Estimate of Volume of Brine in Repository That Leads to a Brine Release." Memorandum to L.H. Brush, April 19, 2005. Carlsbad, NM: Sandia National Laboratories. ERMS 539372.
- Stumm, W., and J.J. Morgan. 1996. *Aquatic Chemistry*, Third Edition. New York, NY: John Wiley and Sons, Inc.
- Tomson, M.B. 1983. "Effect of Precipitation Inhibitors on Calcium Carbonate Scale Formation," *Journal of Crystal Growth*. Vol. 62, 106-112.
- Trovato, E.R. 1997. Untitled letter from E.R. Trovato to G. Dials with enclosures (parameters that are no longer of concern and parameters that DOE must use for the PAVT), April 25, 1997. Washington, DC: U.S. Environmental Protection Agency Office of Radiation and Indoor Air. ERMS 247206.
- U.S. DOE. 1996. *Title 40 CFR Part 191 Compliance Certification Application for the Waste Isolation Pilot Plant, Vol. 1-21*. DOE/CAO-1994-2184. Carlsbad, NM: U.S. Department of Energy Carlsbad Area Office.
- U.S. DOE. 2004. *Title 40 CFR Part 191 Compliance Recertification Application for the Waste Isolation Pilot Plant, Vol. 1-8*. DOE/WIPP 2004-3231. Carlsbad, NM: U.S. Department of Energy Carlsbad Field Office.

- U.S. EPA. 1997. "Compliance Application Review Documents for the Criteria for the Certification and Recertification of the Waste Isolation Pilot Plant's Compliance with the 40 CFR Part 191 Disposal Regulations: Final Certification Decision. CARD 44: Engineered Barrier." EPA Air Docket A-93-02-V-B-2. Washington, DC: U.S. Environmental Protection Agency Office of Radiation and Indoor Air.
- U.S. EPA. 1998a. "Technical Support Document for Section 194.23 – Models and Computer Codes." EPA Air Docket A-93-02-V-B-6. Washington, DC: U.S. Environmental Protection Agency Office of Radiation and Indoor Air.
- U.S. EPA. 1998b. "Technical Support Document for Section 194.24: EPA's Evaluation of DOE's Actinide Source Term." EPA Air Docket A-93-02-V-B-17. Washington, DC: U.S. Environmental Protection Agency Office of Radiation and Indoor Air.
- Wada, N., K. Yamashita, and T. Umegaki. 1995. "Effects of Divalent Cations upon Nucleation, Growth and Transformation of Calcium-Carbonate Polymorphs under Conditions of Double Diffusion," *Journal of Crystal Growth*. Vol. 148, no. 3, 297-304.
- Wang, Y. 1998. "WIPP PA Validation Document for FMT (Version 2.4), Document Version 2.4." Carlsbad, NM: Sandia National Laboratories. ERMS 251587.
- Westin, K., and A.C. Rasmuson. 2005. "Crystal Growth of Aragonite and Calcite in Presence of Citric Acid, DTPA, EDTA and Pyromellitic Acid," *Journal of Colloid and Interface Science*. Vol. 282, no. 2, 359-369.
- Wolery, T.J. 1992a. *EQ3/6, A Software Package for Geochemical Modeling of Aqueous Systems: Package Overview and Installation Guide (Version 7.0)*. UCRL-MA-110662 PT I. Livermore, CA: Lawrence Livermore National Laboratory.
- Wolery, T.J. 1992b. *EQ3NR, A Computer Program for Geochemical Aqueous Speciation-Solubility Calculations: Theoretical Manual, User's Guide, and Related Documentation (Version 7.0)*. UCRL-MA-110662 PT III. Livermore, CA: Lawrence Livermore National Laboratory.
- Wolery, T.J., and S.A. Daveler. 1992. *EQ6, A Computer Program for Reaction-Path Modeling of Aqueous Geochemical Systems: Theoretical Manual, User's Guide, and Related Documentation (Version 7.0)*. UCRL-MA-110662 PT IV. Livermore, CA: Lawrence Livermore National Laboratory.
- Xiong, Y.-L. 2004. "Incorporation of Six Solid Phases Including Hydromagnesite (5424) and Hydromagnesite (4323) into EQ3/6 HMW Database and Its Modified Version HMP." Memorandum to L.H. Brush, August 4, 2004. Carlsbad, NM: Sandia National Laboratories. ERMS 536321.
- Xiong, Y.-L. 2005. "Release of FMT_050405.CHEMDAT." E-mail to J.F. Kanney and J.J. Long, April 5, 2005. Carlsbad, NM: Sandia National Laboratories. ERMS 539304.

- Xiong, Y.-L. 2006a. "Incorporation of Calcium Citrate Hydrate, Earlandite; Calcium Oxalate Monohydrate, Whewellite; and Aqueous Species of Citrate and Oxalate into the EQ3/6 HMP Database and Its Modified Version HMY." Memorandum to L.H. Brush, October 18, 2006. Carlsbad, NM: Sandia National Laboratories. ERMS 544529.
- Xiong, Y.-L. 2006b. "Incorporation of Amorphous Calcium Carbonate into the EQ3/6 HMY Database and Its Modified Version HML." Memorandum to L.H. Brush, October 26, 2006. Carlsbad, NM: Sandia National Laboratories. ERMS 544629.
- Xiong, Y.-L., and A.S. Lord. 2006. "Experimental Investigations of the Reaction Path in the MgO-CO₂-H₂O System in Concentrated Solutions with Ionic Strength up to ~7 M at Ambient Temperature and Ambient Atmospheric CO₂ Partial Pressure, and Their Applications," submitted to *Geochemical Transactions*. Albuquerque, NM: Sandia National Laboratories. SAND2006-7185J.
- Zhang, Y., and R. Dawe. 1998. "The Kinetics of Calcite Precipitation from a High-Salinity Water," *Applied Geochemistry*. Vol. 13, 177-184.
- Zuddas, P., and A. Mucci. 1994. "Kinetics of Calcite Precipitation from Seawater: I. A Classical Chemical Kinetics Description for Strong Electrolyte Solutions," *Geochimica et Cosmochimica Acta*. Vol. 58, 4353-4362.
- Zuddas, P., and A. Mucci. 1998. "Kinetics of Calcite Precipitation from Seawater: II. The Influence of the Ionic Strength," *Geochimica et Cosmochimica Acta*. Vol. 62, no. 5, 757-766.
- Zuddas, P., K. Pachana, and D. Faivre. 2003. "The influence of Dissolved Humic Acids on the Kinetics of Calcite Precipitation from Seawater Solutions," *Chemical Geology*. Vol. 201, 91-101.

9 TABLES

Table 1. Abbreviations, Acronyms, and Initialisms.

Abbreviation, Acronym or Initialism	Definition
acetate, acetic acid	CH_3CO_2^- , $\text{CH}_3\text{CO}_2\text{H}$
Al	aluminum
am	amorphous
anhydrite	CaSO_4
aq	aqueous
aragonite	CaCO_3
$\text{B}(\text{OH})_x^{3-}$	boric acid/borate
Br, Br^-	bromine, bromide (ion)
BRAGFLO	Brine and Gas Flow, a WIPP PA code
Brine A	a synthetic brine representative of intergranular Salado brines
brucite	$\text{Mg}(\text{OH})_2$
C	carbon
Ca, Ca^{2+}	calcium, calcium ion
$\text{CaCO}_3(\text{am})$	amorphous CaCO_3
calcite	CaCO_3
CCA	(WIPP) Compliance Certification Application, submitted to the EPA in October 1996
CH_4	methane
$\text{C}_6\text{H}_{10}\text{O}_5$	cellulose
citrate, citric acid	$(\text{CH}_2\text{CO}_2\text{H})_2\text{C}(\text{OH})(\text{CO}_2)^-$, $(\text{CH}_2\text{CO}_2\text{H})_2\text{C}(\text{OH})(\text{CO}_2\text{H})$
Cl, Cl^-	chlorine, chloride ion
CO_2	carbon dioxide
CO_3 , CO_3^{2-}	carbonate, carbonate ion
CPR	cellulosic, plastic, and rubber
CRA-2004	(WIPP) Compliance Recertification Application, submitted to the EPA in March 2004
DOE	(U.S.) Department of Energy
dolomite	$\text{CaMg}(\text{CO}_3)_2$
DRZ	disturbed rock zone
EDTA	ethylenediaminetetraacetate, $(\text{CH}_2\text{CO}_2\text{H})_2\text{N}(\text{CH}_2)_2\text{N}(\text{CH}_2\text{CO}_2\text{H})(\text{CH}_2\text{CO}_2)^-$; or ethylenediaminetetraacetic acid, $(\text{CH}_2\text{CO}_2\text{H})_2\text{N}(\text{CH}_2)_2\text{N}(\text{CH}_2\text{CO}_2\text{H})_2$
EPA	(U.S.) Environmental Protection Agency
EQ3/6	a geochemical software package for speciation and solubility calculations (EQ3NR) and reaction-path calculations (EQ6)
ERDA-6	Energy Research and Development Administration (WIPP Well) 6, a synthetic brine representative of fluids in Castile brine reservoirs

Table 1. Abbreviations, Acronyms, and Initialisms (cont.).

Abbreviation, Acronym or Initialism	Definition
f_{CO_2}	fugacity (similar to the partial pressure) of CO_2
Fe	iron
Fm.	Formation or formation, depending on usage
FMT	Fracture-Matrix Transport, a geochemical speciation and solubility code
g	gaseous
gaylussite	$\text{Na}_2\text{Ca}(\text{CO}_3)_2 \cdot 5\text{H}_2\text{O}$
GWB	Generic Weep Brine, a synthetic brine representative of intergranular Salado brines
gypsum	$\text{CaSO}_4 \cdot 2\text{H}_2\text{O}$
H_2 , H^+	hydrogen, hydrogen ion
H_2O	water (aq or g)
halite	NaCl
HCO_3^-	bicarbonate ion
H_2CO_3 ,	carbonic acid
H_2S	hydrogen sulfide
hydromagnesite	$\text{Mg}_4(\text{CO}_3)_3(\text{OH})_2 \cdot 3\text{H}_2\text{O}$ or $\text{Mg}_5(\text{CO}_3)_4(\text{OH})_2 \cdot 4\text{H}_2\text{O}$
ikaite	$\text{CaCO}_3 \cdot 6\text{H}_2\text{O}$
K, K^+	potassium, potassium ion
kg	kilogram(s)
L	liter(s)
M	molar
m	molal
magnesite	MgCO_3
Mg, Mg^{2+}	magnesium, magnesium ion
Mg	milligram(s)
MgO	magnesium oxide, used to refer to the WIPP engineered barrier, which includes periclase as the primary constituent and various impurities
mM	millimolar
nm	millimolal
monohydrocalcite	$\text{CaCO}_3 \cdot \text{H}_2\text{O}$
μM	micromolar
μm	micromolal
Na, Na^+	sodium, sodium ion
N_2	nitrogen
NO_3 , NO_3^-	nitrate, nitrate ion
OH^-	hydroxide ion

Table 1. Abbreviations, Acronyms, and Initialisms (cont.).

Abbreviation, Acronym or Initialism	Definition
oxalate, oxalic acid	$(\text{CO}_2\text{H})(\text{CO}_2)^-$, $(\text{CO}_2\text{H})_2$
PA	performance assessment
PABC	Performance Assessment Baseline Calculations, part of the CRA-2004
PAVT	(WIPP) Performance Assessment Verification Test
periclase	pure, crystalline MgO , the primary constituent of the WIPP engineered barrier
pH	the negative, common logarithm of the activity of H^+
pirssonite	$\text{Na}_2\text{Ca}(\text{CO}_3)_2 \cdot 2\text{H}_2\text{O}$
polyhalite	$\text{K}_2\text{MgCa}_2(\text{SO}_4)_4 \cdot 2\text{H}_2\text{O}$
QA	quality assurance
Rev.	Revision
Si	silicon
SO_4 , SO_4^{2-}	sulfate, sulfate ion
TRU	transuranic waste
WIPP	(U.S. DOE) Waste Isolation Pilot Plant
XRD	X-ray diffraction (analysis)

Table 2. Summary of Simulations Carried Out for This Analysis.

EQ6 File Numbers	Brine Type	Brine Volume	Mg-Carbonate Used	Organic Ligands	Polymorph of CaCO ₃ Used	Relevant Tables In This Report (Input, Brine Chemistry, and Results)
Effects of Brine Composition and Brine Volume on Carbonate Precipitation						
	GWB	1,045	Magnesite	No	Calcite	Tables 5, 16, and 21
	ERDA-8	1,045	Magnesite	No	Calcite	Tables 6, 17, and 22
	GWB	7,763	Magnesite	No	Calcite	Tables 7, 18, and 23
	ERDA-6	7,763	Magnesite	No	Calcite	Tables 8, 19, and 24
	ERDA-6	13,267	Magnesite	No	Calcite	Tables 9, 20, and 25
Effects of Hydromagnesite on Carbonate Precipitation						
	GWB	7,763	Hydromagnesite	No	Calcite	Tables 10, 26, and 28
	ERDA-6	7,763	Hydromagnesite	No	Calcite	Tables 11, 27, and 29
Effects of Organic Ligands on Carbonate Precipitation						
	GWB	1,045	Magnesite	Yes	Calcite	Tables 12, 30, and 32
	ERDA-8	1,045	Magnesite	Yes	Calcite	Tables 13, 31, and 33
Effects of CaCO ₃ (am) on Carbonate Precipitation						
	GWB	1,045	Magnesite	Yes	CaCO ₃ (am)	Tables 14, 34, and 36
	ERDA-8	1,045	Magnesite	Yes	CaCO ₃ (am)	Tables 15, 35, and 37

Table 3. Compositions of GWB and ERDA-6 Before and After Equilibration with MgO, Halite and Anhydrite (M, unless otherwise noted).

Element or Property	GWB Before Reaction with MgO, Halite, and Anhydrite ^A	GWB After Reaction with MgO, Halite, and Anhydrite ^B	ERDA-6 Before Reaction with MgO, Halite, and Anhydrite ^C	ERDA-6 After Reaction with MgO, Halite, and Anhydrite ^D
B(OH) _x ^{3-x}	0.158	0.166	0.063	0.0624
Na ⁺	3.53	4.35	4.87	5.24
Mg ²⁺	1.02	0.578	0.019	157
K ⁺	0.467	0.490	0.097	0.0961
Ca ²⁺	0.014	0.00895	0.012	0.0107
SO ₄ ²⁻	0.177	0.228	0.170	0.179
Cl ⁻	5.86	5.38	4.8	5.24
Br ⁻	0.0266	0.0278	0.011	0.0109
Total inorganic C	-	0.350 mM	16 mM	0.428 mM
Ionic strength	-	7.66 m	-	6.80 m
log f _{CO₂}	-	-5.50	-	-5.50
pH	-	8.69	6.17	8.94
Relative humidity	-	0.732	-	0.748
Specific gravity	1.2	1.23	1.216	1.22

A. From Snider (2003).

B. FMT Run 7 (Brush, 2005).

C. From Popielak et al. (1993).

D. FMT Run 11 (Brush, 2005).

Table 4. Suffixes for EQ3/6 Files (“*” denotes wild card).

Suffix	File Definition
*.3i	EQ3NR input files
*.3o	EQ3NR output files
*.3p	EQ3NR pickup files
*.6i	EQ6 input files
*.6o	EQ6 output files
*.6p	EQ6 pickup files
*.6t	EQ6 tab files
*.6tx	EQ6 tabx files

Table 5. Input Parameters for the Simulation with 1,045 m³ of GWB.^{A, B} Assumed that carbonation of brucite produces magnesite and that calcite precipitates, no organic ligands.

Input Parameter	Value for the Repository	Value for a Seven-Room Panel	Value Used in EQ6 Input File for Step 1
Vol. of GWB	$1.001 \times 10^4 \text{ m}^3$	$1.045 \times 10^3 \text{ m}^3$	$1.15 \times 10^0 \text{ L}$
Dissolved solids in GWB ^C	$3.62 \times 10^6 \text{ kg}$	$3.78 \times 10^5 \text{ kg}$	$4.16 \times 10^{-1} \text{ kg}$
H ₂ O in GWB ^D	$8.71 \times 10^9 \text{ kg}$	$9.10 \times 10^8 \text{ kg}$	$1.00 \times 10^0 \text{ kg}$
Organic C remaining in CPR materials ^E	$1.04 \times 10^9 \text{ mol}$	$1.08 \times 10^8 \text{ mol}$	$1.19 \times 10^2 \text{ mol}$
Brucite remaining ^F	$1.26 \times 10^9 \text{ mol}$	$1.32 \times 10^8 \text{ mol}$	$1.45 \times 10^2 \text{ mol}$
SO ₄ ²⁻ required ^G	$5.18 \times 10^8 \text{ mol}$	$5.41 \times 10^7 \text{ mol}$	$5.95 \times 10^1 \text{ mol}$
DRZ required ^G	$1.54 \times 10^9 \text{ kg};$ $7.07 \times 10^5 \text{ m}^3$	$1.61 \times 10^8 \text{ kg};$ $7.38 \times 10^4 \text{ m}^3$	$1.77 \times 10^2 \text{ kg};$ $8.12 \times 10^1 \text{ L}$
Halite present ^H	$2.46 \times 10^{10} \text{ mol}$	$2.57 \times 10^9 \text{ mol}$	$2.81 \times 10^3 \text{ mol}$
Anhydrite required ^G	$1.92 \times 10^8 \text{ mol}$	$2.01 \times 10^7 \text{ mol}$	$2.21 \times 10^1 \text{ mol}$
Gypsum required ^G	$1.52 \times 10^8 \text{ mol}$	$1.59 \times 10^7 \text{ mol}$	$1.75 \times 10^1 \text{ mol}$
Magnesite present ^H	$3.11 \times 10^8 \text{ mol}$	$3.24 \times 10^7 \text{ mol}$	$3.57 \times 10^1 \text{ mol}$
Polyhalite required ^G	$4.35 \times 10^7 \text{ mol}$	$4.54 \times 10^6 \text{ mol}$	$4.99 \times 10^0 \text{ mol}$
CO ₂ required ^I	$1.04 \times 10^9 \text{ mol}$	$1.08 \times 10^8 \text{ mol}$	$1.19 \times 10^2 \text{ mol}$

A. Used for EQ6 input file 06GMIN01.6I.

B. Scaling factor = L GWB/repository ÷ L GWB/EQ6 input file = 8.7122×10^6 .

C. 1 L of GWB contains 0.3617108 kg dissolved solids, based on the chemical composition in Table 2 (see above) and a specific gravity of 1.2321 kg/L from FMT Run 7 for the CRA-2004 PABC.

D. 1 L of GWB contains 0.8703892 kg H₂O, based on the chemical composition in Table 2 and a specific gravity of 1.2321 kg/L from FMT Run 7 for the CRA-2004 PABC.

E. After microbial denitrification and SO₄²⁻ reduction using SO₄²⁻ in the waste.

F. After formation of magnesite resulting from microbial denitrification and SO₄²⁻ reduction using SO₄²⁻ in the waste.

G. For consumption via SO₄²⁻ reduction (see Reaction 2) of CPR materials remaining after microbial denitrification and SO₄²⁻ reduction using SO₄²⁻ in the waste.

H. In the DRZ along with the required quantities of anhydrite, gypsum, and polyhalite.

I. To simulate production from SO₄²⁻ reduction (Reaction 2) of CPR materials remaining after microbial denitrification and SO₄²⁻ reduction using SO₄²⁻ in the waste.

Table 6. Input Parameters for the Simulation with 1,045 m³ of ERDA-6.^{A, B} Assumed that carbonation of brucite produces magnesite and that calcite precipitates, no organic ligands.

Input Parameter	Value for the Repository	Value for a Seven-Room Panel	Value Used in EQ6 Input File for Step 1
Vol. of ERDA-6	$1.001 \times 10^4 \text{ m}^3$	$1.045 \times 10^3 \text{ m}^3$	$1.10 \times 10^0 \text{ L}$
Dissolved solids in ERDA-6 ^C	$3.08 \times 10^6 \text{ kg}$	$3.22 \times 10^5 \text{ kg}$	$3.39 \times 10^{-1} \text{ kg}$
H ₂ O in ERDA-6 ^D	$9.09 \times 10^9 \text{ kg}$	$9.49 \times 10^8 \text{ kg}$	$1.00 \times 10^0 \text{ kg}$
Organic C remaining in CPR materials ^E	$1.04 \times 10^9 \text{ mol}$	$1.08 \times 10^8 \text{ mol}$	$1.14 \times 10^2 \text{ mol}$
Brucite remaining ^F	$1.26 \times 10^9 \text{ mol}$	$1.32 \times 10^8 \text{ mol}$	$1.39 \times 10^2 \text{ mol}$
SO ₄ ²⁻ required ^G	$5.18 \times 10^8 \text{ mol}$	$5.41 \times 10^7 \text{ mol}$	$5.70 \times 10^1 \text{ mol}$
DRZ required ^G	$1.54 \times 10^9 \text{ kg};$ $7.07 \times 10^5 \text{ m}^3$	$1.61 \times 10^8 \text{ kg};$ $7.38 \times 10^4 \text{ m}^3$	$1.70 \times 10^2 \text{ kg};$ $7.78 \times 10^1 \text{ L}$
Halite present ^H	$2.46 \times 10^{10} \text{ mol}$	$2.57 \times 10^9 \text{ mol}$	$2.70 \times 10^3 \text{ mol}$
Anhydrite required ^G	$1.92 \times 10^8 \text{ mol}$	$2.01 \times 10^7 \text{ mol}$	$2.12 \times 10^1 \text{ mol}$
Gypsum required ^G	$1.52 \times 10^8 \text{ mol}$	$1.59 \times 10^7 \text{ mol}$	$1.67 \times 10^1 \text{ mol}$
Magnesite present ^H	$3.11 \times 10^8 \text{ mol}$	$3.24 \times 10^7 \text{ mol}$	$3.42 \times 10^1 \text{ mol}$
Polyhalite required ^G	$4.35 \times 10^7 \text{ mol}$	$4.54 \times 10^6 \text{ mol}$	$4.78 \times 10^0 \text{ mol}$
CO ₂ required ^I	$1.04 \times 10^9 \text{ mol}$	$1.08 \times 10^8 \text{ mol}$	$1.14 \times 10^2 \text{ mol}$

A. Used for EQ6 input file 06EMIN01.6I.

B. Scaling factor = L ERDA-6/repository ÷ L ERDA-6/EQ6 input file = 9.0887×10^6 .

C. 1 L of ERDA-6 contains 0.308002 kg dissolved solids, based on the chemical composition in Table 2 (see above) and a specific gravity of 1.216 kg/L from Table 2.

D. 1 L of ERDA-6 contains 0.907998 kg H₂O, based on the chemical composition in Table 2 and a specific gravity of 1.216 kg/L from Table 2.

E. After microbial denitrification and SO₄²⁻ reduction using SO₄²⁻ in the waste.

F. After formation of magnesite resulting from microbial denitrification and SO₄²⁻ reduction using SO₄²⁻ in the waste.

G. For consumption via SO₄²⁻ reduction (see Reaction 2) of CPR materials remaining after microbial denitrification and SO₄²⁻ reduction using SO₄²⁻ in the waste.

H. In the DRZ along with the required quantities of anhydrite, gypsum, and polyhalite.

I. To simulate production from SO₄²⁻ reduction (Reaction 2) of CPR materials remaining after microbial denitrification and SO₄²⁻ reduction using SO₄²⁻ in the waste.

Table 7. Input Parameters for the Simulation with 7,763 m³ of GWB.^{A, B} Assumed that carbonation of brucite produces magnesite and that calcite precipitates, no organic ligands.

Input Parameter	Value for the Repository	Value for a Seven-Room Panel	Value Used in EQ6 Input File for Step 1
Vol. of GWB	$7.436 \times 10^4 \text{ m}^3$	$7.763 \times 10^3 \text{ m}^3$	$1.15 \times 10^0 \text{ L}$
Dissolved solids in GWB ^C	$2.69 \times 10^7 \text{ kg}$	$2.81 \times 10^6 \text{ kg}$	$4.16 \times 10^{-1} \text{ kg}$
H ₂ O in GWB ^D	$6.47 \times 10^{10} \text{ kg}$	$6.76 \times 10^9 \text{ kg}$	$1.00 \times 10^0 \text{ kg}$
Organic C remaining in CPR materials ^E	$1.04 \times 10^9 \text{ mol}$	$1.08 \times 10^8 \text{ mol}$	$1.60 \times 10^1 \text{ mol}$
Brucite remaining ^F	$1.26 \times 10^9 \text{ mol}$	$1.32 \times 10^8 \text{ mol}$	$1.95 \times 10^1 \text{ mol}$
SO ₄ ²⁻ required ^G	$5.18 \times 10^8 \text{ mol}$	$5.41 \times 10^7 \text{ mol}$	$8.01 \times 10^0 \text{ mol}$
DRZ required ^G	$1.54 \times 10^9 \text{ kg};$ $7.07 \times 10^5 \text{ m}^3$	$1.61 \times 10^8 \text{ kg};$ $7.38 \times 10^4 \text{ m}^3$	$2.38 \times 10^1 \text{ kg};$ $1.09 \times 10^1 \text{ L}$
Halite present ^H	$2.46 \times 10^{10} \text{ mol}$	$2.57 \times 10^9 \text{ mol}$	$3.80 \times 10^2 \text{ mol}$
Anhydrite required ^G	$1.92 \times 10^8 \text{ mol}$	$2.01 \times 10^7 \text{ mol}$	$2.97 \times 10^0 \text{ mol}$
Gypsum required ^G	$1.52 \times 10^8 \text{ mol}$	$1.59 \times 10^7 \text{ mol}$	$2.35 \times 10^0 \text{ mol}$
Magnesite present ^H	$3.11 \times 10^8 \text{ mol}$	$3.24 \times 10^7 \text{ mol}$	$4.80 \times 10^0 \text{ mol}$
Polyhalite required ^G	$4.35 \times 10^7 \text{ mol}$	$4.54 \times 10^6 \text{ mol}$	$6.71 \times 10^{-1} \text{ mol}$
CO ₂ required ^I	$1.04 \times 10^9 \text{ mol}$	$1.08 \times 10^8 \text{ mol}$	$1.60 \times 10^1 \text{ mol}$

A. Used for EQ6 input file 06GMID01.6I.

B. Scaling factor = L GWB/repository ÷ L GWB/EQ6 input file = 6.4721×10^7 .

C. 1 L of GWB contains 0.3617108 kg dissolved solids, based on the chemical composition in Table 2 (see above) and a specific gravity of 1.2321 kg/L from FMT Run 7 for the CRA-2004 PABC.

D. 1 L of GWB contains 0.8703892 kg H₂O, based on the chemical composition in Table 2 and a specific gravity of 1.2321 kg/L from FMT Run 7 for the CRA-2004 PABC.

E. After microbial denitrification and SO₄²⁻ reduction using SO₄²⁻ in the waste.

F. After formation of magnesite resulting from microbial denitrification and SO₄²⁻ reduction using SO₄²⁻ in the waste.

G. For consumption via SO₄²⁻ reduction (see Reaction 2) of CPR materials remaining after microbial denitrification and SO₄²⁻ reduction using SO₄²⁻ in the waste.

H. In the DRZ along with the required quantities of anhydrite, gypsum, and polyhalite.

I. To simulate production from SO₄²⁻ reduction (Reaction 2) of CPR materials remaining after microbial denitrification and SO₄²⁻ reduction using SO₄²⁻ in the waste.

Table 8. Input Parameters for the Simulation with 7,763 m³ of ERDA-6.^{A, B} Assumed that carbonation of brucite produces magnesite and that calcite precipitates, no organic ligands.

Input Parameter	Value for the Repository	Value for a Seven-Room Panel	Value Used in EQ6 Input File for Step 1
Vol. of ERDA-6	$7.436 \times 10^4 \text{ m}^3$	$7.763 \times 10^3 \text{ m}^3$	$1.10 \times 10^0 \text{ L}$
Dissolved solids in ERDA-6 ^C	$2.29 \times 10^7 \text{ kg}$	$2.39 \times 10^6 \text{ kg}$	$3.39 \times 10^{-1} \text{ kg}$
H ₂ O in ERDA-6 ^D	$6.75 \times 10^{10} \text{ kg}$	$7.05 \times 10^9 \text{ kg}$	$1.00 \times 10^0 \text{ kg}$
Organic C remaining in CPR materials ^E	$1.04 \times 10^9 \text{ mol}$	$1.08 \times 10^8 \text{ mol}$	$1.54 \times 10^1 \text{ mol}$
Brucite remaining ^F	$1.26 \times 10^9 \text{ mol}$	$1.32 \times 10^8 \text{ mol}$	$1.87 \times 10^1 \text{ mol}$
SO ₄ ²⁻ required ^G	$5.18 \times 10^8 \text{ mol}$	$5.41 \times 10^7 \text{ mol}$	$7.67 \times 10^0 \text{ mol}$
DRZ required ^G	$1.54 \times 10^9 \text{ kg};$ $7.07 \times 10^5 \text{ m}^3$	$1.61 \times 10^8 \text{ kg};$ $7.38 \times 10^4 \text{ m}^3$	$2.28 \times 10^1 \text{ kg};$ $1.05 \times 10^1 \text{ L}$
Halite present ^H	$2.46 \times 10^{10} \text{ mol}$	$2.57 \times 10^9 \text{ mol}$	$3.64 \times 10^2 \text{ mol}$
Anhydrite required ^G	$1.92 \times 10^8 \text{ mol}$	$2.01 \times 10^7 \text{ mol}$	$2.85 \times 10^0 \text{ mol}$
Gypsum required ^G	$1.52 \times 10^8 \text{ mol}$	$1.59 \times 10^7 \text{ mol}$	$2.25 \times 10^0 \text{ mol}$
Magnesite present ^H	$3.11 \times 10^8 \text{ mol}$	$3.24 \times 10^7 \text{ mol}$	$4.60 \times 10^0 \text{ mol}$
Polyhalite required ^G	$4.35 \times 10^7 \text{ mol}$	$4.54 \times 10^6 \text{ mol}$	$6.44 \times 10^{-1} \text{ mol}$
CO ₂ required ^I	$1.04 \times 10^9 \text{ mol}$	$1.08 \times 10^8 \text{ mol}$	$1.54 \times 10^1 \text{ mol}$

A. Used for EQ6 input file 06EMID01.6I.

B. Scaling factor = L ERDA-6/repository ÷ L ERDA-6/EQ6 input file = 6.7517×10^7 .

C. 1 L of ERDA-6 contains 0.308002 kg dissolved solids, based on the chemical composition in Table 2 (see above) and a specific gravity of 1.216 kg/L from Table 2.

D. 1 L of ERDA-6 contains 0.907998 kg H₂O, based on the chemical composition in Table 2 and a specific gravity of 1.216 kg/L from Table 2.

E. After microbial denitrification and SO₄²⁻ reduction using SO₄²⁻ in the waste.

F. After formation of magnesite resulting from microbial denitrification and SO₄²⁻ reduction using SO₄²⁻ in the waste.

G. For consumption via SO₄²⁻ reduction (see Reaction 2) of CPR materials remaining after microbial denitrification and SO₄²⁻ reduction using SO₄²⁻ in the waste.

H. In the DRZ along with the required quantities of anhydrite, gypsum, and polyhalite.

I. To simulate production from SO₄²⁻ reduction (Reaction 2) of CPR materials remaining after microbial denitrification and SO₄²⁻ reduction using SO₄²⁻ in the waste.

Table 9. Input Parameters for the Simulation with 13,267 of m³ ERDA-6.^{A, B} Assumed that carbonation of brucite produces magnesite and that calcite precipitates, no organic ligands.

Input Parameter	Value for the Repository	Value for a Seven-Room Panel	Value Used in EQ6 Input File for Step 1
Vol. of ERDA-6	$1.2708 \times 10^5 \text{ m}^3$	$1.3267 \times 10^4 \text{ m}^3$	$1.10 \times 10^0 \text{ L}$
Dissolved solids in ERDA-6 ^C	$3.91 \times 10^7 \text{ kg}$	$4.09 \times 10^6 \text{ kg}$	$3.39 \times 10^{-1} \text{ kg}$
H ₂ O in ERDA-6 ^D	$1.15 \times 10^{11} \text{ kg}$	$1.20 \times 10^{10} \text{ kg}$	$1.00 \times 10^0 \text{ kg}$
Organic C remaining in CPR materials ^E	$1.04 \times 10^9 \text{ mol}$	$1.08 \times 10^8 \text{ mol}$	$8.99 \times 10^0 \text{ mol}$
Brucite remaining ^F	$1.26 \times 10^9 \text{ mol}$	$1.32 \times 10^8 \text{ mol}$	$1.09 \times 10^1 \text{ mol}$
SO ₄ ²⁻ required ^G	$5.18 \times 10^8 \text{ mol}$	$5.41 \times 10^7 \text{ mol}$	$4.49 \times 10^0 \text{ mol}$
DRZ required ^G	$1.54 \times 10^9 \text{ kg};$ $7.07 \times 10^5 \text{ m}^3$	$1.61 \times 10^8 \text{ kg};$ $7.38 \times 10^4 \text{ m}^3$	$1.34 \times 10^1 \text{ kg};$ $6.13 \times 10^0 \text{ L}$
Halite present ^H	$2.46 \times 10^{10} \text{ mol}$	$2.57 \times 10^9 \text{ mol}$	$2.13 \times 10^2 \text{ mol}$
Anhydrite required ^G	$1.92 \times 10^8 \text{ mol}$	$2.01 \times 10^7 \text{ mol}$	$1.67 \times 10^0 \text{ mol}$
Gypsum required ^G	$1.52 \times 10^8 \text{ mol}$	$1.59 \times 10^7 \text{ mol}$	$1.32 \times 10^0 \text{ mol}$
Magnesite present ^H	$3.11 \times 10^8 \text{ mol}$	$3.24 \times 10^7 \text{ mol}$	$2.69 \times 10^0 \text{ mol}$
Polyhalite required ^G	$4.35 \times 10^7 \text{ mol}$	$4.54 \times 10^6 \text{ mol}$	$3.77 \times 10^{-1} \text{ mol}$
CO ₂ required ^I	$1.04 \times 10^9 \text{ mol}$	$1.08 \times 10^8 \text{ mol}$	$8.99 \times 10^0 \text{ mol}$

A. Used for EQ6 input file 06EMAX01.6I.

B. Scaling factor = L ERDA-6/repository ÷ L ERDA-6/EQ6 input file = 1.1061×10^8 .

C. 1 L of ERDA-6 contains 0.308002 kg dissolved solids, based on the chemical composition in Table 2 (see above) and a specific gravity of 1.216 kg/L from Table 2.

D. 1 L of ERDA-6 contains 0.907998 kg H₂O, based on the chemical composition in Table 2 and a specific gravity of 1.216 kg/L from Table 2.

E. After microbial denitrification and SO₄²⁻ reduction using SO₄²⁻ in the waste.

F. After formation of magnesite resulting from microbial denitrification and SO₄²⁻ reduction using SO₄²⁻ in the waste.

G. For consumption via SO₄²⁻ reduction (see Reaction 2) of CPR materials remaining after microbial denitrification and SO₄²⁻ reduction using SO₄²⁻ in the waste.

H. In the DRZ along with the required quantities of anhydrite, gypsum, and polyhalite.

I. To simulate production from SO₄²⁻ reduction (Reaction 2) of CPR materials remaining after microbial denitrification and SO₄²⁻ reduction using SO₄²⁻ in the waste.

Table 10. Input Parameters for the Simulation with 7,763 m³ of GWB and Hydromagnesite.^{A, B}
Assumed that carbonation of brucite produces hydromagnesite and that calcite precipitates, no organic ligands.

Input Parameter	Value for the Repository	Value for a Seven-Room Panel	Value Used in EQ6 Input File for Step 1
Vol. of GWB	$7.436 \times 10^4 \text{ m}^3$	$7.763 \times 10^3 \text{ m}^3$	$1.15 \times 10^0 \text{ L}$
Dissolved solids in GWB ^C	$2.69 \times 10^7 \text{ kg}$	$2.81 \times 10^6 \text{ kg}$	$4.16 \times 10^{-1} \text{ kg}$
H ₂ O in GWB ^D	$6.47 \times 10^{10} \text{ kg}$	$6.76 \times 10^9 \text{ kg}$	$1.00 \times 10^0 \text{ kg}$
Organic C remaining in CPR materials ^E	$1.04 \times 10^9 \text{ mol}$	$1.08 \times 10^8 \text{ mol}$	$1.60 \times 10^1 \text{ mol}$
Brucite remaining ^F	$1.26 \times 10^9 \text{ mol}$	$1.32 \times 10^8 \text{ mol}$	$1.95 \times 10^1 \text{ mol}$
SO ₄ ²⁻ required ^G	$5.18 \times 10^8 \text{ mol}$	$5.41 \times 10^7 \text{ mol}$	$8.01 \times 10^0 \text{ mol}$
DRZ required ^G	$1.54 \times 10^9 \text{ kg};$ $7.07 \times 10^5 \text{ m}^3$	$1.61 \times 10^8 \text{ kg};$ $7.38 \times 10^4 \text{ m}^3$	$2.38 \times 10^1 \text{ kg};$ $1.09 \times 10^1 \text{ L}$
Halite present ^H	$2.46 \times 10^{10} \text{ mol}$	$2.57 \times 10^9 \text{ mol}$	$3.80 \times 10^2 \text{ mol}$
Anhydrite required ^G	$1.92 \times 10^8 \text{ mol}$	$2.01 \times 10^7 \text{ mol}$	$2.97 \times 10^0 \text{ mol}$
Gypsum required ^G	$1.52 \times 10^8 \text{ mol}$	$1.59 \times 10^7 \text{ mol}$	$2.35 \times 10^0 \text{ mol}$
Hydromagnesite present ^I	$6.21 \times 10^7 \text{ mol}$	$6.49 \times 10^6 \text{ mol}$	$9.60 \times 10^{-1} \text{ mol}$
Polyhalite required ^G	$4.35 \times 10^7 \text{ mol}$	$4.54 \times 10^6 \text{ mol}$	$6.71 \times 10^{-1} \text{ mol}$
CO ₂ required ^J	$1.04 \times 10^9 \text{ mol}$	$1.08 \times 10^8 \text{ mol}$	$1.60 \times 10^1 \text{ mol}$

A. Used for EQ6 input file 06GMID03.6I.

B. Scaling factor = L GWB/repository ÷ L GWB/EQ6 input file = 6.4721×10^7 .

C. 1 L of GWB contains 0.3617108 kg dissolved solids, based on the chemical composition in Table 2 (see above) and a specific gravity of 1.2321 kg/L from FMT Run 7 for the CRA-2004 PABC.

D. 1 L of GWB contains 0.8703892 kg H₂O, based on the chemical composition in Table 2 and a specific gravity of 1.2321 kg/L from FMT Run 7 for the CRA-2004 PABC.

E. After microbial denitrification and SO₄²⁻ reduction using SO₄²⁻ in the waste.

F. After formation of magnesite resulting from microbial denitrification and SO₄²⁻ reduction using SO₄²⁻ in the waste.

G. For consumption via SO₄²⁻ reduction (see Reaction 2) of CPR materials remaining after microbial denitrification and SO₄²⁻ reduction using SO₄²⁻ in the waste.

See next page for more footnotes.

Table 10. Input Parameters for the Simulation with 7,763 m³ of GWB and Hydromagnesite^{A, B} (cont.).

- H. In the DRZ along with the required quantities of anhydrite, gypsum, and polyhalite.
- I. Calculated quantity of hydromagnesite in the DRZ by assuming that mol hydromagnesite = $1/5 \times$ mol magnesite.
- J. To simulate production from SO_4^{2-} reduction (Reaction 2) of CPR materials remaining after microbial denitrification and SO_4^{2-} reduction using SO_4^{2-} in the waste.

Table 11. Input Parameters for the Simulation with 7,763 m³ of ERDA-6 and Hydromagnesite.^{A, B} Assumed that carbonation of brucite produces hydromagnesite and that calcite precipitates, no organic ligands.

Input Parameter	Value for the Repository	Value for a Seven-Room Panel	Value Used in EQ6 Input File for Step 1
Vol. of ERDA-6	$7.436 \times 10^4 \text{ m}^3$	$7.763 \times 10^3 \text{ m}^3$	$1.10 \times 10^0 \text{ L}$
Dissolved solids in ERDA-6 ^C	$2.29 \times 10^7 \text{ kg}$	$2.39 \times 10^6 \text{ kg}$	$3.39 \times 10^{-1} \text{ kg}$
H ₂ O in ERDA-6 ^D	$6.75 \times 10^{10} \text{ kg}$	$7.05 \times 10^9 \text{ kg}$	$1.00 \times 10^0 \text{ kg}$
Organic C remaining in CPR materials ^E	$1.04 \times 10^9 \text{ mol}$	$1.08 \times 10^8 \text{ mol}$	$1.54 \times 10^1 \text{ mol}$
Brucite remaining ^F	$1.26 \times 10^9 \text{ mol}$	$1.32 \times 10^8 \text{ mol}$	$1.87 \times 10^1 \text{ mol}$
SO ₄ ²⁻ required ^G	$5.18 \times 10^8 \text{ mol}$	$5.41 \times 10^7 \text{ mol}$	$7.67 \times 10^0 \text{ mol}$
DRZ required ^G	$1.54 \times 10^9 \text{ kg};$ $7.07 \times 10^5 \text{ m}^3$	$1.61 \times 10^8 \text{ kg};$ $7.38 \times 10^4 \text{ m}^3$	$2.28 \times 10^1 \text{ kg};$ $1.05 \times 10^1 \text{ L}$
Halite present ^H	$2.46 \times 10^{10} \text{ mol}$	$2.57 \times 10^9 \text{ mol}$	$3.64 \times 10^2 \text{ mol}$
Anhydrite required ^G	$1.92 \times 10^8 \text{ mol}$	$2.01 \times 10^7 \text{ mol}$	$2.85 \times 10^0 \text{ mol}$
Gypsum required ^G	$1.52 \times 10^8 \text{ mol}$	$1.59 \times 10^7 \text{ mol}$	$2.25 \times 10^0 \text{ mol}$
Hydromagnesite present ^I	$6.21 \times 10^7 \text{ mol}$	$6.49 \times 10^6 \text{ mol}$	$9.20 \times 10^{-1} \text{ mol}$
Polyhalite required ^G	$4.35 \times 10^7 \text{ mol}$	$4.54 \times 10^6 \text{ mol}$	$6.44 \times 10^{-1} \text{ mol}$
CO ₂ required ^I	$1.04 \times 10^9 \text{ mol}$	$1.08 \times 10^8 \text{ mol}$	$1.54 \times 10^1 \text{ mol}$

A. Used for EQ6 input file 06EMID03.6I.

B. Scaling factor = L ERDA-6/repository ÷ L ERDA-6/EQ6 input file = 6.7517×10^7 .

C. 1 L of ERDA-6 contains 0.308002 kg dissolved solids, based on the chemical composition in Table 2 (see above) and a specific gravity of 1.216 kg/L from Table 2.

D. 1 L of ERDA-6 contains 0.907998 kg H₂O, based on the chemical composition in Table 2 and a specific gravity of 1.216 kg/L from Table 2.

E. After microbial denitrification and SO₄²⁻ reduction using SO₄²⁻ in the waste.

F. After formation of magnesite resulting from microbial denitrification and SO₄²⁻ reduction using SO₄²⁻ in the waste.

G. For consumption via SO₄²⁻ reduction (see Reaction 2) of CPR materials remaining after microbial denitrification and SO₄²⁻ reduction using SO₄²⁻ in the waste.

H. In the DRZ along with the required quantities of anhydrite, gypsum, and polyhalite.

See next page for more footnotes.

Table 11. Input Parameters for the Simulation with 7,763 m³ of ERDA-6 and Hydromagnesite^{A, B} (cont.).

- I. Calculated quantity of hydromagnesite in the DRZ by assuming that mol hydromagnesite = $1/5 \times$ mol magnesite.
- J. To simulate production from SO_4^{2-} reduction (Reaction 2) of CPR materials remaining after microbial denitrification and SO_4^{2-} reduction using SO_4^{2-} in the waste.

Table 12. Input Parameters for the Simulations with 1,045 m³ of GWB and Organic Ligands.^{A, B}
Assumed that carbonation of brucite produces magnesite and that calcite precipitates.

Input Parameter	Value for the Repository	Value for a Seven-Room Panel	Value Used in EQ6 Input File for Step 1
Vol. of GWB	$1.001 \times 10^4 \text{ m}^3$	$1.045 \times 10^3 \text{ m}^3$	$1.15 \times 10^0 \text{ L}$
Dissolved solids in GWB ^C	$3.62 \times 10^6 \text{ kg}$	$3.78 \times 10^5 \text{ kg}$	$4.16 \times 10^{-1} \text{ kg}$
H ₂ O in GWB ^D	$8.71 \times 10^9 \text{ kg}$	$9.10 \times 10^8 \text{ kg}$	$1.00 \times 10^0 \text{ kg}$
Organic C remaining in CPR materials ^E	$1.04 \times 10^9 \text{ mol}$	$1.08 \times 10^8 \text{ mol}$	$1.19 \times 10^2 \text{ mol}$
Brucite remaining ^F	$1.26 \times 10^9 \text{ mol}$	$1.32 \times 10^8 \text{ mol}$	$1.45 \times 10^2 \text{ mol}$
SO ₄ ²⁻ required ^G	$5.18 \times 10^8 \text{ mol}$	$5.41 \times 10^7 \text{ mol}$	$5.95 \times 10^1 \text{ mol}$
DRZ required ^G	$1.54 \times 10^9 \text{ kg};$ $7.07 \times 10^5 \text{ m}^3$	$1.61 \times 10^8 \text{ kg};$ $7.38 \times 10^4 \text{ m}^3$	$1.77 \times 10^2 \text{ kg};$ $8.11 \times 10^1 \text{ L}$
Halite present ^H	$2.46 \times 10^{10} \text{ mol}$	$2.57 \times 10^9 \text{ mol}$	$2.82 \times 10^3 \text{ mol}$
Anhydrite required ^G	$1.92 \times 10^8 \text{ mol}$	$2.01 \times 10^7 \text{ mol}$	$2.21 \times 10^1 \text{ mol}$
Gypsum required ^G	$1.52 \times 10^8 \text{ mol}$	$1.59 \times 10^7 \text{ mol}$	$1.75 \times 10^1 \text{ mol}$
Magnesite present ^H	$3.11 \times 10^8 \text{ mol}$	$3.24 \times 10^7 \text{ mol}$	$3.57 \times 10^1 \text{ mol}$
Polyhalite required ^G	$4.35 \times 10^7 \text{ mol}$	$4.54 \times 10^6 \text{ mol}$	$4.99 \times 10^0 \text{ mol}$
CO ₂ required ^I	$1.04 \times 10^9 \text{ mol}$	$1.08 \times 10^8 \text{ mol}$	$1.19 \times 10^2 \text{ mol}$
Initial citrate conc. ^J	$8.06 \times 10^{-4} \text{ M}$	$8.06 \times 10^{-4} \text{ M}$	$8.06 \times 10^{-4} \text{ M}$
Initial oxalate conc. ^J	$4.55 \times 10^{-2} \text{ M}$	$4.55 \times 10^{-2} \text{ M}$	$4.55 \times 10^{-2} \text{ M}$

A. Used for EQ6 input file 06GMIN03.6I.

B. Scaling factor = L GWB/repository ÷ L GWB/EQ6 input file = 8.7122×10^6 .

C. 1 L of GWB contains 0.3617108 kg dissolved solids, based on the chemical composition in Table 2 (see above) and a specific gravity of 1.2321 kg/L from FMT Run 7 for the CRA-2004 PABC.

D. 1 L of GWB contains 0.8703892 kg H₂O, based on the chemical composition in Table 2 and a specific gravity of 1.2321 kg/L from FMT Run 7 for the CRA-2004 PABC.

E. After microbial denitrification and SO₄²⁻ reduction using SO₄²⁻ in the waste.

F. After formation of magnesite resulting from microbial denitrification and SO₄²⁻ reduction using SO₄²⁻ in the waste.

G. For consumption via SO₄²⁻ reduction (see Reaction 2) of CPR materials remaining after microbial denitrification and SO₄²⁻ reduction using SO₄²⁻ in the waste.

See next page for more footnotes.

Table 12. Input Parameters for the Simulations with 1,045 m³ of GWB and Organic Ligands^{A, B}
(cont.)

- H. In the DRZ along with the required quantities of anhydrite, gypsum, and polyhalite.
- I. To simulate production from SO_4^{2-} reduction (Reaction 2) of CPR materials remaining after microbial denitrification and SO_4^{2-} reduction using SO_4^{2-} in the waste.
- J. Initial citrate and oxalate concentrations from Brush and Xiong (2005b).

Table 13. Input Parameters for the Simulations with 1,045 m³ of ERDA-6 and Organic Ligands.^{A, B} Assumed that carbonation of brucite produces magnesite and that calcite precipitates.

Input Parameter	Value for the Repository	Value for a Seven-Room Panel	Value Used in EQ6 Input File for Step 1
Vol. of ERDA-6	$1.001 \times 10^4 \text{ m}^3$	$1.045 \times 10^3 \text{ m}^3$	$1.10 \times 10^0 \text{ L}$
Dissolved solids in ERDA-6 ^C	$3.08 \times 10^6 \text{ kg}$	$3.22 \times 10^5 \text{ kg}$	$3.39 \times 10^{-1} \text{ kg}$
H ₂ O in ERDA-6 ^D	$9.09 \times 10^9 \text{ kg}$	$9.49 \times 10^8 \text{ kg}$	$1.00 \times 10^0 \text{ kg}$
Organic C remaining in CPR materials ^E	$1.04 \times 10^9 \text{ mol}$	$1.08 \times 10^8 \text{ mol}$	$1.14 \times 10^2 \text{ mol}$
Brucite remaining ^F	$1.26 \times 10^9 \text{ mol}$	$1.32 \times 10^8 \text{ mol}$	$1.39 \times 10^2 \text{ mol}$
SO ₄ ²⁻ required ^G	$5.18 \times 10^8 \text{ mol}$	$5.41 \times 10^7 \text{ mol}$	$5.70 \times 10^1 \text{ mol}$
DRZ required ^G	$1.54 \times 10^9 \text{ kg};$ $7.07 \times 10^5 \text{ m}^3$	$1.61 \times 10^8 \text{ kg};$ $7.38 \times 10^4 \text{ m}^3$	$1.70 \times 10^2 \text{ kg};$ $7.78 \times 10^1 \text{ L}$
Halite present ^H	$2.46 \times 10^{10} \text{ mol}$	$2.57 \times 10^9 \text{ mol}$	$2.70 \times 10^3 \text{ mol}$
Anhydrite required ^G	$1.92 \times 10^8 \text{ mol}$	$2.01 \times 10^7 \text{ mol}$	$2.12 \times 10^1 \text{ mol}$
Gypsum required ^G	$1.52 \times 10^8 \text{ mol}$	$1.59 \times 10^7 \text{ mol}$	$1.67 \times 10^1 \text{ mol}$
Magnesite present ^H	$3.11 \times 10^8 \text{ mol}$	$3.24 \times 10^7 \text{ mol}$	$3.42 \times 10^1 \text{ mol}$
Polyhalite required ^G	$4.35 \times 10^7 \text{ mol}$	$4.54 \times 10^6 \text{ mol}$	$4.78 \times 10^0 \text{ mol}$
CO ₂ required ^I	$1.04 \times 10^9 \text{ mol}$	$1.08 \times 10^8 \text{ mol}$	$1.14 \times 10^2 \text{ mol}$
Initial citrate conc. ^J	$8.06 \times 10^{-4} \text{ M}$	$8.06 \times 10^{-4} \text{ M}$	$8.06 \times 10^{-4} \text{ M}$
Initial oxalate conc. ^J	$4.55 \times 10^{-2} \text{ M}$	$4.55 \times 10^{-2} \text{ M}$	$4.55 \times 10^{-2} \text{ M}$

A. Used for EQ6 input file 06EMIN03.6I.

B. Scaling factor = L ERDA-6/repository ÷ L ERDA-6/EQ6 input file = 9.0887×10^6 .

C. 1 L of ERDA-6 contains 0.308002 kg dissolved solids, based on the chemical composition in Table 2 (see above) and a specific gravity of 1.216 kg/L from Table 2.

D. 1 L of ERDA-6 contains 0.907998 kg H₂O, based on the chemical composition in Table 2 and a specific gravity of 1.216 kg/L from Table 2.

E. After microbial denitrification and SO₄²⁻ reduction using SO₄²⁻ in the waste.

F. After formation of magnesite resulting from microbial denitrification and SO₄²⁻ reduction using SO₄²⁻ in the waste.

G. For consumption via SO₄²⁻ reduction (see Reaction 2) of CPR materials remaining after microbial denitrification and SO₄²⁻ reduction using SO₄²⁻ in the waste.

See next page for more footnotes.

Table 13. Input Parameters for the Simulations with 1,045 m³ of ERDA-6 and Organic Ligands^{A, B} (cont.)

- H. In the DRZ along with the required quantities of anhydrite, gypsum, and polyhalite.
- I. To simulate production from SO₄²⁻ reduction (Reaction 2) of CPR materials remaining after microbial denitrification and SO₄²⁻ reduction using SO₄²⁻ in the waste.
- J. Initial citrate and oxalate concentrations from Brush and Xiong (2005b).

Table 14. Input Parameters for the Simulations with 1,045 m³ of GWB, Organic Ligands, and CaCO₃(am).^{A, B} Assumed that carbonation of brucite produces magnesite and that CaCO₃(am) precipitates instead of calcite.

Input Parameter	Value for the Repository	Value for a Seven-Room Panel	Value Used in EQ6 Input File for Step 1
Vol. of GWB	$1.001 \times 10^4 \text{ m}^3$	$1.045 \times 10^3 \text{ m}^3$	$1.15 \times 10^0 \text{ L}$
Dissolved solids in GWB ^C	$3.62 \times 10^6 \text{ kg}$	$3.78 \times 10^5 \text{ kg}$	$4.16 \times 10^{-1} \text{ kg}$
H ₂ O in GWB ^D	$8.71 \times 10^9 \text{ kg}$	$9.10 \times 10^8 \text{ kg}$	$1.00 \times 10^0 \text{ kg}$
Organic C remaining in CPR materials ^E	$1.04 \times 10^9 \text{ mol}$	$1.08 \times 10^8 \text{ mol}$	$1.19 \times 10^2 \text{ mol}$
Brucite remaining ^F	$1.26 \times 10^9 \text{ mol}$	$1.32 \times 10^8 \text{ mol}$	$1.45 \times 10^2 \text{ mol}$
SO ₄ ²⁻ required ^G	$5.18 \times 10^8 \text{ mol}$	$5.41 \times 10^7 \text{ mol}$	$5.95 \times 10^1 \text{ mol}$
DRZ required ^G	$1.54 \times 10^9 \text{ kg};$ $7.07 \times 10^5 \text{ m}^3$	$1.61 \times 10^8 \text{ kg};$ $7.38 \times 10^4 \text{ m}^3$	$1.77 \times 10^2 \text{ kg};$ $8.11 \times 10^1 \text{ L}$
Halite present ^H	$2.46 \times 10^{10} \text{ mol}$	$2.57 \times 10^9 \text{ mol}$	$2.82 \times 10^3 \text{ mol}$
Anhydrite required ^G	$1.92 \times 10^8 \text{ mol}$	$2.01 \times 10^7 \text{ mol}$	$2.21 \times 10^1 \text{ mol}$
Gypsum required ^G	$1.52 \times 10^8 \text{ mol}$	$1.59 \times 10^7 \text{ mol}$	$1.75 \times 10^1 \text{ mol}$
Magnesite present ^H	$3.11 \times 10^8 \text{ mol}$	$3.24 \times 10^7 \text{ mol}$	$3.57 \times 10^1 \text{ mol}$
Polyhalite required ^G	$4.35 \times 10^7 \text{ mol}$	$4.54 \times 10^6 \text{ mol}$	$4.99 \times 10^0 \text{ mol}$
CO ₂ required ^I	$1.04 \times 10^9 \text{ mol}$	$1.08 \times 10^8 \text{ mol}$	$1.19 \times 10^2 \text{ mol}$
Initial citrate conc. ^J	$8.06 \times 10^{-4} \text{ M}$	$8.06 \times 10^{-4} \text{ M}$	$8.06 \times 10^{-4} \text{ M}$
Initial oxalate conc. ^J	4.55×10^{-2}	4.55×10^{-2}	4.55×10^{-2}

A. Used for EQ6 input file 06GMIN05.6I.

B. Scaling factor = L GWB/repository ÷ L GWB/EQ6 input file = 8.7122×10^6 .

C. 1 L of GWB contains 0.3617108 kg dissolved solids, based on the chemical composition in Table 2 (see above) and a specific gravity of 1.2321 kg/L from FMT Run 7 for the CRA-2004 PABC.

D. 1 L of GWB contains 0.8703892 kg H₂O, based on the chemical composition in Table 2 and a specific gravity of 1.2321 kg/L from FMT Run 7 for the CRA-2004 PABC.

E. After microbial denitrification and SO₄²⁻ reduction using SO₄²⁻ in the waste.

F. After formation of magnesite resulting from microbial denitrification and SO₄²⁻ reduction using SO₄²⁻ in the waste.

See next page for more footnotes.

Table 14. Input Parameters for the Simulations with 1,045 m³ of GWB, Organic Ligands, and CaCO₃(am)^{A,B} (cont.).

- G. For consumption via SO₄²⁻ reduction (see Reaction 2) of CPR materials remaining after microbial denitrification and SO₄²⁻ reduction using SO₄²⁻ in the waste.
- H. In the DRZ along with the required quantities of anhydrite, gypsum, and polyhalite.
- I. To simulate production from SO₄²⁻ reduction (Reaction 2) of CPR materials remaining after microbial denitrification and SO₄²⁻ reduction using SO₄²⁻ in the waste.
- J. Initial citrate and oxalate concentrations from Brush and Xiong (2005b)

Table 15. Input Parameters for the Simulations with 1,045 m³ of ERDA-6, Organic Ligands, and CaCO₃(am).^{A,B} Assumed that carbonation of brucite produces magnesite and that CaCO₃(am) precipitates instead of calcite.

Input Parameter	Value for the Repository	Value for a Seven-Room Panel	Value Used in EQ6 Input File for Step 1
Vol. of ERDA-6	$1.001 \times 10^4 \text{ m}^3$	$1.045 \times 10^3 \text{ m}^3$	$1.10 \times 10^0 \text{ L}$
Dissolved solids in ERDA-6 ^C	$3.08 \times 10^6 \text{ kg}$	$3.22 \times 10^5 \text{ kg}$	$3.39 \times 10^{-1} \text{ kg}$
H ₂ O in ERDA-6 ^D	$9.09 \times 10^9 \text{ kg}$	$9.49 \times 10^8 \text{ kg}$	$1.00 \times 10^0 \text{ kg}$
Organic C remaining in CPR materials ^E	$1.04 \times 10^9 \text{ mol}$	$1.08 \times 10^8 \text{ mol}$	$1.14 \times 10^2 \text{ mol}$
Brucite remaining ^F	$1.26 \times 10^9 \text{ mol}$	$1.32 \times 10^8 \text{ mol}$	$1.39 \times 10^2 \text{ mol}$
SO ₄ ²⁻ required ^G	$5.18 \times 10^8 \text{ mol}$	$5.41 \times 10^7 \text{ mol}$	$5.70 \times 10^1 \text{ mol}$
DRZ required ^G	$1.54 \times 10^9 \text{ kg};$ $7.07 \times 10^5 \text{ m}^3$	$1.61 \times 10^8 \text{ kg};$ $7.38 \times 10^4 \text{ m}^3$	$1.70 \times 10^2 \text{ kg};$ $7.78 \times 10^1 \text{ L}$
Halite present ^H	$2.46 \times 10^{10} \text{ mol}$	$2.57 \times 10^9 \text{ mol}$	$2.70 \times 10^3 \text{ mol}$
Anhydrite required ^G	$1.92 \times 10^8 \text{ mol}$	$2.01 \times 10^7 \text{ mol}$	$2.12 \times 10^1 \text{ mol}$
Gypsum required ^G	$1.52 \times 10^8 \text{ mol}$	$1.59 \times 10^7 \text{ mol}$	$1.67 \times 10^1 \text{ mol}$
Magnesite present ^H	$3.11 \times 10^8 \text{ mol}$	$3.24 \times 10^7 \text{ mol}$	$3.42 \times 10^1 \text{ mol}$
Polyhalite required ^G	$4.35 \times 10^7 \text{ mol}$	$4.54 \times 10^6 \text{ mol}$	$4.78 \times 10^0 \text{ mol}$
CO ₂ required ^I	$1.04 \times 10^9 \text{ mol}$	$1.08 \times 10^8 \text{ mol}$	$1.14 \times 10^2 \text{ mol}$
Initial citrate conc. ^J	$8.06 \times 10^{-4} \text{ M}$	$8.06 \times 10^{-4} \text{ M}$	$8.06 \times 10^{-4} \text{ M}$
Initial oxalate conc. ^J	4.55×10^{-2}	4.55×10^{-2}	4.55×10^{-2}

A. Used for EQ6 input file 06EMIN05.6I.

B. Scaling factor = L ERDA-6/repository ÷ L ERDA-6/EQ6 input file = 9.0887×10^6 .

C. 1 L of ERDA-6 contains 0.308002 kg dissolved solids, based on the chemical composition in Table 2 (see above) and a specific gravity of 1.216 kg/L from Table 2.

D. 1 L of ERDA-6 contains 0.907998 kg H₂O, based on the chemical composition in Table 2 and a specific gravity of 1.216 kg/L from Table 2.

E. After microbial denitrification and SO₄²⁻ reduction using SO₄²⁻ in the waste.

F. After formation of magnesite resulting from microbial denitrification and SO₄²⁻ reduction using SO₄²⁻ in the waste.

G. For consumption via SO₄²⁻ reduction (see Reaction 2) of CPR materials remaining after microbial denitrification and SO₄²⁻ reduction using SO₄²⁻ in the waste.

See next page for more footnotes.

Table 15. Input Parameters for the Simulations with 1,045 m³ of ERDA-6, Organic Ligands, and CaCO₃(am)^{A, B} (cont.).

- H. In the DRZ along with the required quantities of anhydrite, gypsum, and polyhalite.
- I. To simulate production from SO₄²⁻ reduction (Reaction 2) of CPR materials remaining after microbial denitrification and SO₄²⁻ reduction using SO₄²⁻ in the waste.
- J. Initial citrate and oxalate concentrations from Brush and Xiong (2005b).

Table 16. Brine Compositions from the Simulation with 1,045 m³ of GWB. Assumed that carbonation of brucite produces magnesite and that calcite precipitates, no organic ligands.

Element or Property	GWB before Step 1 ^A	GWB after Step 1 ^B	GWB after Step 2 ^C
$B(OH)_x^{3-x}$	158 mM	-	-
Na^+	3.53 M	5.15 m	5.38 m
Mg^{2+}	1.02 M	667 mm	16.1 μ m
K^+	467 mM	705 mm	2.14 m
Ca^{2+}	14 mM	4.18 mm	6.04 μ m
SO_4^{2-}	177 mM	700 mm	120 mm
Cl^-	5.86 M	6.02 m	6.88 m
Br^-	26.6 mM	-	-
Total inorganic C	-	15.3 μ m	257 mm
Ionic strength	-	8.68	7.95
$\log f_{CO_2}$	-	-6.92	-6.93
pH	-	8.27	11.3
Relative humidity	-	72.4%	71.8%
Specific gravity	1.232	-	-

A. From Snider (2003).

B. From EQ6 output file 06GMIN01.6O.

C. From EQ6 output file 06GMIN02.6O.

Table 17. Brine Compositions from the Simulation with 1,045 m³ of ERDA-6. Assumed that carbonation of brucite produces magnesite and that calcite precipitates, no organic ligands.

Element or Property	ERDA-6 before Step 1 ^A	ERDA-6 after Step 1 ^B	ERDA-6 after Step 2 ^C
B(OH) _x ^{3-x}	0.063 M	-	-
Na ⁺	4.87 M	5.15 m	5.38 m
Mg ²⁺	19 mM	683 mm	16.1 μm
K ⁺	97 mM	706 mm	2.14 m
Ca ²⁺	12 mM	4.27 mm	6.04 μm
SO ₄ ²⁻	170 mM	700 mm	112 mm
Cl ⁻	4.8 M	5.98 m	6.88 m
Br ⁻	11 mM	-	-
Total inorganic C	16 mM	15.4 μm	256 mm
Ionic strength	-	8.69	7.94
log f _{CO₂}	-	-6.92	-6.93
pH	6.17	8.27	11.3
Relative humidity	-	72.4%	71.8%
Specific gravity	1.216	-	-

A. From Popielak et al. (1983).

B. From EQ6 output file 06EMIN01.6O.

C. From EQ6 output file 06EMIN02.6O.

Table 18. Brine Compositions from the Simulation with 7,763 m³ of GWB. Assumed that carbonation of brucite produces magnesite and that calcite precipitates, no organic ligands.

Element or Property	GWB before Step 1 ^A	GWB after Step 1 ^B	GWB after Step 2 ^C
$B(OH)_x^{3-x}$	0.158 M	-	-
Na^+	3.53 M	5.15 m	4.67 m
Mg^{2+}	1.02 M	671 mm	220 mm
K^+	467 mM	706 mm	1.70 m
Ca^{2+}	14 mM	4.21 mm	102 mm
SO_4^{2-}	177 mM	700 mm	19.6 mm
Cl^-	5.86 M	6.013 m	7.15 m
Br^-	26.6 mM	-	-
Total inorganic C	-	15.3 μ m	216 mm
Ionic strength	-	8.68	7.44
$\log f_{CO_2}$	-	-6.92	-6.93
pH	-	8.27	8.53
Relative humidity	-	72.4%	72.0%
Specific gravity	1.232	-	-

A. From Snider (2003).

B. From EQ6 output file 06GMID01.6O.

C. From EQ6 output file 06GMID02.6O.

Table 19. Brine Compositions from the Simulation with 7,763 m³ of ERDA-6. Assumed that carbonation of brucite produces magnesite and that calcite precipitates, no organic ligands.

Element or Property	ERDA-6 before Step 1 ^A	ERDA-6 after Step 1 ^B	ERDA-6 after Step 2 ^C
B(OH) _x ^{3-x}	0.063 M	-	-
Na ⁺	4.87 M	5.287 m	5.85 m
Mg ²⁺	19 mM	594 mm	16.4 μm
K ⁺	97 mM	714 mm	1.28 m
Ca ²⁺	12 mM	4.44 mm	6.15 μm
SO ₄ ²⁻	170 mM	0.670 m	175 mm
Cl ⁻	4.8 M	6.00 m	6.40 m
Br ⁻	11 mM	-	-
Total inorganic C	16 mM	15.5 μm	259 mm
Ionic strength	-	8.53	7.63
log f _{CO₂}	-	-6.92	-6.92
pH	6.17	8.31	11.3
Relative humidity	-	72.6%	73.2%
Specific gravity	1.216	-	-

A. From Popielak et al. (1983).

B. From EQ6 output file 06EMID01.6O.

C. From EQ6 output file 06EMID02.6O.

Table 20. Brine Compositions from the Simulation with 13,267 m³ of ERDA-6. Assumed that carbonation of brucite produces magnesite and that calcite precipitates, no organic ligands.

Element or Property	ERDA-6 before Step 1 ^A	ERDA-6 after Step 1 ^B	ERDA-6 after Step 2 ^C
B(OH) _x ^{3-x}	0.063 M	-	-
Na ⁺	4.87 M	5.63 m	6.09 m
Mg ²⁺	19 mM	362 mm	16.5 μm
K ⁺	97 mM	733 mm	813 mm
Ca ²⁺	12 mM	4.86 mm	6.22 μm
SO ₄ ²⁻	170 mM	599 mm	180 mm
Cl ⁻	4.8 M	6.05 m	6.17 m
Br ⁻	11 mM	-	-
Total inorganic C	16 mM	16.4 μm	262 mm
Ionic strength	-	8.14	7.42
log f _{CO₂}	-	-6.92	-6.92
pH	6.17	8.45	11.3
Relative humidity	-	73.1%	73.8%
Specific gravity	1.216	-	-

A. From Popielak et al. (1983).

B. From EQ6 output file 06EMAX01.6O.

C. From EQ6 output file 06EMAX02.6O.

Table 21. Quantities of CO₂ Consumed by Magnesite, Calcite, and Pirssonite; and Effective CO₂ Yield in the Simulation with 1,045 m³ of GWB. Assumed that carbonation of brucite produces magnesite and that calcite precipitates, no organic ligands.

Phase of Microbial Activity	CO ₂ Consumed By Magnesite (mol, %)	CO ₂ Consumed By Calcite (mol, %)	CO ₂ Consumed By Pirssonite (mol, %)	Effective CO ₂ Yield (mol CO ₂ /mol organic C)
Begin (0% of CPR materials consumed)	0, 0	0, 0	0, 0	0
Denitrification (4.89% of CPR materials) ^A	5.379×10^7 , 100	0, 0	0, 0	1
SO ₄ ²⁻ reduction w. SO ₄ ²⁻ in waste (0.84% of CPR materials) ^A	9.24×10^6 , 100	0, 0	0, 0	1
SO ₄ ²⁻ reduction w. SO ₄ ²⁻ in DRZ (94.27% of CPR materials) ^B	5.72×10^8 , 55	4.03×10^8 , 39	5.80×10^7 , 6	0.55
End (100% of CPR materials)	6.35×10^8 , 58	4.03×10^8 , 37	5.80×10^7 , 5	0.58

A. Not included in EQ6 simulation, but accounted for by adjusting inventory parameters in the EQ6 input file.

B. From EQ6 output file 06GMIN02.6P.

Table 22. Quantities of CO₂ Consumed by Magnesite, Calcite, and Pirssonite; and Effective CO₂ Yield in the Simulation with 1,045 m³ of ERDA-6. Assumed that carbonation of brucite produces magnesite and that calcite precipitates, no organic ligands.

Phase of Microbial Activity	CO ₂ Consumed By Magnesite (mol, %)	CO ₂ Consumed By Calcite (mol, %)	CO ₂ Consumed By Pirssonite (mol, %)	Effective CO ₂ Yield (mol CO ₂ /mol organic C)
Begin (0% of CPR materials consumed)	0, 0	0, 0	0, 0	0
Denitrification (4.89% of CPR materials) ^A	5.379×10^7 , 100	0, 0	0, 0	1
SO ₄ ²⁻ reduction w. SO ₄ ²⁻ in waste (0.84% of CPR materials) ^A	9.24×10^6 , 100	0, 0	0, 0	1
SO ₄ ²⁻ reduction w. SO ₄ ²⁻ in DRZ (94.27% of CPR materials) ^B	5.62×10^8 , 54	3.92×10^8 , 38	7.89×10^7 , 8	0.54
End (100% of CPR materials)	6.25×10^8 , 57	3.92×10^8 , 36	7.89×10^7 , 7	0.57

A. Not included in EQ6 simulation, but accounted for by adjusting inventory parameters in the EQ6 input file.

B. From EQ6 output file 06EMIN02.6P.

Table 23. Quantities of CO₂ Consumed by Magnesite, Calcite, and Pirssonite; and Effective CO₂ Yield in the Simulation with 7,763 m³ of GWB. Assumed that carbonation of brucite produces magnesite and that calcite precipitates, no organic ligands.

Phase of Microbial Activity	CO ₂ Consumed By Magnesite (mol, %)	CO ₂ Consumed By Calcite (mol, %)	CO ₂ Consumed By Pirssonite (mol, %)	Effective CO ₂ Yield (mol CO ₂ /mol organic C)
Begin (0% of CPR materials consumed)	0, 0	0, 0	0, 0	0
Denitrification (4.89% of CPR materials) ^A	5.379×10^7 , 100	0, 0	0, 0	1
SO ₄ ²⁻ reduction w. SO ₄ ²⁻ in waste (0.84% of CPR materials) ^A	9.24×10^6 , 100	0, 0	0, 0	1
SO ₄ ²⁻ reduction w. SO ₄ ²⁻ in DRZ (94.27% of CPR materials) ^B	6.23×10^8 , 60	4.14×10^8 , 40	0, 0	0.60
End (100% of CPR materials)	6.86×10^8 , 62	4.14×10^8 , 38	0, 0	0.62

A. Not included in EQ6 simulation, but accounted for by adjusting inventory parameters in the EQ6 input file.

B. From EQ6 output file 06GMID02.6P.

Table 24. Quantities of CO₂ Consumed by Magnesite, Calcite, and Pirssonite; and Effective CO₂ Yield in the Simulation with 7,763 m³ of ERDA-6. Assumed that carbonation of brucite produces magnesite and that calcite precipitates, no organic ligands.

Phase of Microbial Activity	CO ₂ Consumed By Magnesite (mol, %)	CO ₂ Consumed By Calcite (mol, %)	CO ₂ Consumed By Pirssonite (mol, %)	Effective CO ₂ Yield (mol CO ₂ /mol organic C)
Begin (0% of CPR materials consumed)	0, 0	0, 0	0, 0	0
Denitrification (4.89% of CPR materials) ^A	5.379×10^7 , 100	0, 0	0, 0	1
SO ₄ ²⁻ reduction w. SO ₄ ²⁻ in waste (0.84% of CPR materials) ^A	9.24×10^6 , 100	0, 0	0, 0	1
SO ₄ ²⁻ reduction w. SO ₄ ²⁻ in DRZ (94.27% of CPR materials) ^B	5.64×10^8 , 55	4.10×10^8 , 40	4.59×10^7 , 5	0.55
End (100% of CPR materials)	6.27×10^8 , 58	4.10×10^8 , 38	4.59×10^7 , 4	0.58

A. Not included in EQ6 simulation, but accounted for by adjusting inventory parameters in the EQ6 input file.

B. From EQ6 output file 06EMID02.6P.

Table 25. Quantities of CO₂ Consumed by Magnesite, Calcite, and Pirssonite; and Effective CO₂ Yield in the Simulation with 13,267 m³ of ERDA-6. Assumed that carbonation of brucite produces magnesite and that calcite precipitates, no organic ligands.

Phase of Microbial Activity	CO ₂ Consumed By Magnesite (mol, %)	CO ₂ Consumed By Calcite (mol, %)	CO ₂ Consumed By Pirssonite (mol, %)	Effective CO ₂ Yield (mol CO ₂ /mol organic C)
Begin (0% of CPR materials consumed)	0, 0	0, 0	0, 0	0
Denitrification (4.89% of CPR materials) ^A	5.379×10^7 , 100	0, 0	0, 0	1
SO ₄ ²⁻ reduction w. SO ₄ ²⁻ in waste (0.84% of CPR materials) ^A	9.24×10^6 , 100	0, 0	0, 0	1
SO ₄ ²⁻ reduction w. SO ₄ ²⁻ in DRZ (94.27% of CPR materials) ^B	5.64×10^8 , 56	4.25×10^8 , 42	1.85×10^7 , 2	0.56
End (100% of CPR materials)	6.27×10^8 , 59	4.25×10^8 , 40	1.85×10^7 , 2	0.59

A. Not included in EQ6 simulation, but accounted for by adjusting inventory parameters in the EQ6 input file.

B. From EQ6 output file 06EMAX02.6P.

Table 26. Brine Compositions from the Simulation with 7,763 m³ of GWB and Hydromagnesite. Assumed that carbonation of brucite produces hydromagnesite and that calcite precipitates, no organic ligands.

Element or Property	GWB before Step 1 ^A	GWB after Step 1 ^B	GWB after Step 2 ^C
$B(OH)_x^{3-x}$	0.158 M	-	-
Na^+	3.53 M	5.15 m	4.33 m
Mg^{2+}	1.02 M	672 mm	506 mm
K^+	0.467 M	706 mm	1.93 m
Ca^{2+}	14 mM	4.21 mm	9.05 mm
SO_4^{2-}	177 mM	700 mm	138 mm
Cl^-	5.86 M	6.01 m	7.22 m
Br^-	26.6 mM	-	-
Total inorganic C	-	428 μ m	428 μ m
Ionic strength	-	8.68	8.05
$\log f_{CO_2}$	-	-5.48	-5.48
pH	-	8.27	8.32
Relative humidity	-	72.6%	70.9%
Specific gravity	1.232	-	-

A. From Snider (2003).

B. From EQ6 output file 06GMID03.6O.

C. From EQ6 output file 06GMID04.6O.

Table 27. Brine Compositions from the Simulation with 7,763 m³ of ERDA-6 and Hydromagnesite. Assumed that carbonation of brucite produces hydromagnesite and that calcite precipitates, no organic ligands.

Element or Property	ERDA-6 before Step 1 ^A	ERDA-6 after Step 1 ^B	ERDA-6 after Step 2 ^C
B(OH) _x ^{3-x}	0.063 M	-	-
Na ⁺	4.87 M	5.29 m	5.77 m
Mg ²⁺	19 mM	595 mm	393 μm
K ⁺	97 mM	714 mm	1.48 m
Ca ²⁺	12 mM	4.44 mm	6.13 μm
SO ₄ ²⁻	170 mM	670 mm	209 mm
Cl ⁻	4.8 M	6.00 m	6.48 m
Br ⁻	11 mM	-	-
Total inorganic C	16 mM	4.32 μm	265 mm
Ionic strength	-	8.53	7.80
log f _{CO₂}	-	-5.48	-5.48
pH	6.17	8.31	10.6
Relative humidity	-	72.6%	72.8%
Specific gravity	1.216	-	-

A. From Popielak et al. (1983).

B. From EQ6 output file 06EMID03.6O.

C. From EQ6 output file 06EMID04.6O.

Table 28. Quantities of CO₂ Consumed by Hydromagnesite, Calcite, and Pirssonite; and Effective CO₂ Yield in the Simulation with 7,763 m³ of GWB. Assumed that carbonation of brucite produces hydromagnesite and that calcite precipitates, no organic ligands.

Phase of Microbial Activity	CO ₂ Consumed By Hydromagnesite (mol, %)	CO ₂ Consumed By Calcite (mol, %)	CO ₂ Consumed By Pirssonite (mol, %)	Effective CO ₂ Yield (mol CO ₂ /mol organic C)
Begin (0% of CPR materials consumed)	0, 0	0, 0	0, 0	0
Denitrification (4.89% of CPR materials) ^A	5.379×10^7 , 100	0, 0	0, 0	1
SO ₄ ²⁻ reduction w. SO ₄ ²⁻ in waste (0.84% of CPR materials) ^A	9.24×10^6 , 100	0, 0	0, 0	1
SO ₄ ²⁻ reduction w. SO ₄ ²⁻ in DRZ (94.27% of CPR materials) ^B	6.06×10^8 , 59	4.14×10^8 , 41	0, 0	0.59
End (100% of CPR materials)	6.69×10^8 , 62	4.14×10^8 , 38	0, 0	0.62

A. Not included in EQ6 simulation, but accounted for by adjusting inventory parameters in the EQ6 input file.

B. From EQ6 output file 06GMID04.6P.

Table 29. Quantities of CO₂ Consumed by Hydromagnesite, Calcite, and Pirssonite; and Effective CO₂ Yield in the Simulation with 7,763 m³ of ERDA-6. Assumed that carbonation of brucite produces hydromagnesite and that calcite precipitates, no organic ligands.

Phase of Microbial Activity	CO ₂ Consumed By Hydromagnesite (mol, %)	CO ₂ Consumed By Calcite (mol, %)	CO ₂ Consumed By Pirssonite (mol, %)	Effective CO ₂ Yield (mol CO ₂ /mol organic C)
Begin (0% of CPR materials consumed)	0, 0	0, 0	0, 0	0
Denitrification (4.89% of CPR materials) ^A	5.379×10^7 , 100	0, 0	0, 0	1
SO ₄ ²⁻ reduction w. SO ₄ ²⁻ in waste (0.84% of CPR materials) ^A	9.24×10^6 , 100	0, 0	0, 0	1
SO ₄ ²⁻ reduction w. SO ₄ ²⁻ in DRZ (94.27% of CPR materials) ^B	5.64×10^8 , 55	4.08×10^8 , 40	5.00×10^7 , 5	0.55
End (100% of CPR materials)	6.27×10^8 , 58	4.08×10^8 , 38	5.00×10^7 , 5	0.58

A. Not included in EQ6 simulation, but accounted for by adjusting inventory parameters in the EQ6 input file.

B. From EQ6 output file 06EMID04.6P.

Table 30. Brine Compositions from the Simulation with 1,045 m³ of GWB and Organic Ligands. Assumed that carbonation of brucite produces magnesite and that calcite precipitates.

Element or Property	GWB before Step 1 ^A	GWB after Step 1 ^B	GWB after Step 2 ^C
B(OH) _x ^{3-x}	0.158 M	-	-
Na ⁺	3.53 M	5.13 m	5.38 m
Mg ²⁺	1.02 M	642 mm	16.2 μm
K ⁺	467 mM	704 mm	2.16 m
Ca ²⁺	14 mM	4.06 mm	6.05 μm
SO ₄ ²⁻	177 mM	701 mm	121 mm
Cl ⁻	5.86 M	6.09 m	6.90 m
Br ⁻	26.6 mM	-	-
Total inorganic C	-	15.3 μm	259 mm
Ionic strength	-	8.66	8.04
log f _{CO₂}	-	-6.92	-6.93
pH	-	8.27	11.3
Relative humidity	-	72.4%	71.8%
Specific gravity	1.232	-	-
Citrate ^D	806 μM	1.15 mm	560 μm
Oxalate ^D	45.5 mM	396 μm	31.6 mm

A. From Snider (2003).

B. From EQ6 output file 06GMIN03.6O.

C. From EQ6 output file 06GMIN04.6O.

D. Initial citrate and oxalate concentrations from Brush and Xiong (2005b).

Table 31. Brine Compositions from the Simulation with 1,045 m³ of ERDA and Organic Ligands. Assumed that carbonation of brucite produces magnesite and that calcite precipitates.

Element or Property	ERDA-6 before Step 1 ^A	ERDA-6 after Step 1 ^B	ERDA-6 after Step 2 ^C
B(OH) _x ^{3-x}	63 mM	-	-
Na ⁺	4.87 M	5.14 m	5.38 m
Mg ²⁺	19 mM	664 mM	16.2 μm
K ⁺	97 mM	705 mM	2.16 m
Ca ²⁺	12 mM	4.17 mM	6.05 μm
SO ₄ ²⁻	170 mM	701 mM	112 mM
Cl ⁻	4.8 M	6.03 m	6.89 m
Br ⁻	11 mM	-	-
Total inorganic C	16 mM	15.3 μm	258 mM
Ionic strength	-	8.68	8.02
Log f _{CO₂}	-	-6.92	-6.93
pH	6.17	8.27	11.3
Relative humidity	-	72.4%	71.8%
Specific gravity	1.216	-	-
Citrate ^D	806 μm	889 μm	561 μm
Oxalate ^D	45.5 mM	402 μm	31.7 mM

A. From Popielak et al. (1983).

See next page for more footnotes.

Table 31. Brine Compositions from the Simulation with 1,045 m³ of ERDA and Organic Ligands (cont.).

B. From EQ6 output file 06EMIN03.6O.

C. From EQ6 output file 06EMIN04.6O.

D. Initial citrate and oxalate concentrations from Brush and Xiong (2005b).

Table 32. Quantities of CO₂ Consumed by Magnesite, Calcite, and Pirssonite; and Effective CO₂ Yield in the Simulation with 1,045 m³ of GWB and Organic Ligands. Assumed that carbonation of brucite produces magnesite and that calcite precipitates.

Phase of Microbial Activity	CO ₂ Consumed By Magnesite (mol, %)	CO ₂ Consumed By Calcite (mol, %)	CO ₂ Consumed By Pirssonite (mol, %)	Effective CO ₂ Yield (mol CO ₂ /mol organic C)
Begin (0% of CPR materials consumed)	0, 0	0, 0	0, 0	0
Denitrification (4.89% of CPR materials) ^A	5.379×10^7 , 100	0, 0	0, 0	1
SO ₄ ²⁻ reduction w. SO ₄ ²⁻ in waste (0.84% of CPR materials) ^A	9.24×10^6 , 100	0, 0	0, 0	1
SO ₄ ²⁻ reduction w. SO ₄ ²⁻ in DRZ (94.27% of CPR materials) ^B	5.72×10^8 , 55	4.03×10^8 , 39	5.80×10^7 , 6	0.55
End (100% of CPR materials)	6.35×10^8 , 58	4.03×10^8 , 37	5.80×10^7 , 5	0.58

A. Not included in EQ6 simulation, but accounted for by adjusting inventory parameters in the EQ6 input file.

B. From EQ6 output file 06GMIN04.6P.

Table 33. Quantities of CO₂ Consumed by Magnesite, Calcite, and Pirssonite; and Effective CO₂ Yield in the Simulation with 1,045 m³ of ERDA-6 and Organic Ligands. Assumed that carbonation of brucite produces magnesite and that calcite precipitates.

Phase of Microbial Activity	CO ₂ Consumed By Magnesite (mol, %)	CO ₂ Consumed By Calcite (mol, %)	CO ₂ Consumed By Pirssonite (mol, %)	Effective CO ₂ Yield (mol CO ₂ /mol organic C)
Begin (0% of CPR materials consumed)	0, 0	0, 0	0, 0	0
Denitrification (4.89% of CPR materials) ^A	5.379×10^7 , 100	0, 0	0, 0	1
SO ₄ ²⁻ reduction w. SO ₄ ²⁻ in waste (0.84% of CPR materials) ^A	9.24×10^6 , 100	0, 0	0, 0	1
SO ₄ ²⁻ reduction w. SO ₄ ²⁻ in DRZ (94.27% of CPR materials) ^B	5.62×10^8 , 54	3.92×10^8 , 38	7.89×10^7 , 8	0.54
End (100% of CPR materials)	6.25×10^8 , 57	3.92×10^8 , 36	7.89×10^7 , 7	0.57

A. Not included in EQ6 simulation, but accounted for by adjusting inventory parameters in the EQ6 input file.

B. From EQ6 output file 06EMIN04.6P.

Table 34. Brine Compositions from the Simulation with 1,045 m³ of GWB, Organic Ligands, and CaCO₃(am). Assumed that carbonation of brucite produces magnesite and that CaCO₃(am) precipitates instead of calcite.

Element or Property	GWB before Step 1 ^A	GWB after Step 1 ^B	GWB after Step 2 ^C
*			
B(OH) _x ^{3-x}	158 mM	-	-
Na ⁺	3.53 M	5.13 m	5.11 m
Mg ²⁺	1.02 M	642 mm	99.6 μm
K ⁺	467 mM	704 mm	2.16 m
Ca ²⁺	14 mM	4.06 mm	3.65 mm
SO ₄ ²⁻	177 mM	701 mm	121 mm
Cl ⁻	5.86 M	6.09 m	7.20 m
Br ⁻	26.6 mM	-	-
Total inorganic C	-	15.3 μm	3.49 mm
Ionic strength	-	8.66	7.49
log f _{CO₂}	-	-6.92	-6.93
pH	-	8.27	10.3
Relative humidity	-	72.4%	72.0%
Specific gravity	1.232	-	-
Citrate ^D	806 μm	1.15 mm	567 μm
Oxalate ^D	45.5 mm	396 μm	287 μm

A. From Snider (2003).

B. From EQ6 output file 06GMIN05.6O.

C. From EQ6 output file 06GMIN06.6O.

D. Initial citrate and oxalate concentrations from Brush and Xiong (2005b).

Table 35. Brine Compositions from the Simulation with 1,045 m³ of ERDA-6, Organic Ligands, and CaCO₃(am). Assumed that carbonation of brucite produces magnesite and that CaCO₃(am) precipitates instead of calcite.

Element or Property	ERDA-6 before Step 1 ^A	ERDA-6 after Step 1 ^B	ERDA-6 after Step 2 ^C
B(OH) _x ^{3-x}	63 mM	-	-
Na ⁺	4.87 M	5.14 m	5.11 m
Mg ²⁺	19 mM	664 mm	99.7 μm
K ⁺	97 mM	705 mm	2.16 m
Ca ²⁺	12 mM	4.17 mm	3.65 mm
SO ₄ ²⁻	170 mM	701 mm	113 mm
Cl ⁻	4.8 M	6.03 m	7.20 m
Br ⁻	11 mM	-	-
Total inorganic C	16 mM	15.3 μm	3.49 mm
Ionic strength	-	8.68	7.47
Log f _{CO₂}	-	-6.92	-6.93
pH	6.17	8.27	10.3
Relative humidity	-	72.4%	72.0%
Specific gravity	1.216	-	-
Citrate ^D	806 μm	889 μm	567 μm
Oxalate ^D	45.5 mm	402 μm	286 μm

A. From Popielak et al. (1983).

See next page for more footnotes.

Table 35. Brine Compositions from the Simulation with 1,045 m³ of ERDA-6, Organic Ligands, and CaCO₃(am) (cont.).

B. From EQ6 output file 06EMIN05.6O.

C. From EQ6 output file 06EMIN06.6O.

D. Initial citrate and oxalate concentrations from Brush and Xiong (2005b).

Table 36. Quantities of CO₂ Consumed by Magnesite, CaCO₃(am), and Pirssonite; and Effective CO₂ Yield in the Simulation with 1,045 m³ of GWB and Organic Ligands. Assumed that carbonation of brucite produces magnesite and that CaCO₃(am) precipitates instead of calcite.

Phase of Microbial Activity	CO ₂ Consumed By Magnesite (mol, %)	CO ₂ Consumed By CaCO ₃ (am) (mol, %)	CO ₂ Consumed By Pirssonite (mol, %)	Effective CO ₂ Yield (mol CO ₂ /mol organic C)
Begin (0% of CPR materials consumed)	0, 0	0, 0	0, 0	0
Denitrification (4.89% of CPR materials) ^A	5.379×10^7 , 100	0, 0	0, 0	1
SO ₄ ²⁻ reduction w. SO ₄ ²⁻ in waste (0.84% of CPR materials) ^A	9.24×10^6 , 100	0, 0	0, 0	1
SO ₄ ²⁻ reduction w. SO ₄ ²⁻ in DRZ (94.27% of CPR materials) ^B	5.72×10^8 , 55	3.98×10^8 , 38	6.66×10^7 , 6	0.55
End (100% of CPR materials)	6.35×10^8 , 58	3.98×10^8 , 36	6.66×10^7 , 6	0.58

A. Not included in EQ6 simulation, but accounted for by adjusting inventory parameters in the EQ6 input file.

B. From EQ6 output file 06GMIN06.6P.

Table 37. Quantities of CO₂ Consumed by Magnesite, CaCO₃(am), and Pirssonite; and Effective CO₂ Yield in the Simulation with 1,045 m³ of ERDA-6 and Organic Ligands. Assumed that carbonation of brucite produces magnesite and that CaCO₃(am) precipitates instead of calcite.

Phase of Microbial Activity	CO ₂ Consumed By Magnesite (mol, %)	CO ₂ Consumed By CaCO ₃ (am) (mol, %)	CO ₂ Consumed By Pirssonite (mol, %)	Effective CO ₂ Yield (mol CO ₂ /mol organic C)
Begin (0% of CPR materials consumed)	0, 0	0, 0	0, 0	0
Denitrification (4.89% of CPR materials) ^A	5.379×10^7 , 100	0, 0	0, 0	1
SO ₄ ²⁻ reduction w. SO ₄ ²⁻ in waste (0.84% of CPR materials) ^A	9.24×10^6 , 100	0, 0	0, 0	1
SO ₄ ²⁻ reduction w. SO ₄ ²⁻ in DRZ (94.27% of CPR materials) ^B	5.62×10^8 , 54	3.88×10^8 , 37	8.74×10^7 , 8	0.54
End (100% of CPR materials)	6.25×10^8 , 57	3.88×10^8 , 35	8.74×10^7 , 8	0.57

A. Not included in EQ6 simulation, but accounted for by adjusting inventory parameters in the EQ6 input file.

B. From EQ6 output file 06EMIN06.6P.

Table 38. Logs of the Solubility Products for Minerals with the Composition CaCO_3 or $\text{CaCO}_3 \cdot x\text{H}_2\text{O}$.

Mineral	Log K_{sp}
Calcite ^A	-8.496
Aragonite ^A	-8.357
Vaterite ^A	-7.937
Ikaite ^B	-6.568
Monohydrocalcite ^B	Not reported
$\text{CaCO}_3(\text{am})^{\text{C, D}}$	-6.401
$\text{CaCO}_3(\text{am})^{\text{B}}$	-6.081

A. From Plummer and Busenberg (1992).

B. From Clarkson et al. (1992).

C. From Brečević and Nielsen (1989).

D. Xiong (2006b) selected this value of K_{sp} to assess the effects of $\text{CaCO}_3(\text{am})$ on brine composition, precipitation of carbonate minerals, and effective CO_2 yield because Gal et al (1996) recommended this K_{sp} based on their critical review of the literature.

APPENDIX A. DOCUMENTATION OF EQ3/6 CALCULATIONS

Software: EQ3/6, Version 7.2c.

Executable Name and Path: C:\eq3_6v7.2c\bin\eq3nr.exe, eq6.exe, eqpt.exe, runeq3.exe, runeq6.exe, and runeqpt.exe.

Databases and Path: C:\eq3_6v7.2c\db\data1.hmp; data1.hmy; data1.hml.

Hardware System: Dell Precision Workstation model 340, S843806.

Input Files and Path for EQ3NR Calculations Concerning ERDA-6:

C:\eq3_6v7.2c\xiong\gwb_drz\epa_sul\qa_2006\erda_dr3.3i (without organic ligands; magnesite not suppressed).

C:\eq3_6v7.2c\xiong\gwb_drz\epa_sul\qa_2006\erda_dr4.3i (without organic ligands; magnesite suppressed).

C:\eq3_6v7.2c\xiong\gwb_drz\epa_sul\qa_2006\erda_orc.3i (with organic ligands; aragonite, calcite and magnesite not suppressed).

C:\eq3_6v7.2c\xiong\gwb_drz\epa_sul\qa_2006\erda_ora.3i (with organic ligands; aragonite and calcite suppressed; magnesite not suppressed).

Input Files and Path for EQ6 Calculations Concerning ERDA-6:

C:\eq3_6v7.2c\xiong\gwb_drz\epa_sul\qa_2006\06emin01.6i; 06emin02.6i; 06emin03.6i; 06emin04.6i; 06emin05.6i; 06emin06.6i; 06emid01.6i; 06emid02.6i; 06emid03.6i; 06emid04.6i; 06emax01.6i; 06emax02.6i; 06emax01.6i.

Input File and Path for EQ3NR Calculations Concerning GWB:

C:\eq3_6v7.2c\xiong\gwb_drz\epa_sul\qa_2006\06gwbdrz.3i (without organic ligands; magnesite not suppressed).

C:\eq3_6v7.2c\xiong\gwb_drz\epa_sul\qa_2006\06gwbdrf1.3i (without organic ligands; magnesite suppressed).

C:\eq3_6v7.2c\xiong\gwb_drz\epa_sul\qa_2006\06gwborg.3i (with organic ligands; aragonite, calcite and magnesite not suppressed).

C:\eq3_6v7.2c\xiong\gwb_drz\epa_sul\qa_2006\06gwbora.3i (with organic ligands; aragonite and calcite suppressed; magnesite not suppressed).

Input Files and Path for EQ6 Calculations Concerning GWB:

C:\eq3_6v7.2c\xiong\gwb_drz\epa_sul\qa_2006\06gmin01.6i; 06gmin02.6i; 06gmin03.6i; 06gmin04.6i; 06gmin05.6i; 06gmin06.6i; 06gmid01.6i; 06gmid02.6i; 06gmid03.6i; 06gmid04.6i.

APPENDIX B. LIST OF EQ6 INPUT FILES

Run Number	/Brine	Brine Volume (m ³)	Remarks
06emin01.6i	ERDA-6	1,045	Titrated solids into ERDA-6 without organic ligands
06emin02.6i	ERDA-6	1,045	Simulated removal of SO ₄ ²⁻ and 2H ⁺ by microbial SO ₄ ²⁻ reduction, titrated CO ₂ into ERDA-6 without organic ligands, magnesite precipitation allowed
06emin03.6i	ERDA-6	1,045	Titrated solids into ERDA-6 with organic ligands
06emin04.6i	ERDA-6	1,045	Simulated removal of SO ₄ ²⁻ and 2H ⁺ by microbial SO ₄ ²⁻ reduction, titrated CO ₂ into ERDA-6 with organic ligands, calcite precipitation allowed
06emin05.6i	ERDA-6	1,045	Titrated the solids into ERDA-6 with organic ligands
06emin06.6i	ERDA-6	1,045	Simulated removal of SO ₄ ²⁻ and 2H ⁺ by microbial SO ₄ ²⁻ reduction, titrated CO ₂ into ERDA-6 with organic ligands, aragonite and calcite suppressed, CaCO ₃ (am) precipitation allowed
06emid01.6i	ERDA-6	7,763	Titrated solids into ERDA-6 without organic ligands

Run Number	/Brine	Brine Volume (m ³)	Remarks
06emid02.6i	ERDA-6	7,763	Simulated removal of SO ₄ ²⁻ and 2H ⁺ by microbial SO ₄ ²⁻ reduction, titrated CO ₂ into ERDA-6 without organic ligands, magnesite precipitation allowed
06emid03.6i	ERDA-6	7,763	Titrated solids into ERDA-6 without organic ligands
06emid04.6i	ERDA-6	7,763	Simulated removal of SO ₄ ²⁻ and 2H ⁺ by microbial SO ₄ ²⁻ reduction, titrated CO ₂ into ERDA-6 without organic ligands, magnesite suppressed, hydromagnesite (5424) precipitation allowed
06emax01.6i	ERDA-6	13,267	Titrated solids into ERDA-6 without organic ligands
06emax02.6i	ERDA-6	13,267	Simulated removal of SO ₄ ²⁻ and 2H ⁺ by microbial SO ₄ ²⁻ reduction, titrated CO ₂ into ERDA-6 without organic ligands. magnesite precipitation allowed
06gmin01.6i	GWB	1,045	Titrated solids into GWB without organic ligands
06gmin02.6i	GWB	1,045	Simulated removal of SO ₄ ²⁻ and 2H ⁺ by microbial SO ₄ ²⁻ reduction, titrated CO ₂ into GWB without organic ligands, magnesite precipitation allowed
06gmin03.6i	GWB	1,045	Titrated solids into GWB with organic ligands

Run Number	/Brine	Brine Volume (m ³)	Remarks
06gmin04.6i	GWB	1,045	Simulated removal of SO ₄ ²⁻ and 2H ⁺ by microbial SO ₄ ²⁻ reduction, titrated CO ₂ into GWB with organic ligands, calcite precipitation allowed
06gmin05.6i	GWB	1,045	Titrated solids into GWB with organic ligands
06gmin06.6i	GWB	1,045	Simulated removal of SO ₄ ²⁻ and 2H ⁺ by microbial SO ₄ ²⁻ reduction, titrated CO ₂ into GWB with organic ligands, aragonite and calcite suppressed, CaCO ₃ (am) precipitation allowed
06gmid01.6i	GWB	7,763	Titrated solids into GWB without organic ligands
06gmid02.6i	GWB	7,763	Simulated removal of SO ₄ ²⁻ and 2H ⁺ by microbial SO ₄ ²⁻ reduction, titrated CO ₂ into GWB without organic ligands, magnesite precipitation allowed
06gmid03.6i	GWB	7,763	Titrated solids into GWB without organic ligands
06gmid04.6i	GWB	7,763	Simulated removal of SO ₄ ²⁻ and 2H ⁺ by microbial SO ₄ ²⁻ reduction, titrated CO ₂ into GWB without organic ligands, magnesite suppressed, hydromagnesite (5424) precipitation allowed
